

University of Southampton

Faculty of Engineering, Science and Mathematics

School of Civil Engineering and the Environment
& School of Ocean and Earth Science

Sediment Exchange between the Dutch Coast and the Tidal Basin Western Scheldt

Annelies Oscar Margaretha Bolle

A dissertation submitted in partial fulfilment of the degree of MSc in
Engineering in the Coastal Environment by instructional course.

December 2006

Summary

To understand the sediment exchange between the Dutch coast and the tidal basin Western Scheldt, the mechanism responsible for this transport must be identified. This study focusses the interaction between tide and bathymetry.

An existing numerical, depth-averaged model of the Western Scheldt in the DELFT3D software (WL|Delft Hydraulics) is applied. The bathymetry of the years 1970, 1983 and 2002 are selected based on previous sand balance studies. In this way three different situations at the mouth are represented: respectively strong import, import and export of sediments. Each model is forced by the same morphological tide.

After comparison of the vertical tidal asymmetry in the model with field data, both the vertical and horizontal tide are analysed. Time series of water levels, velocities and discharges are harmonically analysed in terms of the M_2 , M_4 and M_6 tidal constituents. The tidal asymmetry is expressed by the amplitude ratios M_4/M_2 and M_6/M_2 , and the phase differences $2\phi_2 - \phi_4$ and $3\phi_2 - \phi_6$.

Further the tide driven sediment transport according to a certain bathymetry is determined. Bed-load and suspended load are distinguished and the Engelund-Hansen and Van Rijn formulation are compared. The residual transport patterns are analysed and a sand balance is derived from the modelled transports. This leads to the evolution in time of the sediment exchange between and the erosion/sedimentation within the different macro cells in the Western Scheldt.

To conclude the human interventions, the changes in tidal asymmetry and the evolutions in the sediment transport are related to each other. The increased eastward transport is reproduced in the model, however the change to sediment export at the mouth can not be explained by the tidal asymmetry only. Other processes such as wind and waves should be studied as well to determine the mechanisms which influence the sediment exchange the most.

Acknowledgements

You don't make a good dissertation entirely on your own. Many people contribute small peaces and help you to let the work grow bit by bit. Others are there to form the counterweight for all this work. They listen to your worries and make you laugh when you need it.

Therefore, it would like to express my special thanks to:

- Carl Amos, my supervisor at the University of Southampton,
- WL|Delft Hydraulics which offered me the project and the facilities to work on it,
- Zheng Bing Wang and Edwin Elias from WL, for there guidance, the interesting discussions and the comments on my work,
- John de Ronde from Rijkswaterstaat for his never ending interest in the project,
- all the other employees at WL who didn't mind using some of there valuable time to answer my questions,
- my fellow students in Southampton,
- the students at WL: Frank, Bas, Marieke, Nathanael, Robert-Jan, Pieter, Joana, Inge, Maria and Ali who where always willing to chat and who made me feel at home in the Netherlands,
- and last but not least my boyfriend Wim, my sister Evelien and my parents who supported me through my entire period of study in Leuven, Southampton and Delft.

Contents

List of Figures

List of Tables

List of Abbreviations

Glossary

1	Introduction	1—1
1.1	Problem Definition.....	1—1
1.2	Framework.....	1—3
1.3	Structure of the Report	1—4
2	Study Area.....	2—1
2.1	Topography	2—1
2.2	Hydrodynamic Characteristics.....	2—2
2.3	Morphodynamic Characteristics	2—4
3	Literature Review	3—1
3.1	Estuarine Morphodynamics	3—1
3.2	Sand Balance	3—2
3.3	Tide-driven Sediment Transport	3—8
4	Model Description	4—1
4.1	The Model	4—1
4.2	Simulations	4—3
5	Tidal Asymmetry	5—1
5.1	Applicability of the Model	5—1
5.2	Vertical Tidal Asymmetry.....	5—10

5.3	Horizontal Tidal Asymmetry	5—22
6	Sediment Transport	6—1
6.1	Residual Sediment Transport Patterns.....	6—1
6.2	Tidally Averaged Bed-load Transport	6—8
6.3	Sand Balance Derived from the Model	6—10
6.4	Relation Sediment Transport & Tidal Asymmetry	6—17
7	Conclusions	7—1
8	Recommendations.....	8—1
References		

List of Figures

Figure 2-1: The Scheldt estuary from Gent to the Western Scheldt mouth	2—1
Figure 2-2: Map of the Western Scheldt mouth	2—3
Figure 2-3: Bathymetric parameters along the Western Scheldt basin.....	2—4
Figure 2-4: The multiple channel system as schematised with macro and meso cells.....	2—5
Figure 2-5: Map showing the accretion and consecutive embankment of the intertidal flats and salt marshes along the Scheldt estuary between 1650 and 1968.	2—7
Figure 2-6: Evolution of the Western Scheldt mouth between 1800 and 1997.....	2—8
Figure 3-1: Schematic overview of factors influencing estuarine bathymetry.	3—1
Figure 3-2: The aggregated morphological division of the Western Scheldt.....	3—4
Figure 3-3: The aggregated morphological division of the Western Scheldt mouth.	3—5
Figure 3-4: Sand balance of the Sea Scheldt: boundary condition at the Belgian-Dutch boundary	3—6
Figure 3-5: Cumulative sand volumes since 1955 in the Western Scheldt.....	3—7
Figure 3-6: Changes of the asymmetry of the vertical tide over the period 1971-1996, based on water level measurements.....	3—11
Figure 3-7: Contour plots of the parameters that determine nonlinear distortion as a function of a/h and V_s/V_o , resulting from 84 model systems.	3—13
Figure 4-1: Morphologic, curvilinear grid of the Western Scheldt model in DELFT3D....	4—1
Figure 4-2: Cumulative sand volume since 1955 in the Western Scheldt	4—3
Figure 4-3: Bathymetry for the year 2002.....	4—4
Figure 5-1: Location of the measurement stations for the water levels.....	5—2
Figure 5-2: Comparison of the amplitude of the M_2 tidal constituent derived from the model (relative to 2002) with the measurements (relative to 2000) at the stations Terneuzen, Hansweert and Bath.....	5—4
Figure 5-3: Comparison of the amplitude of the M_2 tidal constituent derived from the model (relative to 2002) with the measurements (relative to 2000) at the stations Westkapelle, Cadzand and Vlissingen.....	5—5
Figure 5-4: Comparison of the phase of the M_2 tidal constituent derived from the model (relative to 2002) with the measurements (relative to 2000) at the stations Terneuzen, Hansweert and Bath.....	5—5
Figure 5-5: Comparison of the phase of the M_2 tidal constituent derived from the model (relative to 2002) with the measurements (relative to 2000) at the stations Westkapelle, Cadzand and Vlissingen.....	5—6
Figure 5-6: Comparison of the phase of the amplitude ratio M_4/M_2 derived from the model (relative to 2002) with the measurements (relative to 2000) at the stations Terneuzen, Hansweert and Bath.....	5—7

Figure 5-7: Comparison of the phase of phase difference $2\phi_2-\phi_4$ derived from the model (relative to 2002) with the measurements (relative to 2000) at the stations Terneuzen, Hansweert and Bath.....	5—7
Figure 5-8: Comparison of the phase of the amplitude ratio M_6/M_2 derived from the model (relative to 2002) with the measurements (relative to 2000) at the stations Terneuzen, Hansweert and Bath.....	5—8
Figure 5-9: Comparison of the phase of phase difference $3\phi_2-\phi_6$ derived from the model (relative to 2002) with the measurements (relative to 2000) at the stations Terneuzen, Hansweert and Bath.....	5—8
Figure 5-10: Location of the lines of observation points in the model along the ebb and flood channels.....	5—10
Figure 5-11: Evolution of the amplitude of M_2 , M_4 and M_6 along the ebb channels in the Western Scheldt.	5—12
Figure 5-12: Evolution of the amplitude of M_2 , M_4 and M_6 along the flood channels in the Western Scheldt.	5—13
Figure 5-13: Evolution of the phase of M_2 , M_4 and M_6 along the ebb channels in the Western Scheldt.....	5—14
Figure 5-14: Evolution of the phase of M_2 , M_4 and M_6 along the flood channels in the Western Scheldt.	5—14
Figure 5-15: Bathymetry near the ‘Drempel of Valkenisse’ for the years 1970, 1983 and 2002.....	5—15
Figure 5-16: Evolution of the amplitude ratios M_4/M_2 and M_6/M_2 along the ebb channels in the Western Scheldt.....	5—16
Figure 5-17: Evolution of the amplitude ratios M_4/M_2 and M_6/M_2 along the flood channels in the Western Scheldt.....	5—16
Figure 5-18: Evolution of the phase differences $2\phi_2-\phi_4$ and $3\phi_2-\phi_6$ along the ebb channels in the Western Scheldt.....	5—17
Figure 5-19: Evolution of the phase differences $2\phi_2-\phi_4$ and $3\phi_2-\phi_6$ along the flood channels in the Western Scheldt.....	5—17
Figure 5-20: Bathymetry in macro cell 6 and 7 for the years 1970, 1983 and 2002.....	5—19
Figure 5-21: Location of the observation points and cross-sections in the model.....	5—22
Figure 5-22: The profile of the cross-section in macro cell 6.....	5—23
Figure 5-23: Tidal ellipses for the M_2 , M_4 and M_6 tidal constituents derived from the model results for the years 1970, 1983 and 2002 for the observation point in the flood channel of macro cell 6.	5—24
Figure 5-24: Tidal ellipses for the M_2 , M_4 and M_6 tidal constituents derived from the model results for the years 1970, 1983 and 2002 for the observation point in the ebb channel of macro cell 6.....	5—25
Figure 5-25: The amplitude ratios M_0/M_2 , M_4/M_2 and M_6/M_2 , and the phase differences $2\phi_2-\phi_4$ and $3\phi_2-\phi_6$ of the velocity at the observation points in the ebb and flood channel of macro cell 6 for the years 1970, 1983 and 2002.....	5—27

Figure 5-26: The amplitude ratios M_0/M_2 , M_4/M_2 and M_6/M_2 for the discharge through the cross-sections in the ebb and flood channel of macro cell 6 derived from the model results for the years 1970, 1983 and 2002.....	5—28
Figure 5-27: Evolution of the amplitude of the M_2 , M_4 and M_6 components of the horizontal tide along the flood channels in the Western Scheldt.	5—29
Figure 5-28: Evolution of the amplitude of the M_2 , M_4 and M_6 components of the horizontal tide along the ebb channels in the Western Scheldt.	5—30
Figure 5-29: Evolution of the phase of the M_2 , M_4 and M_6 components of the horizontal tide along the flood channels in the Western Scheldt.....	5—31
Figure 5-30: Evolution of the phase of the M_2 , M_4 and M_6 components of the horizontal tide along the ebb channels in the Western Scheldt.	5—31
Figure 5-31: Evolution of the amplitude ratio of the M_2 , M_4 and M_6 components of the horizontal tide along the flood channels in the Western Scheldt.	5—32
Figure 5-32: Evolution of the amplitude ratio of the M_2 , M_4 and M_6 components of the horizontal tide along the ebb channels in the Western Scheldt.	5—33
Figure 5-33: Evolution of the phase differences of the M_2 , M_4 and M_6 components of the horizontal tide along the flood channels in the Western Scheldt.	5—33
Figure 5-34: Evolution of the phase differences of the M_2 , M_4 and M_6 components of the horizontal tide along the ebb channels in the Western Scheldt.	5—34
Figure 6-1: Residual transport patterns in the western part of the Western Scheldt for 2002 as calculated with the Engelund Hansen formulation for the total load.	6—2
Figure 6-2: Residual transport patterns in the western part of the Western Scheldt for 1970 and 2002 according to the Engelund Hansen formulation for total load.	6—3
Figure 6-3: Residual transport patterns in the western part of the Western Scheldt for 2002 as calculated with the Van Rijn formulation for the suspended load.....	6—4
Figure 6-4: Residual transport patterns in the western part of the Western Scheldt for 2002 as calculated with the Van Rijn formulation for the bed-load.....	6—5
Figure 6-5: Residual transport patterns in the western part of the Western Scheldt for 1970 and 2002 according to the Van Rijn formulation for suspended load.	6—6
Figure 6-6: The different contributing terms and the total dimensionless tide-averaged bed-load transport according to Van de Kreeke and Robaczewska (2003) at the observation points in macro cell 6 for the years 1970, 1983 and 2002. ...	6—9
Figure 6-7: Division of the Western Scheldt in cells for the sand balance.	6—10
Figure 6-8: Transport between the macro cells in the Western Scheldt in m^3 /tidal cycle for the total , bed-load and suspended transport according to Van Rijn	6—13
Figure 6-9: Sedimentation and erosion in the macro cells in the Western Scheldt for the total, bed-load, and suspended transport according to Van Rijn.	6—14
Figure 8-1: Aerial photo of the shoals “de Hooge platen” in 1996 and 2001.	8—2

List of Tables

Table 5-1: Average deviation of amplitude and phase from M_2 , M_4 and M_6 derived from the model results from the field data.....	5—2
Table 5-2: Comparison of the amplitudes (absolute) and phases (relative to Cadzand) for the M_2 , M_4 and M_6 constituents derived from the measurements and the model results for the year 1983.	5—3
Table 5-3: Location of the measurement stations and the crossings of the ebb and flood channels along the Western Scheldt.	5—11
Table 5-4: Overview of the dredging, dumping and sand mining in macro cell 6.	5—19
Table 6-1: Transport across the macro cell borders according to the Van Rijn formula..	6—11
Table 6-2: Erosion and sedimentation in the macro cells according to the Van Rijn formulation.	6—12
Table 6-3: Most important evolutions of the amplitude ratios and the phase differences of the M_2 , M_4 and M_6 components of the vertical tide.....	6—17

List of Abbreviations

AD	Anno Domino
ADCP	Acoustic Doppler Current Profiler
NAP	Nieuw Amsterdams Peil (= Dutch gravitational reference level, \approx mean sea level)
RCMG	Renard Centre of Marine Geology (at the University of Gent, Belgium)
RWS RIKZ	Rijkswaterstaat Rijksinstituut voor Kust en Zee (= ‘National Institute for Coastal and Marine Management’ which is a specialist service of the Directorate General of Public Works and Water Management in the Netherlands)
TNO	Nederlandse Organisatie voor Toegepast-Natuurwetenschappelijk Onderzoek (= Dutch organisation for applied-natural scientific research)

Glossary

Scheldt estuary	the part of the Scheldt River that is subject to tidal action, consisting of the Sea Scheldt, the Western Scheldt and the mouth region
Sea Scheldt	the part of the Scheldt River between Gent and the Belgian-Dutch border
Western Scheldt	the part of the Scheldt River between the Belgian-Dutch border and Vlissingen
Mouth region or Voordelta	the part of the Scheldt River seawards of Vlissingen (=the area between Oostende-Westkapelle and Vlissingen-Breskens)

I Introduction

I.1 Problem Definition

The main research question for this study is: “Which are the mechanisms governing the sediment exchange between the Dutch coast and the tidal basin Western Scheldt?”

This question is answered by addressing the following three sub-questions:

- Is there a change in tidal asymmetry over the years?
 - Does the asymmetry of the vertical tide determined from the model agree with the asymmetry derived from field measurements?
 - How does the asymmetry of the vertical tide in the estuary change over the years?
 - How does the asymmetry of the horizontal tide in the estuary change over the years?
- How do changes in the bathymetry modify the tidal asymmetry? Is there a relation between the changes in the tidal asymmetry and the import/export of sediments at the mouth?
 - Which changes in the bathymetry have influenced the tidal asymmetry the most?
 - Does the residual transport derived from the model agree with previous sand balances?
 - Does bed-load and suspended load sediment follow different trends?
 - Can different transport formulations influence the results significantly?
- Which characteristics of the bottom geometry are responsible for the import/export of sediments at the Western Scheldt mouth?

The main objective of this study is to identify the mechanisms governing the import/export of sediments at the mouth of the Western Scheldt. The evaluation of the relative importance of the tide-driven sediment transport in this phenomenon is an essential first step. In general, the principal forcing factors of water motion in well mixed estuaries are: the astronomical tide, the meteorological factors and the river flow (Wang et al., 1999). However, in this study only the influence of the tide will be examined. This for a number of reasons:

First, the tidal asymmetry is an important factor for the generation of residual transport in estuaries. In the Western Scheldt this is possibly a principal factor influencing the sediment exchange between the ebb-tidal delta and the estuary (ibid.). Among others, Aubrey and Speer (1985), Boon and Byrne (1981) and Friedrichs and Aubrey (1988) showed that basin morphology can affect the tidal asymmetry due to the local generation by non-linear bottom friction, non-linear advection of momentum or tidal interaction with the morphology inside the basin such as the hypsometry effect leading to asymmetric flooding and drying of the inter-tidal shoals and bathymetry related residual flow circulations. These two arguments suggest that it is worth looking at the tidal asymmetry as possible determinative process in the sediment exchange.

The mean river outflow is about $5 \times 10^6 \text{ m}^3$ per semi-diurnal tide, which is less than 1% of the tidal prism of about $2 \times 10^9 \text{ m}^3$ (Wang et al., 2002). The Western Scheldt can be considered as well-mixed, only during high river discharges the part between Rupelmonde and Hansweert is considered as partially mixed (Verlaan, 1998). Therefore the influence of density differences on the water movement and water levels is small (Technische Scheldecommissie, 1984) and will be neglected in this study. We also do not address the importance of wind and waves. Although these can contribute significantly to the transports in a tidal inlet Elias et al. (2006).

In this study a DELFT3D-model is used to study the interaction between bathymetry and tide in the Western Scheldt. If one wants to apply a numerical model for this purpose, the first step is to investigate whether or not the asymmetry observed in field measurements, can be reproduced in the model. If the model is able to reproduce the tidal asymmetry, it can further be used to analyse the influence of the bottom geometry on the import/export regime at the estuary mouth. Therefore, a comparison between the vertical tidal asymmetry derived from model results and field measurements is made. This gives an idea of the accuracy of the model concerning the tidal asymmetry. The other questions aim at identifying the relative importance of various factors influencing the residual transport in the estuary.

I.2 Framework

The topic “Sediment exchange between the Dutch coast and the tidal basin Western Scheldt” fits into the study “Interaction between the long-term developments of the Dutch coast and the tidal basins Marsdiep and Western Scheldt” which is undertaken by WL|Delft Hydraulics in the Netherlands. This research is commissioned by the RWS National Institute for Coastal and Marine Management (RWS RIKZ). An important mission of RWS RIKZ is to gather and supply information, services and advice concerning the sustainable use of coasts and seas and the protection of the land against tidal flooding.

The present policy in the Netherlands is to hold the coastline in its current position (RIKZ, 2006). Sand nourishment is applied for the maintenance of the basis coastline and the larger-scale foundation of the coast. To maintain this foundation, which is defined as the area between the toe of the dune and the NAP-20m depth contour, sufficient sand should be supplied to keep pace with the sea level rise and to compensate the sand losses. For the Dutch coast also the losses at the coastal inlets have to be taken into account (ibid.).

Another point of concern is the safety against flooding, accessibility and natural quality of the Scheldt Estuary. The policy for the near future is outlined in the “Scheldt Estuary Development Plan 2010” (OS2010, 2006). The preservation of the estuarine dynamics in the Western Scheldt such as the multiple channel system, the tide and the total sand volume is one of the challenges for the future.

The study commissioned by RWS RIKZ concerns the exchange of sediment between the coast and the tidal basins Western Scheldt and Wadden Sea, the most important basins along the Dutch Coast, over different time-scales. For both basins, questions about the evolution of the import/export at the mouth recently arose. In case of the Western Scheldt, which is the subject of this study, mainly the uncertainty about the future developments after the change from import to export at the mouth was noticed in the nineties, necessitated a more detailed study of this area.

I.3 Structure of the Report

This report contains 8 chapters. In chapter 2 the topography and the hydrodynamic and the morphodynamic characteristics of the study area are described. This is followed by a literature review concerning the sand balance concept and factors influencing the sediment transport in chapter 3. The focus is on tidal asymmetry due to interaction between tide and bathymetry.

Chapter 4 describes the numerical model and the model method used in this study. A brief introduction into the different simulations is given.

The results are described in the next two chapters: the vertical and horizontal tidal asymmetry are described in chapter 5, whereas the residual sediment transport patterns and the sand balance derived from the model results is presented in chapter 6. The relation between the changes in tidal asymmetry and sediment transport are discussed as well.

The main conclusions from this study and recommendations for further research are formulated in respectively chapters 7 and 8.

2 Study Area

2.1 Topography

The Scheldt rises in the north of France near St. Quentin, 350 km upstream of the mouth. (Figure 2-1) The entire part downstream of the weir at Gentbrugge is tidally influenced. The upstream part in Belgium from Gent to the Belgian-Dutch border forms the Sea Scheldt. The Dutch part of the estuary consists of the Western Scheldt and its mouth. The total surface of the river basin is around 21000 km², from which 1000 km² is located on Dutch territory (Kramer, 2002). The fall of the river is 95 m from which 79 m in France.

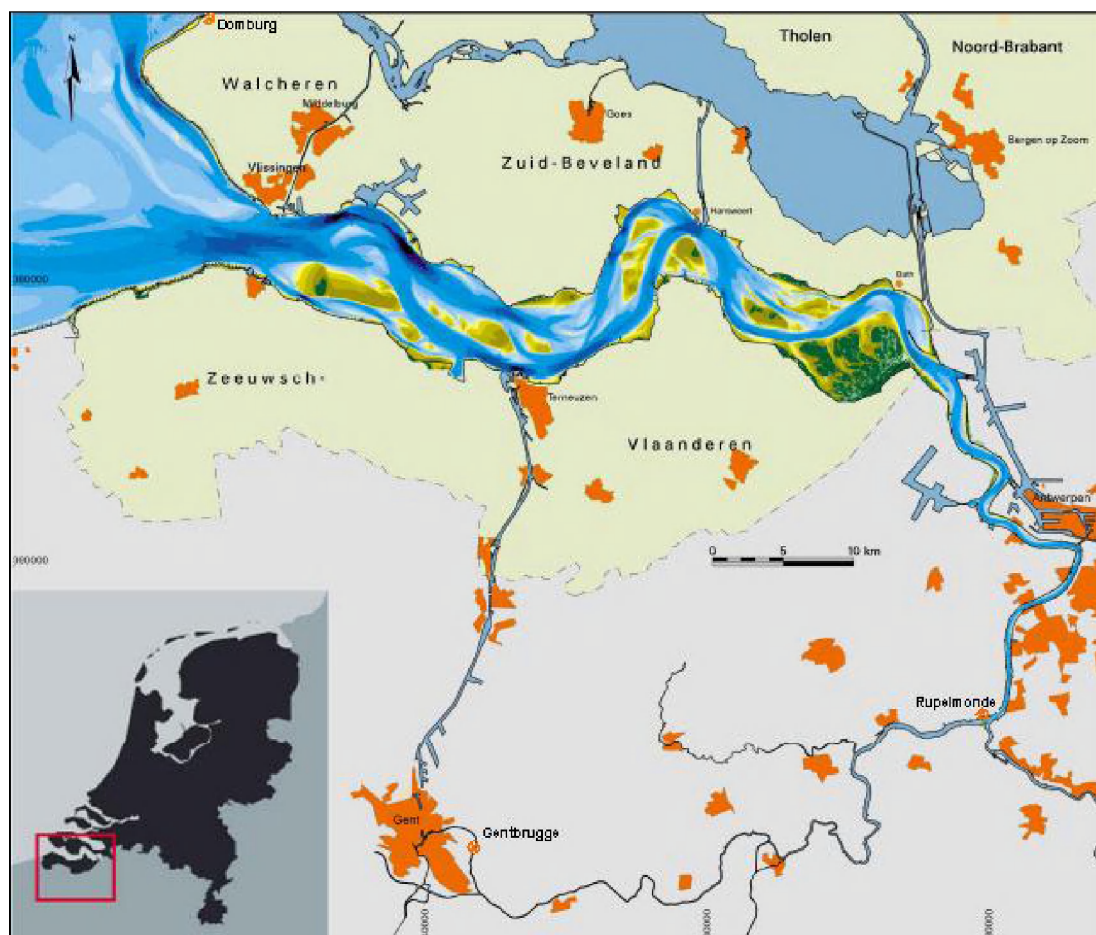


Figure 2-1: The Scheldt estuary from Gent to the Western Scheldt mouth (after Groenendaal, 2005).

2.2 Hydrodynamic Characteristics

The tides in the estuary are dominantly semi-diurnal. The tidal prism is in the order of $2.2 \times 10^9 \text{ m}^3$ at Vlissingen, $0.2 \times 10^9 \text{ m}^3$ at the Belgian-Dutch border and $0.1 \times 10^9 \text{ m}^3$ at Antwerpen (Verlaan, 1998). The mean tidal range increases between Vlissingen and Antwerpen from 3.8 to 5.2 m and decreases again to 1.9 m near Gent. The vertical tide is asymmetric and flood-dominant. This effect increases going upstream: the ratio between the rise and fall time of the tidal wave decreases from 0.88 at Vlissingen to 0.75 at Rupelmonde and 0.39 at Gent (Kuijper et al., 2004).

The mean river outflow is about $120 \text{ m}^3/\text{s}$ or $5 \times 10^6 \text{ m}^3$ of water per semi-diurnal tide. This is less than 1% of the tidal prism of about $2 \times 10^9 \text{ m}^3$ (Wang et al., 2002). Based on the ratio of the freshwater discharge and the tidal volume the estuary can be considered as partially mixed between Rupelmonde and Hansweert (only during high river discharges) and well-mixed downstream of Hansweert (Verlaan, 1998). Therefore the influence of density differences on the water movement and water levels is small (Technische Scheldecommissie, 1984). The maximum depth-averaged current velocities in the channels are in the order of 1-1.5 m/s (Wang et al., 2002).

The wave height and the wave period decrease eastwards along the Western Scheldt. Whereas at the most seaward location (Schouwenbank which is located 25 km northwest from Domburg) the mean wave height is 1.1 m, the remaining wave height at Bath is only 20% of this value. The wave period decreases from around 4 to 5 seconds at the seaward end to around 2 seconds near Bath (Gautier and Van De Boomgaard, 2003).

The hydrodynamic characteristics of the mouth were recently described by Dumon et al. (2006). They analysed the data from the measurement networks “Meetnet Vlaamse Banken” from the Flemish government and “Zege Meetnet” from Rijkswaterstaat in the Netherlands. Figure 2-2 shows an overview of this area, the measurement locations are given in Appendix A.1. They found a decreasing mean wave height from 1.47 m near the measurement location Westhinder, over 1.27 m near Akkaert Zuid, to 1.03 m near Bol van Heist (near the seaward border of the mouth). Near Westhinder the wave direction is 37% of the time W-NW, while near Cadzand this is already 53% due to refraction. They noticed that the measured tidal amplitudes at sea are smaller than those in the Western Scheldt, which confirms the theory of the amplification of the tide in a funnel shaped estuary.

Kornman et al. (2000) noticed an increase of the tidal range in the mouth of 4% per century. This is possibly caused by the combination of sea level rise, the interventions related to the Delta-plan and/or the anthropogenic impact within the Western Scheldt estuary (Dumon et al, 2006).



Figure 2-2: Map of the Western Scheldt mouth (Dumon et al. 2006).

Concerning the wind, Dumon et al. noticed that on the Vlakte van de Raan 40% of the time the direction is S-SW to SW-W. Also the highest wind speed comes from these directions. The eastern sector is the most unusual direction. The wind speed is significant higher at sea: at Westhinder the wind speed can be the double compared to Zeebrugge. Also the average wind speed on the Vlakte van de Raan is lower than at locations more to the north. This is explained by the orientation of the coastline which makes the wind from the most important S and SW directions to be more disturbed near the coast than at sea.

2.3 Morphodynamic Characteristics

2.3.1 Morphological Description

The Western Scheldt is a coastal plain estuary in the classical sense. The estuary is tide-dominated with a meso- to macro-tidal regime according to the classification of Dyer (1997). It has a funnel-shaped geometry, where the estuarine width reduces from about 6 km near the mouth, via 2-3 km near Bath to less than 100 m near the estuary head. The width-averaged depth decreases from 15 m at Vlissingen to only 3 m near Gent (Wang et al., 2002). The evolution of the average channel depth, the average propagation depth, the channel width at low water and the basin width at low and high water is visualised in Figure 2-3. Hypsometric curves have been formulated by Mol et al. (1997) for the six echosounding areas located in the Western Scheldt. These areas are given in Appendix A.1.

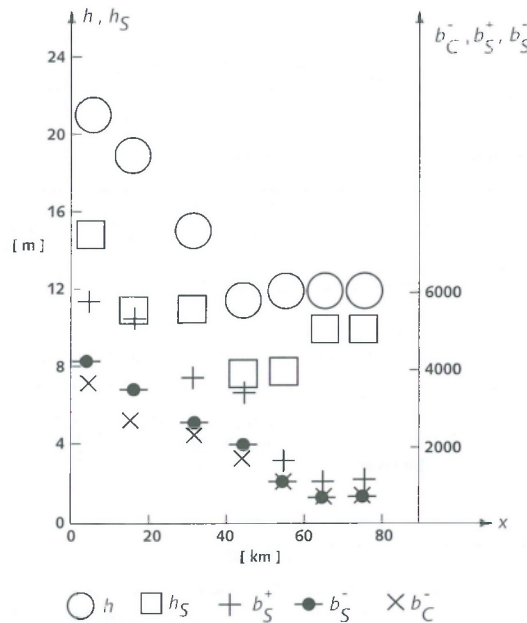


Figure 2-3: Bathymetric parameters along the Western Scheldt basin: the average channel depth h , the average propagation depth h_S , the channel width at low water b_C^- , the basin width at high water b_S^+ and the basin width at low water b_S^- (Dronkers, 2005).

The meandering channel system of the Western Scheldt shows a regular repetitive pattern of ebb and flood channels. Van Veen (1950) classified this as a braided pattern. Lateral boundaries are formed by dikes and bank-protection measures. Bars are found at the seaward side of the ebb channels and at the landward side of the flood channels. The major

transport occurs in the main ebb and flood channels. Winterwerp et al. (2000) used a chain of macro-cells (ebb- and flood channels) and meso cells (connecting channels) to schematise the channel system (Figure 2-4).

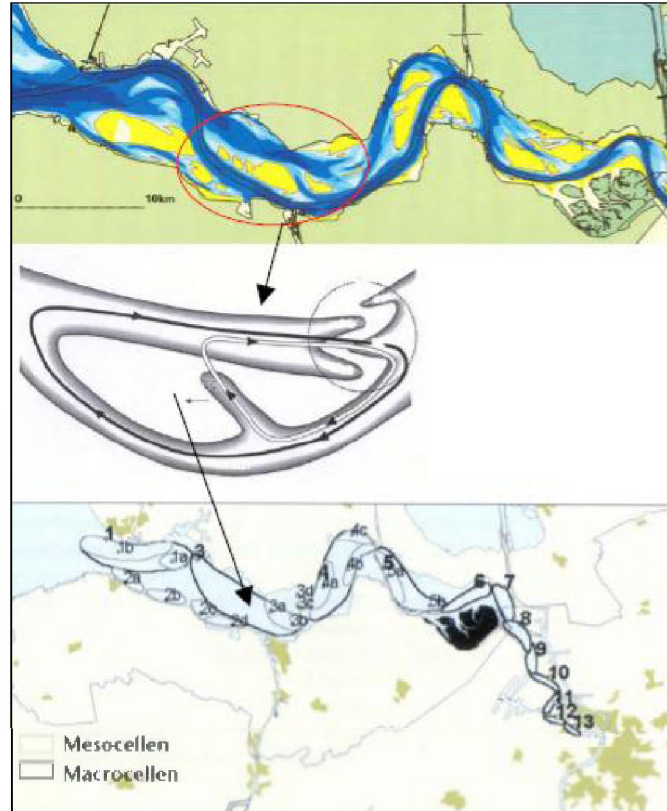


Figure 2-4: The multiple channel system as schematised with macro and meso cells (Kuijper et al., 2004).

In the Western Scheldt mouth the “Scheur/Wielingen” is clearly the main channel and is east-west directed. Another important channel is the “Oostgat” which shorts the Western Scheldt and the North Sea. The function of the shoal area the Raan as breakwater is very important for the coast behind and the entrance of the Western Scheldt (Dumon et al., 2006). The Raan forms a buffer between the sea climate and the Western Scheldt mouth, and weakens the incoming hydrodynamic patterns (waves and currents). Over the shoal area no dominant current direction is present.

The sediment in the Western Scheldt mainly consists of sand with less than 10% mud in the channels and on the shoals. The median diameter d_{50} in the channels is typically larger than 150 μm , on the shoals between 50 and 150 μm and along the estuarine margins (intertidal areas and salt marshes) smaller than 125 μm . The grain size diameter in the channels in the upstream section is somewhat finer than downstream. The bed of the Western Scheldt is

build of alternating erodible sand layers and resistant layers of stiff clay (Kuijper et al., 2004). Maps with the median grain size d_{50} , the percentage of mud and the thickness of the upper erodible sand layer in the Western Scheldt are given in Appendix A.1.

The sediment composition in the mouth is very heterogeneous (Du Four et al., 2006). This is partly due to the natural environment in which this area is located, but also to the numerous human impacts such as dredging and dumping in this region. The Vlake van de Raan, the shoals and the channels in the south-western part of the mouth are characterised by fine sands. Coarse sand is found in the Wielingen (Figure 2-2) which is explained by the strong currents in the throat of the Western Scheldt mouth. The mouth is also characterised by ‘disturbing clay layers’, silt fields and a high turbidity. The Tertiary clay is located close to the bottom surface in the navigation channel Scheur, where clay granules are found (ibid.). Maps with the median grain size and the occurrence of cohesive sediments in the mouth are given in Appendix A.1.

2.3.2 Morphological Changes

The Western Scheldt evolved from the Honte, a tidal channel which has been expanding landward since the early middle Ages. It gradually took over the function of the Eastern Scheldt which was the original mouth of the river Scheldt.

In the 14th century the Western Scheldt had scoured enough to become the new shipping route to the port of Antwerpen. In the 17th century the Western Scheldt had become a large tidal basin. During the following centuries the connections with the Eastern Scheldt and the large branches along the southern shore of the estuary silted up and were consecutively dammed in the 19th and 20th century (Figure 2-5). The intertidal storage decreased from 295 km² in 1650 AD to 104 km² in the recent Western Scheldt (van der Spek, 1997).

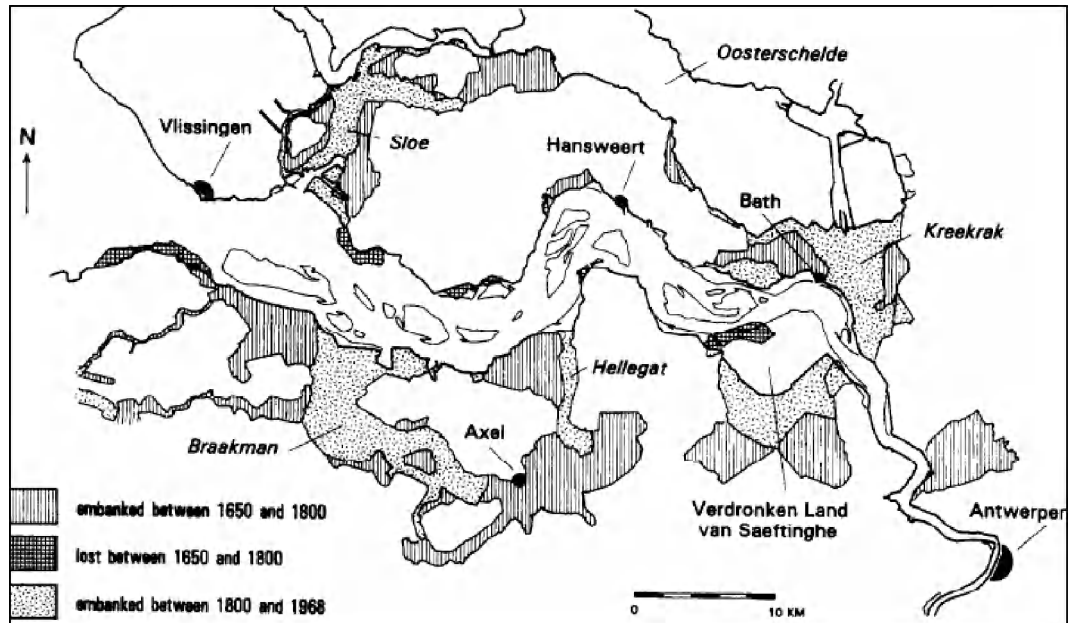


Figure 2-5: Map showing the accretion and consecutive embankment of the intertidal flats and salt marshes along the Scheldt estuary between 1650 and 1968. The intertidal shoals in the estuary, indicated by their mean sea level contours, show the situation for 1968 (Van der Spek, 1997).

The configuration of the main ebb and flood channels remained unaltered in most locations since approximately 1930. However a general steepening of the bathymetry is noticed since 1955. This is indicated by the increases of the shoal area (+20% or 800 ha between 1955 and 1980) and the decrease of the sub-tidal area (-35% between 1955 and 2002) (Kuijper, 2004). Upstream of Antwerpen the geometry of the estuary remained stable. Nowadays the Western Scheldt resembles a classical funnel shaped estuary. The “Verdrongen land van Saeftinghe” is the only remaining substantial intertidal marsh (van der Spek, 1997).

The morphologic changes in the mouth are also related to a lot of different factors of which the tides, the geology and the human interventions are the most important (Peters, 2006). The evolution of this area between 1800 and 1997 is depicted in Figure 2-6. The channels Wielingen and Spleet evolved to one main channel: Scheur. The channel of the Walvisstaart became wider and more important. These changes are related to the evolution of the channels and shoals in the western part of the Western Scheldt, which determine the direction of the ebb-tidal flow as described by Peters (2006).

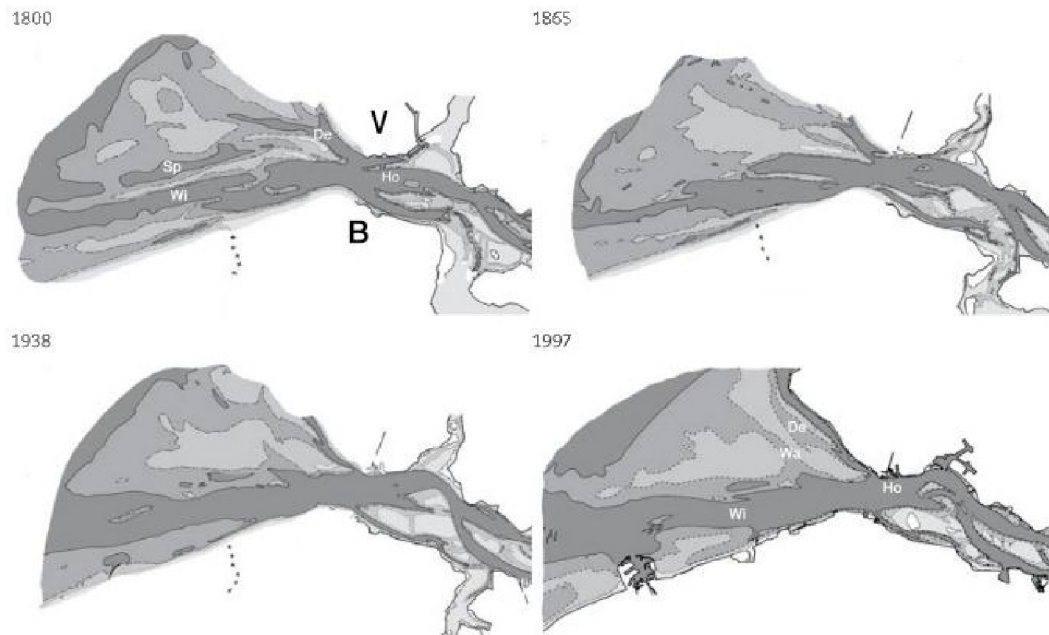


Figure 2-6: Evolution of the Western Scheldt mouth between 1800 and 1997 (V=Vlissingen, B=Breskens, Wi=Wielingen, Sp=Spleet, Wa=geul van de Walvisstaart, Ho=de Honte, De=Deurlo) (Peters, 2006).

The human influences on the morphology of the Western Scheldt are not limited to the large land reclamation in the past, also in the last 50 years several interventions took place. Apart from almost continuous dredging, dumping and sand mining in the estuary, bank protection measures have been placed at the border of a number of channels Peters et al. (2003). This is described in detail in Appendix A.2.

Also the morphological evolution of the mouth is affected by human interventions. The expansion of the port of Zeebrugge (1972-1985) with the construction of the breakwaters and the dumping of large amounts of dredged material northwest of the Vlakte van de Raan for a long time, certainly have an influence although the exact impact can hardly be estimated (Peters, 2006; Port of Zeebrugge, 2006). Also other edifices such as the delta-plan with the storm-surge barrier on the Eastern Scheldt (build between 1976 and 1986) have possibly affected the Western Scheldt mouth area (ibid.).

3 Literature Review

3.1 Estuarine Morphodynamics

The morphology of estuaries is the result of non-linear interactions between bed topography, water and sediment motion (Hibma et al., 2004). This morphodynamic evolution is complex since a wide range of space and time scales are involved: from micro scale features (ripples and dunes on the bed), over meso scale (ebb- and flood channels and shoals) and macro scale features (inlet gorge and ebb-tidal delta) to the mega scale which refers to the entire estuary (ibid.).

Main factors determining meso and macro scale development are tidal currents and wind waves. The relative importance of these two factors is used to make a distinction between tide- and wave-dominated basins (Hayes, 1975). The hypsometry of basins has been related to these forcings by Friedrichs and Aubrey (1996): convex profiles are associated with tide-dominance and concave profiles with wave-dominance.

Apart from natural processes, human interventions such as dredging, dumping, sand mining and reclamation influence the estuarine bathymetry (Prandle, 2004) (Figure 3-1).

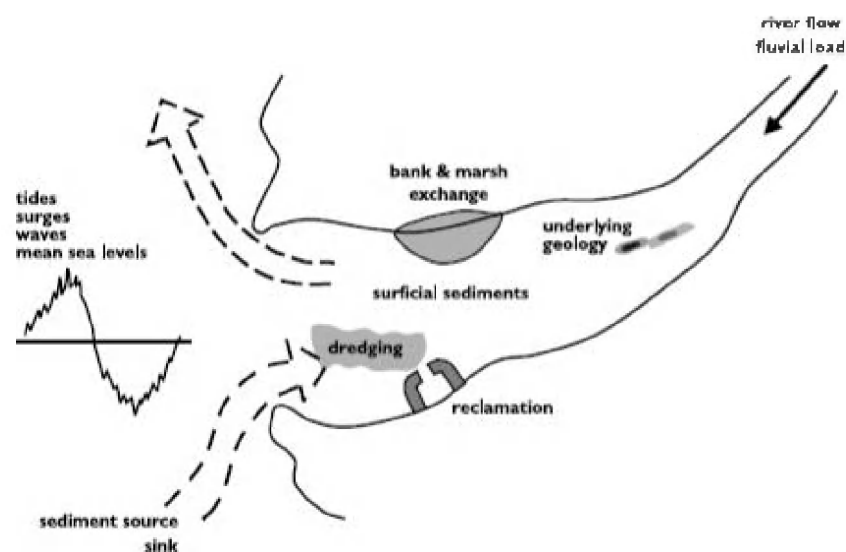


Figure 3-1: Schematic overview of factors influencing estuarine bathymetry (Prandle, 2004).

Since tidal inlets are openings in the coastline through which tides exchange water and sediment between the tidal basin and the open sea, they participate dynamically in the coastal tract due to the capacity to store (or release) large quantities of sand in the deltas (Cowell et al., 2003; Elias et al., 2006). As a result they influence the coastal sand balance. To evaluate this interaction, the residual sediment transport at the mouth has to be determined. The governing processes must be identified and understood to predict the future evolution of the estuary and the coastal sand resources.

3.2 Sand Balance

The morphological management of the Scheldt estuary is based on “integral sand-management” which aims at an optimal sand content and distribution in the Western Scheldt in support of a healthy and complete estuarine ecosystem (LTV, 2001). The Netherlands and Belgium determined in the long-term vision for the Scheldt estuary that the multiple channel system must be preserved since it is essential for the different functions of the estuary: accessibility, safety and natural environment (ibid.). For this management policy, a detailed insight is required into the sand transport in the estuary and how it is governed by the human interventions and natural processes. The sand balance is one tool to study this subject since sand volumes and main transport directions in the estuary can be derived from echo-sounding and intervention data.

3.2.1 General

A sand balance quantifies the erosion and sedimentation of sand under influence of the natural processes and interventions for all the different compartments covering the area of interest, including the sediment exchange between them. The balance is constructed from historical measurements of bottom depth and human interventions such as dredging, dumping, sand mining and suppletion (Jeuken et al., 2002).

Based on the echo-sounding and intervention data, the natural erosion or sedimentation of a compartment can be calculated as follows:

$$\Delta V_{nat} = \Delta V_{tot} - \Delta V_i \quad \text{Equation 3-1}$$

where ΔV_{tot} = the sediment volume change of a balance compartment based on the echo-sounding data (= the measured volume change)

ΔV_i = the net human induced volume change of the balance compartment (dredging, dumping, sand mining and suppletion)

ΔV_{nat} = the corrected or natural sediment volume change

Erosion and net dredging are included as negative values, sedimentation and net dumping as positive values (Nederbragt and Liek, 2004).

The accuracy of the sand balance is influenced by the precision of the bathymetry and the intervention data. Sources of errors related to the depth measurements are:

- the stochastic error (random)
- the systematic error (always the same influence)
- the variable systematic error (human errors)

The stochastic error varies depending on the location. Errors are typically higher in the mouth than on the river. This error decreases over the years as result of evolving measurement and processing techniques. When considering larger areas stochastic errors are balanced. The systematic error disappears when volume changes are calculated as long as the method has remained the same (Marijs and Parée, 2004).

Dredging, dumping and sand mining data introduce errors by the assumption of the conversion factor, the inaccuracies concerning the distribution of the volumes over different compartments and the errors in the reported volumes (Nederbragt and Liek, 2004). It is important to be aware of these errors, so that the sand balances can be interpreted correctly.

3.2.2 Western Scheldt Estuary

The borders of the compartments in both the Western Scheldt and its mouth are defined corresponding to the echo-sounding areas to simplify the synchronisation of data and to allow comparison with previous balances (Jeuken et al., 2002).

Since measurements are made year-round and spread over different locations, data must be synchronised in place and time. In previous studies 1 January of each calendar year has been chosen (Uit den Bogaard, 1995; De Jong, 2000; Nederbragt and Liek, 2004).

Uit den Bogaard (1995) considered two different synchronisation methods: linear interpolation between two consecutive measurements and interpolation based on linear trend lines. The latter method introduces subjectivity since sudden changes are flattened and erosion rates differ according to the considered period. Therefore Jeuken et al. (2002) advise to use the linear interpolation between two successive observations, which has been applied by Nederbragt and Liek (2004).

To determine the sediment exchange between different parts of the Western Scheldt, the morphological compartments are combined to macro-cells (Figure 3-2) and an assumption on one of the borders (for example the sediment exchange across the Dutch-Belgian border) has to be made. As a result the sediment exchange between the Western Scheldt and the mouth is obtained from:

$$S_{sb} = S_{lb} + \Delta V_{nat} \quad \text{Equation 3-2}$$

where S_{sb} = the sediment exchange at the seaward border of the Western Scheldt (between the estuary and the mouth)

S_{lb} = the sediment exchange at the landward border of the Western Scheldt (the Belgian-Dutch border)

ΔV_{nat} = the corrected or natural sediment volume change

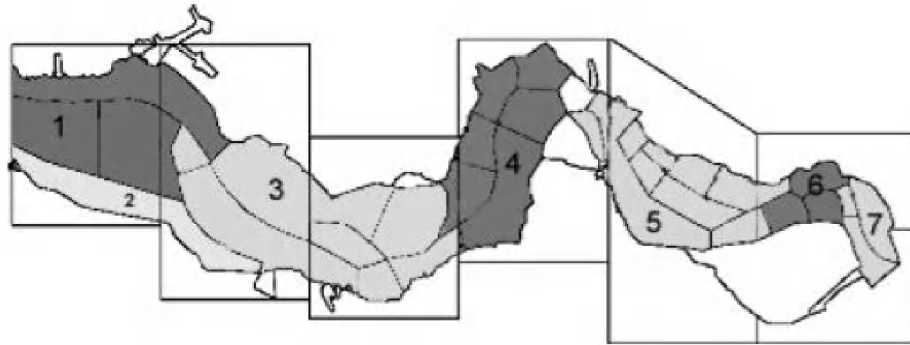


Figure 3-2: The aggregated morphological division of the Western Scheldt into meso (cell 2) and macro cells (rest). The numbers of the cells agree with the macro-cells from Figure 2-4. The rectangles represent the echo-sounding areas (after Nederbragt and Liek, 2004).

Sediment exchange between the different compartments in the mouth (Figure 3-3) can not be calculated since there are too many degrees of freedom because every compartment borders several others. By considering the entire mouth, it is possible to determine the sediment exchange of the Western Scheldt mouth with the Belgian coast, the North Sea, the Eastern Scheldt mouth and the Western Scheldt (Nederbragt and Liek, 2004).

The division in compartments is described in Appendix A.3.1.

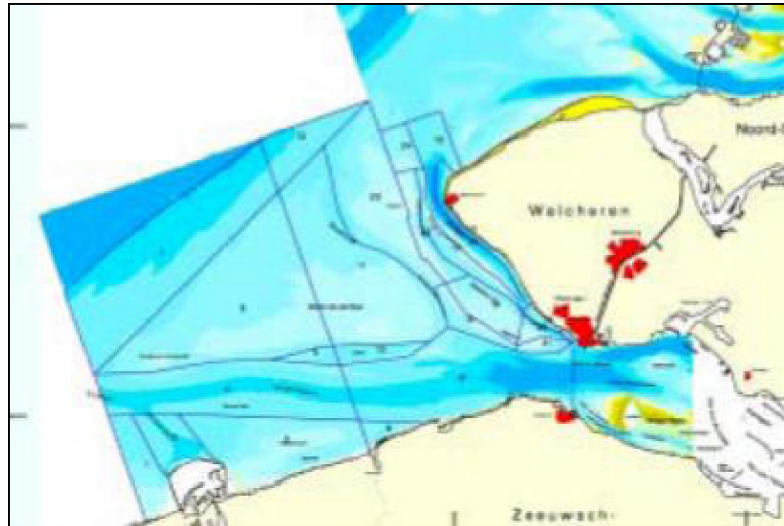


Figure 3-3: The aggregated morphological division of the Western Scheldt mouth (Nederbragt and Liek, 2004).

Results from Previous Studies

Nederbragt and Liek (2004) concluded from their sand balance study that since 1955 alternating periods with sand import and export occur. The Western Scheldt became exporting since the 90's from the previous century. On average, the export was $1.5 \text{ Mm}^3/\text{year}$ over the period 1990-2001. The sediment transport from the west to the east has increased since 1997. The Western Scheldt combined with the mouth also shows an exporting trend over the period 1990-1996.

Duin (2005) performed a trend analysis on the data from the sand balance from Walburg (2006). He found that both the Western and the Eastern Scheldt delta show a significant erosion trend (due to natural transports) over the period 1973-1997 of respectively 2.7 and $1.1 \text{ Mm}^3/\text{year}$.

Recently the sand balance of the Western Scheldt has been updated by Haecon (2006). They expanded the previously developed sand balance model of Nederbragt and Liek (2004) on the landward side with the Sea Scheldt to Rupelmonde and on the western side with the area between Zeebrugge and the Western Scheldt mouth. They included all data for the period 1955-2004. Their sand balance of the Sea Scheldt shows that the assumption in the previous balances of no transport across the Belgian-Dutch border is not valid.

Between 1955 and 2004 a yearly import in the Sea Scheldt of 1.1 million m^3 occurs, although there is a strong fluctuation (Figure 3-4). By considering the transport towards the Sea Scheldt the change from import to export near Vlissingen takes place several years later

(in 1997) compared to the previous balance (in 1990) (Figure 3-5). This agrees with the findings of Nederbragt and Lick (2004).

The results from these three sand balances are extensively described in Appendix A.3.2.

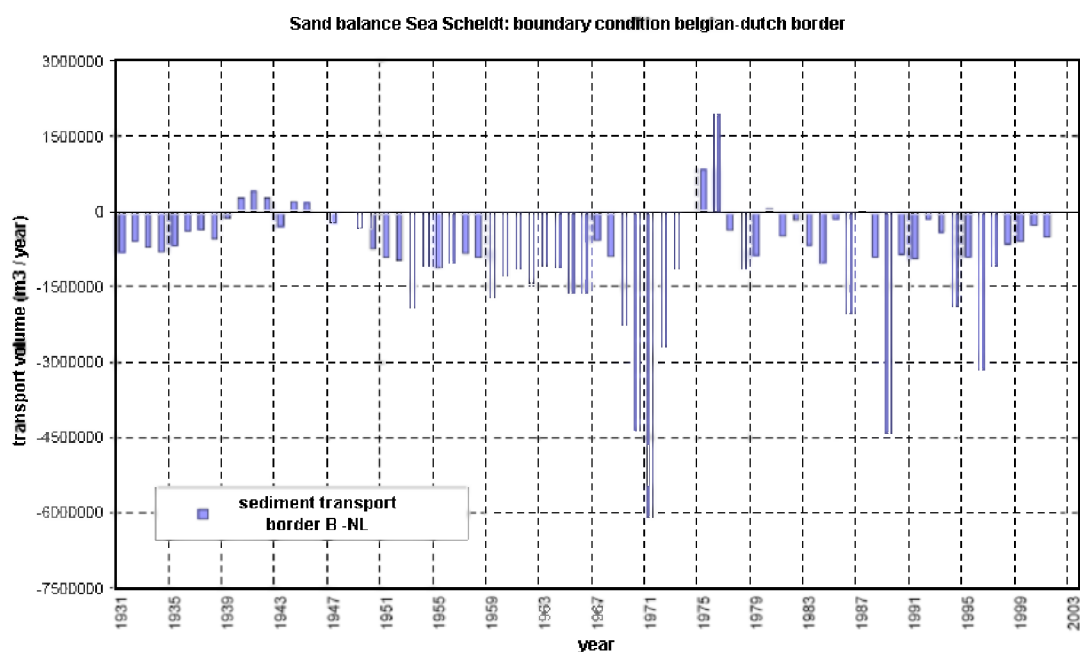


Figure 3-4: Sand balance of the Sea Scheldt: boundary condition at the Belgian-Dutch boundary (Assumption of no transport near Rupelmonde; - = transport towards Belgium) (Haecon, 2006).

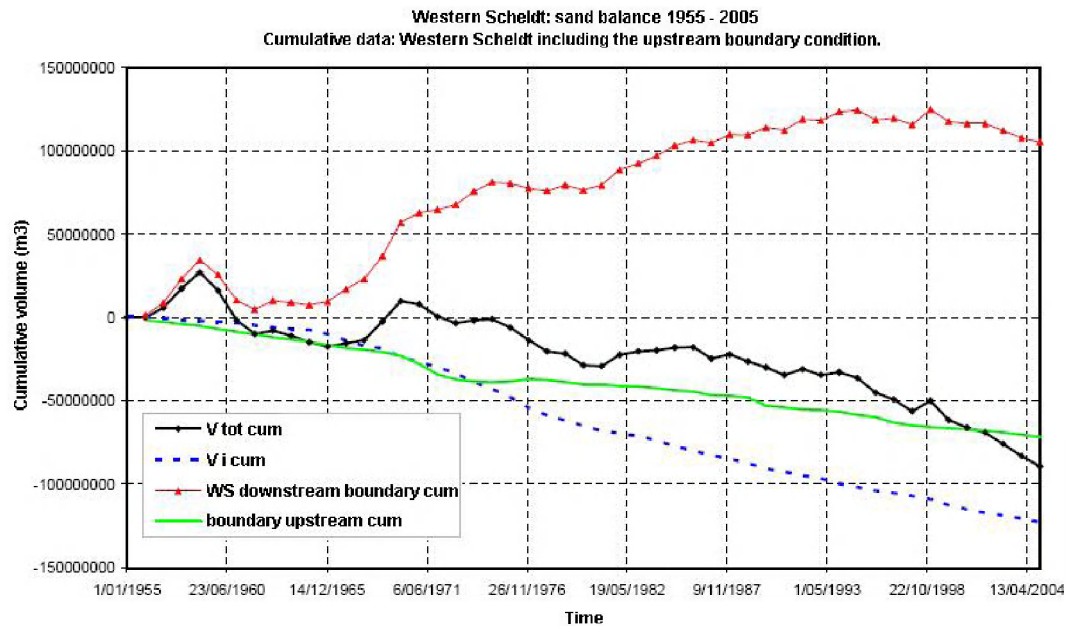


Figure 3-5: Cumulative sand volumes since 1955 in the Western Scheldt. (black line = total volume V_{tot} , blue dashed line = cumulative interventions V_i , green line = upstream boundary condition near the Belgian-Dutch boundary, red line = downstream boundary near Vlissingen). A descending green line means export from the Western Scheldt towards the Sea Scheldt or Saefthinge. A rising red line means import from the mouth towards the Western Scheldt (Haecon, 2006).

Reasons for the Change from Import to Export near Vlissingen

The import/export of sediment near Vlissingen is presumably a natural reaction of the estuarine system on a number of factors: the modified dumping strategy and the further deepening of the navigation channel by which the current and transport patterns can be influenced (Haecon, 2006).

Jeuken et al. (2004) suggest that the change from sand-importing to sand-exporting system has its origin in the western and central part of the Western Scheldt. An explanation for this change is yet unknown, but possibly the cut-off around 1950 of the channel bend in the central part (near Hansweert) and the displacement of the navigation channel from the ebb towards the flood channel around 1980 have influenced this process (Kuijper et al., 2004). The exchange may be further affected by the change in sand mining, dredging and dumping strategy since 1998 (Dauwe, 2001):

- dredging in both eastern and western parts of the Western Scheldt
- relocation of the sand mining activities from the western to the eastern part
- limitation of the dumping locations in the eastern part and expansion of the dumping locations in the western part

3.3 Tide-driven Sediment Transport

This section focusses on the sediment transport due to tidal asymmetry. Other transport mechanisms and the influence of different transport formulations are described in Appendix A.4.

3.3.1 Tidal Asymmetry

An important factor causing residual sediment transport in estuaries is tidal asymmetry. In the Western Scheldt it is possibly a principal factor influencing the sediment exchange between the ebb-tidal delta and the estuary, as well as between the various parts of the estuary (Wang et al., 1999).

3.3.1.1 Generating Mechanisms

The principal forcing factors of the water motion in well-mixed estuaries are:

- the astronomical tide
- the meteorological effects
- the river flow

The astronomical tide can be described in a number of harmonic components. Their frequency can be astronomically determined, their amplitude and phase vary from place to place. As astronomic tides propagate into estuaries, non-linear processes due to the interaction between the oscillating tide and the basin morphology generate high frequency harmonics. When these constituents grow, the tide becomes increasingly asymmetric (Friedrichs and Aubrey, 1988).

Tidal asymmetry can be interpreted in a number of ways. First of all distinction is made between the vertical and the horizontal tide. The vertical tide, which refers to the water level elevation, is called asymmetric when the flood period is unequal to the ebb period. If the period of water level rise is shorter than the period of water level fall, the tide is called flood-dominant and in the opposite case ebb-dominant.

The horizontal tide, referring to the flow velocity, is asymmetric when it generates residual sediment transport (which is the locally-averaged sediment transport within a tidal period). Two sub-types can be distinguished: the first is related to the difference between the ebb and

flood velocities, the second to the duration of the slack water. If the maximum flood velocity is higher than the maximum ebb velocity, residual transport of coarse sediments in the flood direction will occur. If the slack water before ebb is longer than the one before flood a residual transport of fine suspended sediments occurs in the flood direction. Both cases are called flood-dominant (Wang et al., 1999).

The tidal period can be defined in a variety of ways: for the vertical tide between two consecutive high or low waters; for the horizontal tide between two adjacent flood or ebb slack waters. This makes the tidal period variable from one tide to another. In most cases the period of the M_2 tidal constituent is used (Wang et al., 1999).

3.3.1.2 Horizontal Tide

Groen (1967) and Van de Kreeke and Robaczewska (1993) showed that not only the residual flow velocity but also the high-frequency harmonics of the flow can contribute to residual sediment transport.

The residual flow velocity in estuaries is influenced by:

- the upstream discharge
- the wind
- the tidally-induced horizontal circulation

Tides may generate residual currents through (Tee, 1976):

- the non-linear bottom friction
- the non-linear terms in the continuity equation
- the non-linear advection terms in the momentum equation

The 1D-equations for tidal motion in a channel with variable width are given in Appendix A.5.

Tidally induced residual flow is very sensitive to geometry and bathymetry, so only general principles and qualitative features are transferable between different cases (Zimmerman, 1978, 1980, 1981; Riderinkhof, 1988a, 1988b, 1989; Wang et al., 1999).

Li and O'Donnel (1998) explained the flood-dominance in relatively shallow parts and the ebb-dominance in relatively deep parts of the cross-section by using an analytical solution

of the residual current for a prismatic shallow estuary. They found that the inertia effect (the non-linear advection term) is the major source of geometry-induced residual circulation. The bathymetry-induced circulation is mostly caused by non-linear friction.

Van der Male (1993) and Vroon et al. (1997) found that eddies at the scale of the flood- and ebb channel systems and within wide channels dominate the pattern of the residual flow field in the Western Scheldt. The intensity of these bathymetry-induced residual circulations in the ebb and flood channels goes through a spring-neap tidal cycle (Wang et al., 1999).

3.3.1.3 Vertical Tide

The asymmetry of the vertical tide refers to the distortion of the semi-diurnal tide due to the overtides. The strength of the asymmetry depends on the ratio between the amplitude of the semi-diurnal tide and the overtides. The nature of the asymmetry (i.e. ebb- or flood-dominance) is determined by the phase difference. The vertical tide is called flood dominant if the relative phase is between 0° and 180° .

Speer et al. (1991) pointed out that the nature of the tidal asymmetry can be presented by the phase difference between the M_4 and M_2 constituents, since the relative phase-difference between the quarter-diurnal constituents and their semi-diurnal parent constituents is about the same for all constituents at the same station.

Boon (1988) concluded from his study of the temporal variation of tidal asymmetry that the mean values for the amplitude ratio (a_4/a_2) and the phase difference ($2\phi_2 - \phi_4$) found with the Fourier analysis of the tidal data are the same as when computed for the M_2 and M_4 tides only.

Since a tidal period is relatively short compared to the spring-neap cycle, all semi-diurnal constituents can be approximated as having the same frequency, and can be represented by a complex number with the amplitude as a modulus and the phase as a phase angle. The combined semi-diurnal tide can then be obtained by summing up all the constituents. By doing the same for the other tides, the tidal asymmetry can be obtained without producing a time series.

The tidal asymmetry inside the estuary is influenced by the asymmetry of the tide at the seaward boundary of the estuarine system (Dronkers, 1986, 1998; van der Spek, 1997). It is

likely that the asymmetry of the vertical tide at a certain station is influenced by the asymmetry of the tide in the section downstream (Wang et al., 2002).

The tidal asymmetry in the Western Scheldt changed over the last decades as can be seen in Figure 3-6. Apart from the amplitude ratio M_4/M_2 and the phase difference $2\varphi_2 - \varphi_4$ at each station, also the evolution between subsequent stations has been analysed. The change of the tidal asymmetry between two stations is represented by the amplitude and phase parameter:

$$\text{Amplitude parameter } A = \frac{\left(\frac{a_4}{a_2}\right)_{\text{station2}}}{\left(\frac{a_4}{a_2}\right)_{\text{station1}}}$$

$$\text{Phase parameter } P = (2\varphi_2 - \varphi_4)_{\text{station2}} - (2\varphi_2 - \varphi_4)_{\text{station1}}$$

where a_2 = the amplitude of the M_2 tidal component

a_4 = the amplitude of the M_4 tidal component

φ_2 = the phase of the M_2 tidal component

φ_4 = the phase of the M_4 tidal component

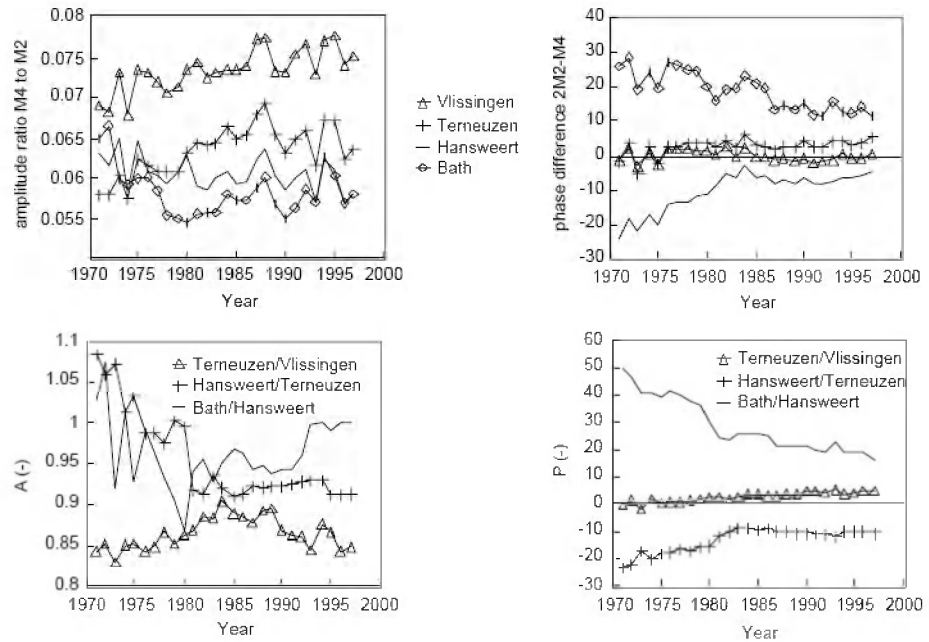


Figure 3-6: Changes of the asymmetry of the vertical tide over the period 1971-1996, based on water level measurements (Wang et al., 2002).

The largest alterations of the tidal asymmetry are observed at Hansweert and Bath with a small decrease in the respective slightly ebb-dominant and flood-dominant asymmetry of the vertical tide. The spatial variation is due to the increase of the M_2 tide towards the head of the Western Scheldt which is not followed by the M_4 (Wang et al., 2002).

3.3.1.4 Relation between the Asymmetry of the Horizontal and Vertical Tide

The continuity equation demonstrates the close relationship between the vertical and horizontal tide:

$$Q_1 - Q_2 = \int_{x_1}^{x_2} b(x, \zeta) \frac{\partial \zeta}{\partial t} dx \quad \text{Equation 3-3}$$

where Q_i = discharge at x_i
 b = storage width
 ζ = water level

Asymmetry in the vertical tide will cause asymmetry in the horizontal tide. However, it is a non-linear relationship since both storage width and cross-sectional area depend on the water level. As a result a flood-dominant duration asymmetry of the vertical tide is not necessarily associated with a flood-dominance of the tidal current.

In the Western Scheldt the hypsometric properties of the channel/shoal system tend to reinforce the asymmetry in the flow rates, whereas the asymmetry in the velocities is weakened (Wang et al., 1999).

The tidal asymmetry increases with the amplitude of the tide: the non-linear interactions are stronger during spring tide than during neap tide. Field measurements have shown that this applies to the Western Scheldt (Wang et al., 1999).

3.3.1.5 Interactions between Tidal Asymmetry, Morphology and Sediment Transport

In general there is a complex interaction between tidal asymmetry, morphology and sediment transport. Other factors such as sea level rise and the 18.6 year tidal cycle

complicate this relationship even further. Friedrichs et al. (1990) concluded that the reaction of an estuary to sea level rise depends on the local estuarine geometry.

Influence of the Morphology on Tidal Asymmetry

The influence of the geometry and bathymetry of short, friction-dominated and well-mixed estuaries has been studied by Speer and Aubrey (1985) and Friedrichs and Aubrey (1988) using 1D numerical models. They defined two parameters to characterise the tidal asymmetry in such an estuary (Figure 3-7):

- the ratio of the tidal amplitude and the mean water depth (a/h)
- the ratio of the volume of water stored between low and high water in tidal flats and marshes and the volume of water contained in the channels below mean sea level (V_s/V_c)

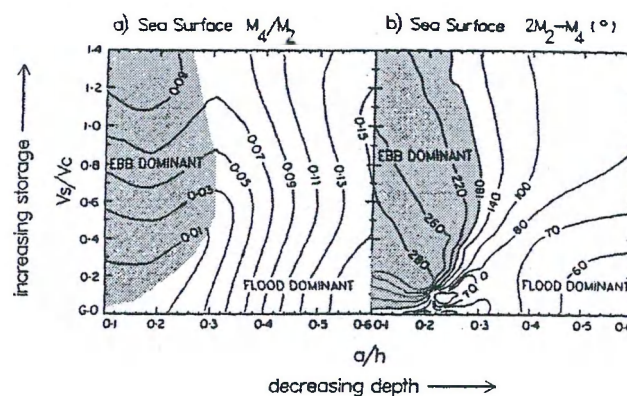


Figure 3-7: Contour plots of the parameters that determine nonlinear distortion as a function of a/h and V_s/V_c , resulting from 84 model systems. The 180° contour separates the plots into flood- and ebb-dominant regions (Friedrichs and Aubrey, 1988).

It has been shown in a number of previous studies that shallow systems tend to be flood-dominant, whereas deep tidal basins tend to be ebb-dominant (Dronkers, 1986; Friedrichs and Aubrey, 1988; Speer et al., 1991; Friedrichs et al., 1992; Wang et al., 2002).

Li and O'Donnell (1997) determined some additional parameters having an influence on the residual flow and tidal asymmetry:

- the ratio of the length of the estuary and the tidal wave length
- the ratio of the length scale of the morphological variation along the estuary and the tidal wave length
- the ratio of the tidal period and the decay time scale due to friction

Dronkers (1986, 1998) concluded that the intertidal area in the estuary is an important parameter. His findings qualitatively agree with those of Speer and Aubrey (1985).

The results from the analytical model of Fortunato and Oliveira (2005) confirm that tidal flats enhance ebb-dominance, whereas large tidal amplitudes promote flood-dominance. Maximum ebb-dominance occurs for tidal flats at or above mean water level, depending on the tidal amplitude and the extent of the tidal flats. They also proved qualitatively that friction enhances flood-dominance as stated before by Speer and Aubrey (1985) and Kang and Jun (2003).

Also Van Dongeren and De Vriend (1994) mentioned that large intertidal flat areas will decrease the flood velocities relative to ebb velocities. As a result the net landward sand transport will diminish and the basin becomes less flood-dominant when tidal flats expand as a result of sediment import. A total compensation of the flood-dominant transport by this mechanism is possible in theory, but not to be expected in reality since the sedimentation of mud, which is based on other processes, will continue and further infilling of the estuary will take place (Van den Berg et al., 1996).

Dronkers (1986) suggest that the aerial extent of the tidal flats in the present-day tidal basins in the Netherlands is too small to overcome the flood-dominance.

The deformation of the tidal wave during propagation through the estuary is a basic mechanism which generates tidal asymmetry since the propagation speed of low and high water will differ. Faster high water causes flood-dominance and faster low water generates ebb-dominance. This mechanism applies not only for short basins, but also for long estuaries such as the Western Scheldt (Wang et al., 2002).

The theory of Speer et al. (1991) has been evaluated for the Western Scheldt by Wang et al. (1999, 2002). Despite the different geometry of the considered systems (the Western Scheldt is long and relatively deep, in contrast to the short friction dominated estuaries considered by Speer) a qualitative agreement was found.

By considering the temporal changes of the tidal asymmetry (of the vertical tide) and the hypsometry, it has been shown that Speer's theory qualitatively explains the observed changes of the tidal asymmetry and morphology. Flood-dominance of the vertical tide is indeed associated with larger values of a/h and V_s/V_c compared to areas where ebb-dominant asymmetry prevails.

The parameter a/h seems to describe the changes due to dredging since 1971 near the head of the Western Scheldt estuary quite well. Therefore this theory could be used to assess the impact of human interference on the asymmetry of the vertical tide in a qualitative way.

Observations for the Western Scheldt indicate that the two morphological parameters a/h and V_s/V_c are mutually dependent. A possible set of independent parameters containing the same information is for example the ratio a/h and the ratio of the horizontal area of intertidal shoals to the total surface area F_f/F (Wang et al., 2002).

Influence of Tidal Asymmetry on Sediment Transport

Tidal asymmetry is important for the morphological development since it strongly influences the residual sediment transport. As mentioned before two main types of transport can be distinguished: bed-load and suspended load transport.

Van de Kreeke and Robaczewska (1993) described the effect of the asymmetry of the horizontal tide on the residual bed-load transport. Assuming that transport is in the form of bed-load (with the transport rate proportional to some power of the local current speed) and that the tidal current is dominated by the M_2 constituent, the long-term mean bed-load transport essentially depends on the residual flow velocity M_0 , the M_2 component and its even overtides (M_4 and M_6). The residual bed-load transport is in the direction of the largest current speed and the threshold of motion tends to enhance the effect of the velocity asymmetry.

Apart from this mechanism, suspended transport can also occur when there is no residual bed-load transport due to the relaxation effect in the sediment concentration as illustrated by Groen (1967). The residual transport will be in the flood direction if the high water slack is longer than the low water slack. Settling and scour lag effects have been described by Van Straaten and Kuenen (1957) and Postma (1970, 1981).

When tide gauge data and sediment transport relations are available, an indication whether tidal asymmetry needs to be considered as a mechanism for net sediment transport in an (shallow water) estuary can be obtained when the relationship between the tidal elevation and the velocity is known. The difference between linear and non-linear relationships has been studied by Fry and Aubrey (1990). The ratio of flood-to-ebb bed-load transport and its relation to an asymmetric elevation gave similar results for the linear and non-linear

relations because of the offsetting effects. Thus for a first estimate of the transport the linear relationship suffices

Bonekamp et al. (2002) used DELFT3D flow simulations in combination with the simple model of Groen (1967) (including the settling lag effect) for the concentration of sediments to model the sediment transport in the Texel inlet and compared their results with ADCP ferry measurements. Their study indicates that DELFT3D flow simulations are able to produce most of the qualitative features of the depth-averaged transport due to tidal asymmetries. Only near the inlet boundaries they found large deviations in transport. However the Groen model is too simplistic to derive the transport from the flow velocity.

4 Model Description

4.1 The Model

The two-dimensional, depth averaged hydrodynamic model of the Western Scheldt used in this study, has been derived from the Kustzuid model within the framework of the study “Long-term vision Scheldt estuary” (Winterwerp et al., 2000) as described by van der Kaaij et al. (2004). The utilised software is DELFT3D (WL|Delft Hydraulics, 2005).

The model includes the lower Sea Scheldt downstream from Rupelmonde, the Western Scheldt, and the Voordelta which is the Western Scheldt mouth region. A curvilinear grid has been applied (Figure 4-1). The dimensions from the grid cells vary between $800 \times 800 \text{ m}^2$ at the open sea to $150 \times 250 \text{ m}^2$ within the estuary. In this way a high computational efficiency is obtained by prescribing a high resolution in the area of interest, in combination with a low resolution far away at the open model boundaries (Kuijper et al., 2004).

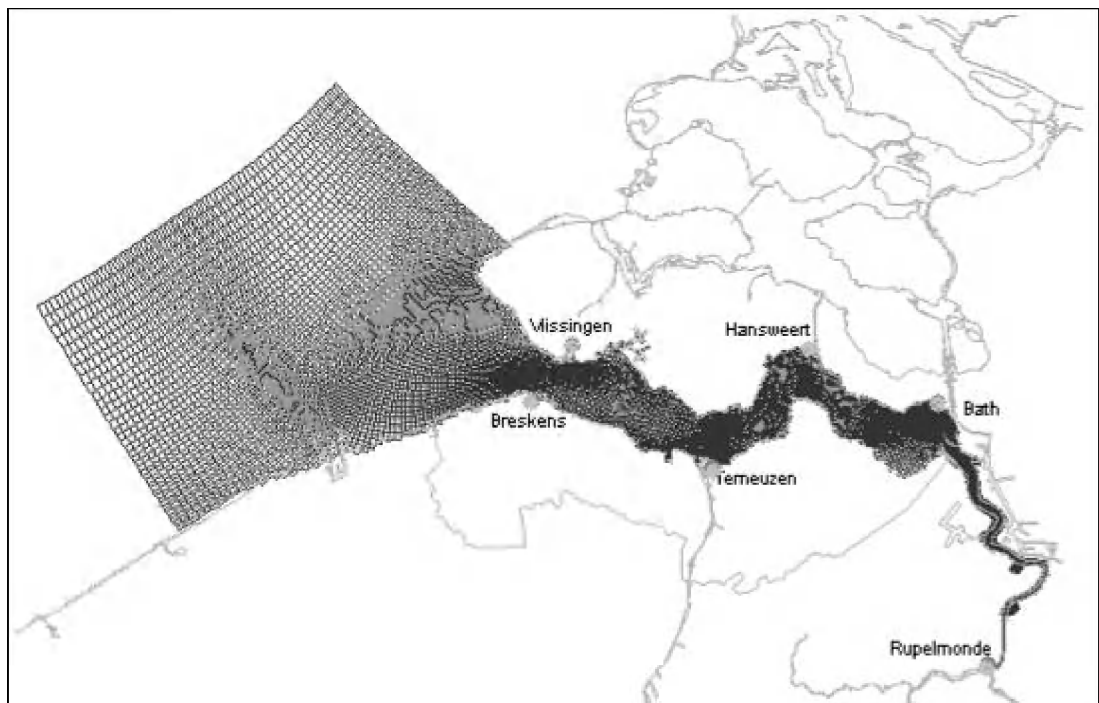


Figure 4-1: Morphologic, curvilinear grid of the Western Scheldt model in DELFT3D.

The open sea boundaries of the model are forced by means of Riemann boundary conditions, i.e. a combination of water levels and velocities. At the open river boundary near Rupelmonde discharges are prescribed. The bed friction is taken from the Scalwest model and is expressed as a Manning roughness with values varying between 0.02 and 0.04 s/m^{1/3} (Kuijper et al., 2004). The sediment grain size is taken uniform at 200 µm which is representative for the medium to fine sands in the Western Scheldt (Wang et al., 2002).

The calibration and verification of the hydrodynamic and morphodynamic model are described by van der Kaaij et al. (2004) and Kuijper et al. (2004). The calibration of the hydrodynamic model was carried out for the years 2000, 2001 and 2002 with the bathymetry of the year 2001. Water level, velocity and discharge measurements are used for the calibration over the period 19-21/06/2000. For the verification of this model the year 1972 was selected, which is during the first deepening of the navigation channel. The bathymetry was adapted to the 1972 situation and time series for the boundary signal at both the sea and river boundary were constructed based on tidal predictions. The roughness schematisation has been kept the same as during the calibration.

During the calibration of the morphodynamic model Kuijper et al. (2004) selected a morphological tide in such a way that during ebb and during flood the computed sediment transport through a cross-section near Vlissingen is similar to the average ebb and flood transport for a complete spring-neap tidal cycle. They found that the computed bed level changes were almost identical compared to the runs with an entire spring-neap cycle.

For a detailed description of the calibration and validation of the model reference is made to the above mentioned documents. An overview of the model specifications relevant for this study is given in Appendix A.6. Other specific properties will be mentioned later on in this report when relevant for the discussion of the model results.

4.2 Simulations

To investigate how the tidal asymmetry is influenced by changes in the bathymetry and which mechanisms determine the import or export of sediments in the Western Scheldt, simulations are performed with the DELFT3D model of the Western Scheldt with different bathymetries.

Because the ultimate aim of this study is the explanation of the import/export at the mouth, three bottoms have been selected based on the results of the sand balance study of Nederbragt and Liek (2004)¹ and the availability of digital data:

- 1970 before the first deepening => strong import
- 1983 after the first deepening => import
- 2002 after the second deepening => export

In this way three different regimes at the inlet are investigated. On Figure 4-2 which shows the cumulative sand volume in the Western Scheldt, the selected years are indicated, together with the periods of the first and second deepening.

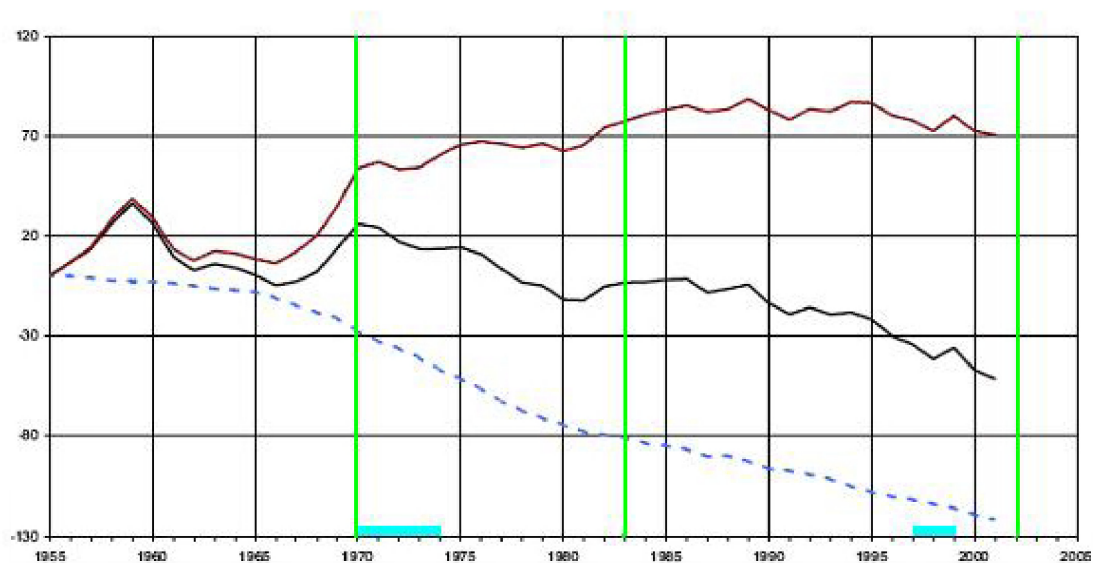


Figure 4-2: Cumulative sand volume (Mm^3) since 1955 in the Western Scheldt. Total volume V_{tot} (black line), cumulative interventions V_i (blue dashed line) and the natural volume V_{nat} . The green lines indicate the years chosen for the analysis. The light blue, thick lines indicate the periods of the first and second deepening (Adapted from Nederbragt and Liek, 2004).

¹ The study of Haecon (2006) was not available at the start of this project. However, similar characteristic periods are mentioned in their study.

The Western Scheldt model as described by Van der Kaaij et al. (2004) and Kuijper et al. (2004) is adapted to these three different situations by importing the respective bathymetry. The bathymetry for 2002 is shown on Figure 4-3, the bathymetry for the years 1970 and 1983 can be found in Appendix A.6. The sediment grain size (200 μm) and roughness schematisation (Manning: 0.02-0.04 $\text{s/m}^{1/3}$) are the same as in the original model for all the situations.

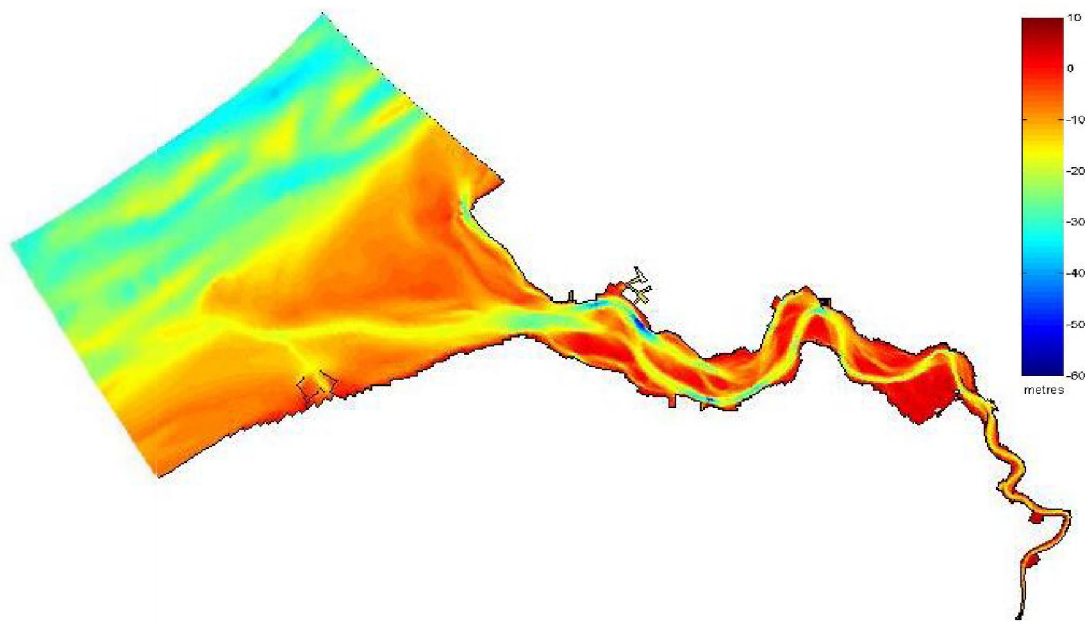


Figure 4-3: Bathymetry for the year 2002.

In all the simulations for this study the morphological tide with duration of 25 hours selected by Kuijper et al. (2004) is applied. As a result the boundary conditions both upstream and downstream are identical for the three years. For the seaward boundary this assumption is likely to be valid since no significant changes have occurred during this period in the North Sea (Kuijper et al., 2004). The main advantage of this approach is the opportunity to compare the results of the different years, only considering the changes of the bathymetry within the Western Scheldt. However, one must keep in mind this assumption, since Kornman et al. (2000) noticed an increase of the tidal range in the mouth of 4% per century. Also the upstream condition has possibly changed over the years; but no reliable data are available.

In all the model runs the simulation time step is 1 minute and a period of 5 days are simulated. To avoid the influence of the spin-up of the model, which is around 16 hours in

the present configuration, results from an entire tidal cycle (ebb-flood) at the end of this period are selected for the analysis.

Observation points and cross-sections have been chosen to monitor the water level, the velocity, the discharge and the sediment transport. Time series with time step 10 minutes are available in all these points. The output of vector quantities can be chosen according to the orientation of the curvilinear grid or according to the x-y coordinate system. The conventions concerning the sign of these parameters and the orientation of the curvilinear grid along the estuary is described in Appendix A.6.

Two main types of model simulations can be distinguished: with and without sediment transport. When only the evolution of the tidal asymmetry is investigated, no sediment transport is simulated. These model results are analysed in chapter 5.

When sediment transport is included, two different transport formulations are used: Engelund Hansen (1967) and Van Rijn (2003). The Engelund Hansen formula only gives the total load and is proportional to a power of the flow velocity.

With the Van Rijn (2003) approach in DELFT3D distinction can be made between bed-load and suspended load. Bed-load transport is calculated for all “sand” sediment fractions by broadly following the approach described by Van Rijn (1993, 2000). It accounts for the near-bed sediment transport occurring below a defined reference height (WL|Delft Hydraulics, 2005). The transport of suspended sediment is calculated by solving the three-dimensional advection-diffusion (mass-balance) equation for the suspended sediment (ibid.). The model results with sediment transport are used in chapter 6.

5 Tidal Asymmetry

The tidal asymmetry is an important factor for the generation of residual transport in estuaries. In the Western Scheldt this is possibly a principal factor influencing the sediment exchange between the ebb-tidal delta and the estuary (Wang et al., 1999). Since field data about the horizontal tide are scarce and limited in time, this will be investigated by means of a numerical model.

As a first step the vertical tidal asymmetry derived from the model is compared with field measurements, which gives an indication of the applicability of the model for this research. Next the effect of a modified bathymetry on the tidal asymmetry is examined.

5.1 Applicability of the Model

5.1.1 Method

Along the Western Scheldt water levels are being measured since 1885. For the stations Westkapelle, Cadzand, Vlissingen, Terneuzen, Hansweert and Bath, time series with a sampling interval of 1 hour (until 1987) and 10 minutes (since 1987) are available from 1971 onwards. The observations over the period 1971-1997 were analysed by the Ministry of Transport, Public Works and Water Management. They determined 94 harmonic components for each year of measurements. The results of the harmonic analysis over this period were used by Wang et al. (2002) to quantify the annual changes of the asymmetry of the vertical tide in the Western Scheldt.

Hereafter, the tidal asymmetry derived from the model results with the bathymetry of the years 1970, 1983 and 2002 are compared with the asymmetry derived from the measured water levels. For the comparison, observation points are selected in the model at the locations of the measurement stations (Figure 5-1). In these points, time series of the water level are available, which are harmonically analysed in terms of the amplitudes and phases of the tidal constituents M_2 , M_4 and M_6 . The differences between the computed and measured amplitudes and phases quantify the model performance with respect to the reproduction of the tidal asymmetry.

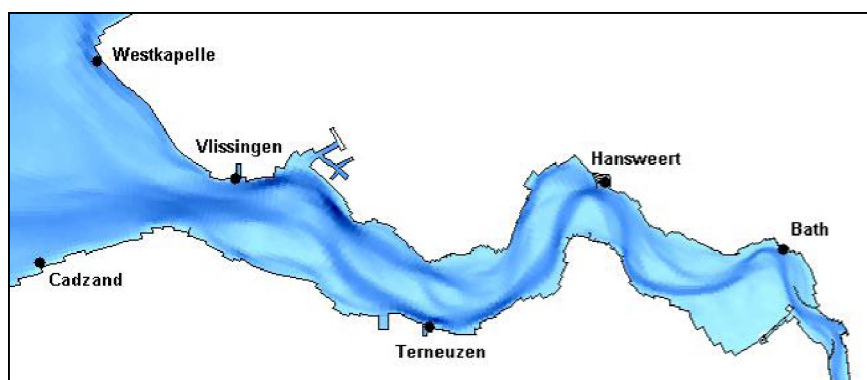


Figure 5-1: Location of the measurement stations for the water levels.

5.1.2 Results

To start with the amplitude and phase of the M_2 , M_4 and M_6 tidal components are compared at the stations Westkapelle, Cadzand, Vlissingen, Terneuzen, Hansweert and Bath. Table 5-1 gives an overview of the deviations of the model results from the field data.

Table 5-1: Average deviation of amplitude and phase from M_2 , M_4 and M_6 derived from the model results from the field data.

	Average Deviation from Field Data			
	Recent Model Results (average of the years 1970, 1983 & 2002)		Average of the Calibration (2000) and Validation (1972) of the Original Model	
Amplitude (m)	entire estuary		entire estuary	
M_2	0.03		0.05	
M_4	0.03		0.02	
M_6	0.10		0.04	
Phase φ (degrees)	downstream	upstream	downstream	upstream
M_2	1	10	1	10
M_4	3	25	10	20
M_6	5	5	5	5

The amplitude of M_2 , the most important tidal constituent in the Western Scheldt, is accurately represented in the model. The deviation is 3 to 5 cm, which is 2 to 3 percent of the amplitude. Table 5-2 gives an example of the amplitudes and phases in the different stations. The other years are given in Appendix A.7.2. Considering the phase of M_2 , the model results show an increasing phase difference upstream in the estuary. The accuracy of

M_4 is comparable for the recent and original model results. Whereas the phase of M_6 is well represented, the amplitude is less accurate in the recent model.

The differences between the recent model results and the measurements are mainly caused by the applied forcing schematisation in the model. A morphological tide is used, which is selected based on optimal correspondence between measured and modelled sedimentation and erosion patterns. Although the morphological tide closely represents the tidal characteristics it is not necessarily the ‘optimal’ representation. The morphological tide does not contain all the different constituents present in reality, and can therefore not be expected to generate exactly the same results. However, as already mentioned above, there is a rather good agreement, especially for the M_2 constituent.

Table 5-2: Comparison of the amplitudes (absolute) and phases (relative to Cadzand) for the M_2 , M_4 and M_6 constituents derived from the measurements and the model results for the year 1983.

1983		Cad-zand	West-kapelle	Vlis-singen	Terneu-zen	Hans-weert	Bath
observa-tions M_2	amplitude (m)	1,68	1,53	1,75	1,87	1,99	2,10
	$\Delta\phi$ (°)	0	4	10	19	30	44
model results M_2	amplitude (m)	1,70	1,55	1,74	1,86	1,96	2,06
	$\Delta\phi$ (°)	0	4	10	21	34	53
observa-tions M_4	amplitude (m)	0,12	0,13	0,13	0,12	0,12	0,12
	$\Delta\phi$ (°)	0	4	27	42	73	76
model results M_4	amplitude (m)	0,15	0,17	0,15	0,14	0,13	0,15
	$\Delta\phi$ (°)	0	6	27	41	87	89
observa-tions M_6	amplitude (m)	0,10	0,09	0,09	0,09	0,10	0,12
	$\Delta\phi$ (°)	0	6	33	76	128	181
model results M_6	amplitude (m)	0,20	0,18	0,18	0,21	0,23	0,20
	$\Delta\phi$ (°)	0	4	38	87	136	187
$\Delta\phi$ is expressed relative to Cadzand.							

More important than absolute values is the model ability to reproduce the relative changes in time. Therefore amplitudes and phases derived from observations and recent model results have been expressed relative to the 2000 (respectively 2002) situation. In this way it is possible to compare the trend in the parameters. A rising line shows an increase of the respective value, whereas a descending line indicates a decrease.

The results for the amplitude and phase of the M_2 constituent are presented in Figures 5-2 to 5-5. For both amplitude and phase it is visible that in the model there is almost no change in

the most seaward located stations (i.e. Westkapelle, Cadzand and Vlissingen). This is logical since for the three different years identical boundary conditions are used. However it is important to be aware of this assumption, because the observations indicate somewhat larger deviations.

More upstream in the estuary (Terneuzen, Hansweert and Bath) the graphs show that the trend in the parameters is well represented in the model (except for the phase in Hansweert).

Similar comparisons are made for the amplitudes and phases of M_4 and M_6 (Appendix A.7.1). The relative change in amplitude for the M_4 component shows not that much agreement; the trends for the amplitude of M_6 are better represented. Concerning the phases, trends come out well in general, with exception from the station Hansweert.

The irregularities at Hansweert are a common problem for all parameters. Two possible causes can be thought of: limitations in the model (the limited information in the morphological tide for example) or the particular location of the measurement station.

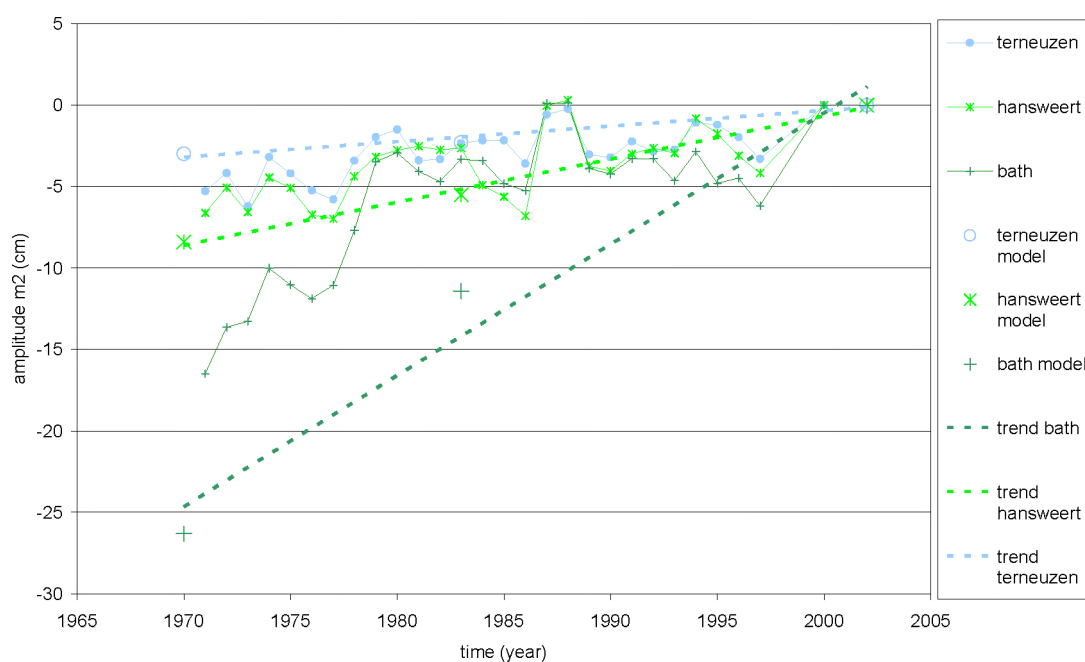


Figure 5-2: Comparison of the amplitude of the M_2 tidal constituent derived from the model (relative to 2002) with the measurements (relative to 2000) at the stations Terneuzen, Hansweert and Bath.

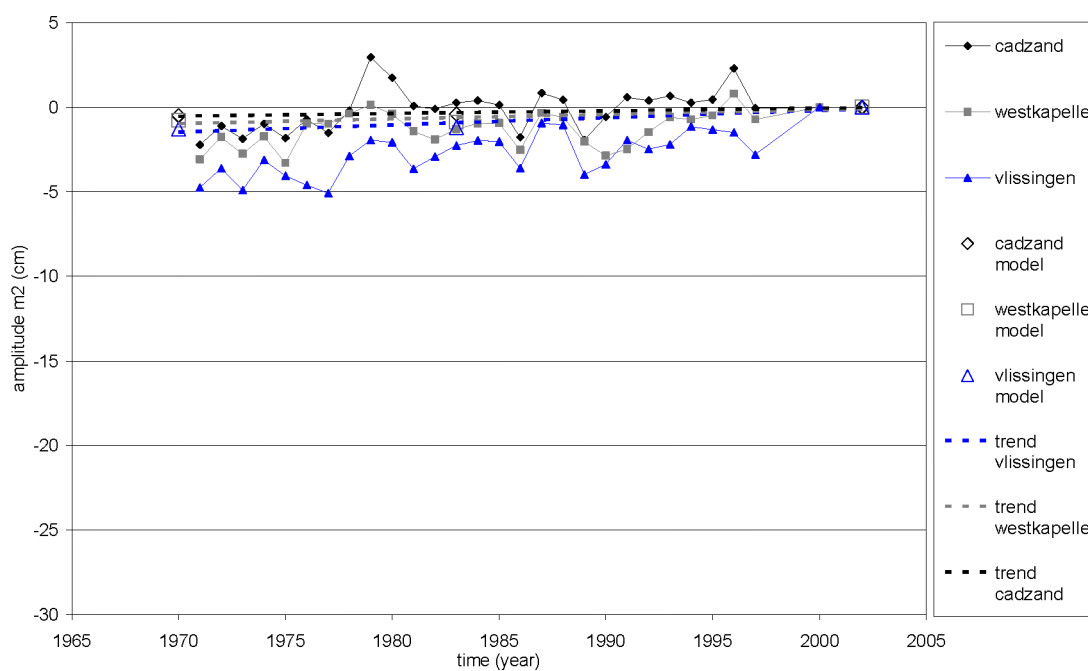


Figure 5-3: Comparison of the amplitude of the M₂ tidal constituent derived from the model (relative to 2002) with the measurements (relative to 2000) at the stations Westkapelle, Cadzand and Vlissingen.

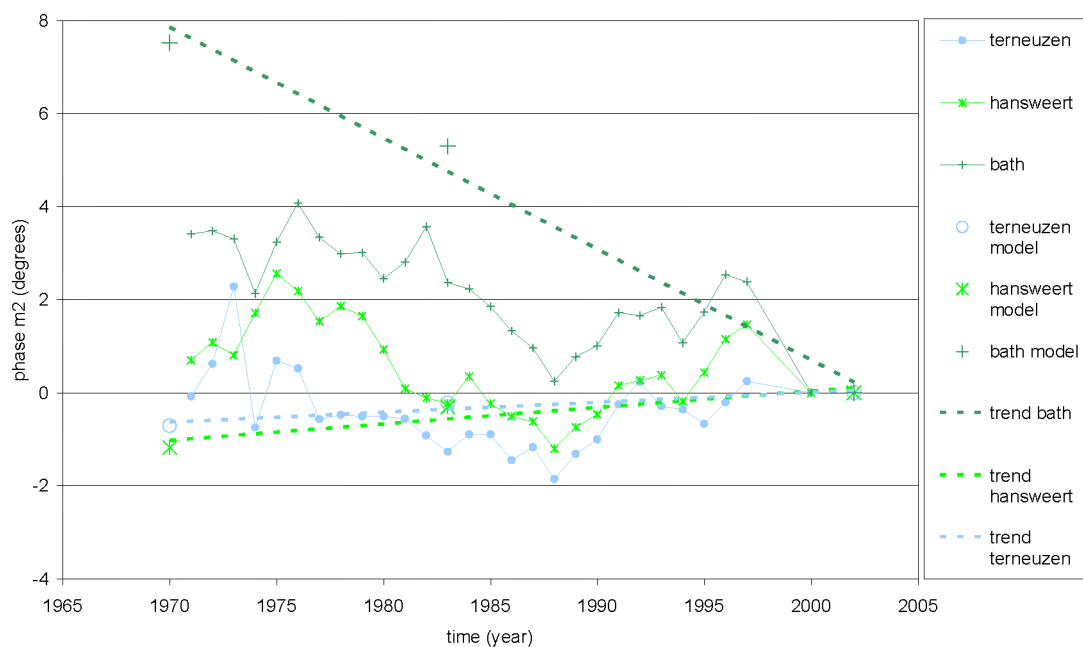


Figure 5-4: Comparison of the phase of the M₂ tidal constituent derived from the model (relative to 2002) with the measurements (relative to 2000) at the stations Terneuzen, Hansweert and Bath.

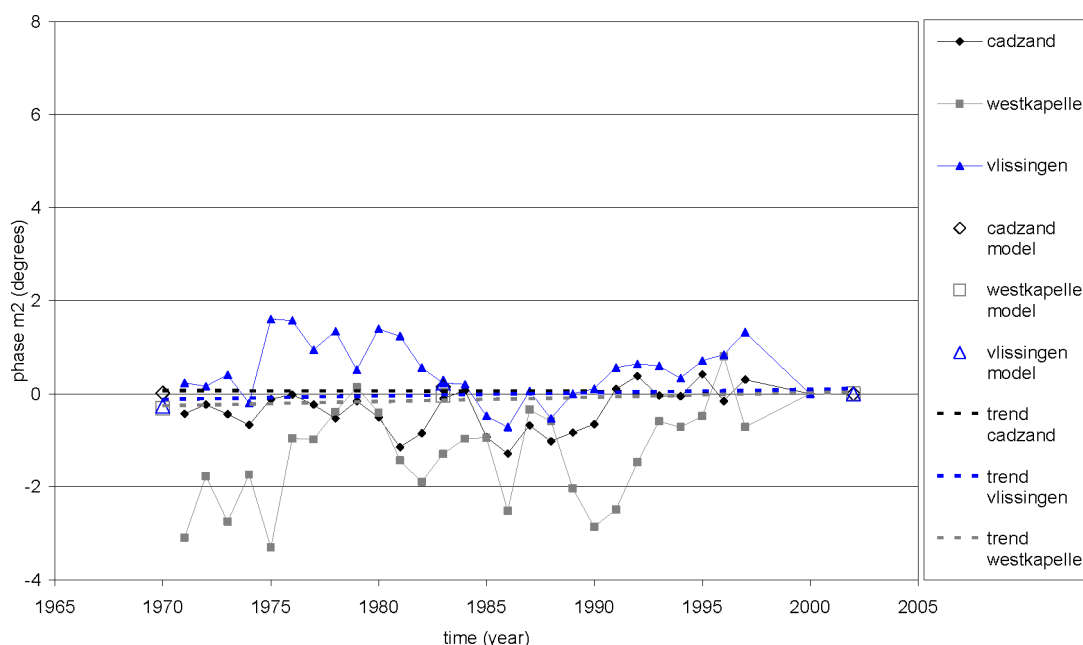


Figure 5-5: Comparison of the phase of the M_2 tidal constituent derived from the model (relative to 2002) with the measurements (relative to 2000) at the stations Westkapelle, Cadzand and Vlissingen.

The tidal asymmetry in the Western Scheldt can be described according to Wang et al. (2002) by:

- the amplitude ratio M_4/M_2 which determines the strength of the asymmetry
- the phase difference $2\phi_2 - \phi_4$ which indicates the flood or ebb-dominance (for a positive respective negative difference, i.e. flood dominant if the relative phase is between 0° and 180°)

Similarly, the relation between the M_2 and M_6 tidal constituents are expressed with the amplitude ratio M_6/M_2 and the phase difference $3\phi_2 - \phi_6$.

For every station the relative differences of these parameters between observations and model results are calculated. (Figures 5-6 to 5-9). The trend of these parameters over the years is in general well represented, although in some cases the trend is more pronounced in the model. Only for the station Hansweert (and the amplitude of M_4 in Terneuzen for 1970), large differences occur. This was to be expected, since differences already came out for the individual quantities as described earlier. Here again, the change is smaller downstream. These graphs are given in Appendix A.7.1.

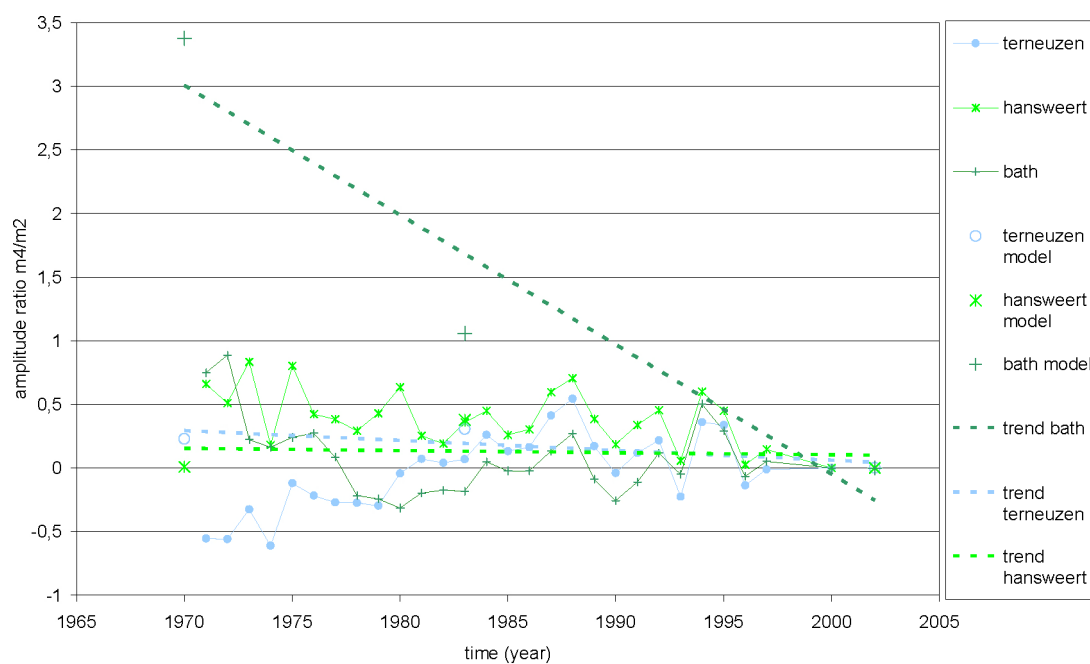


Figure 5-6: Comparison of the phase of the amplitude ratio M_4/M_2 derived from the model (relative to 2002) with the measurements (relative to 2000) at the stations Terneuzen, Hansweert and Bath.

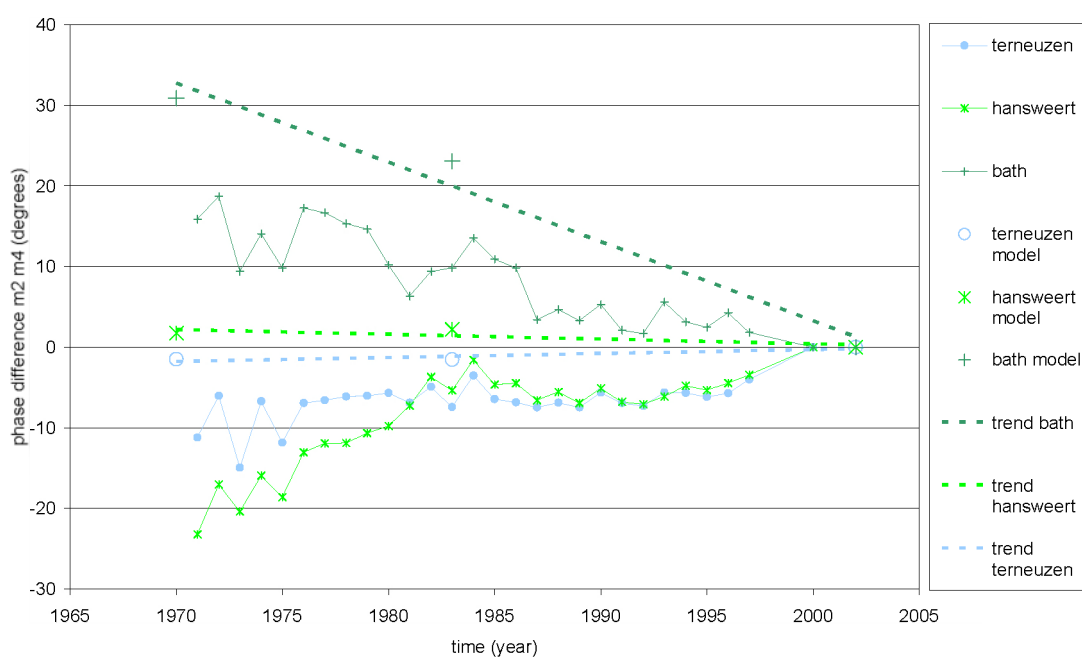


Figure 5-7: Comparison of the phase of phase difference $2\phi_2 - \phi_4$ derived from the model (relative to 2002) with the measurements (relative to 2000) at the stations Terneuzen, Hansweert and Bath.

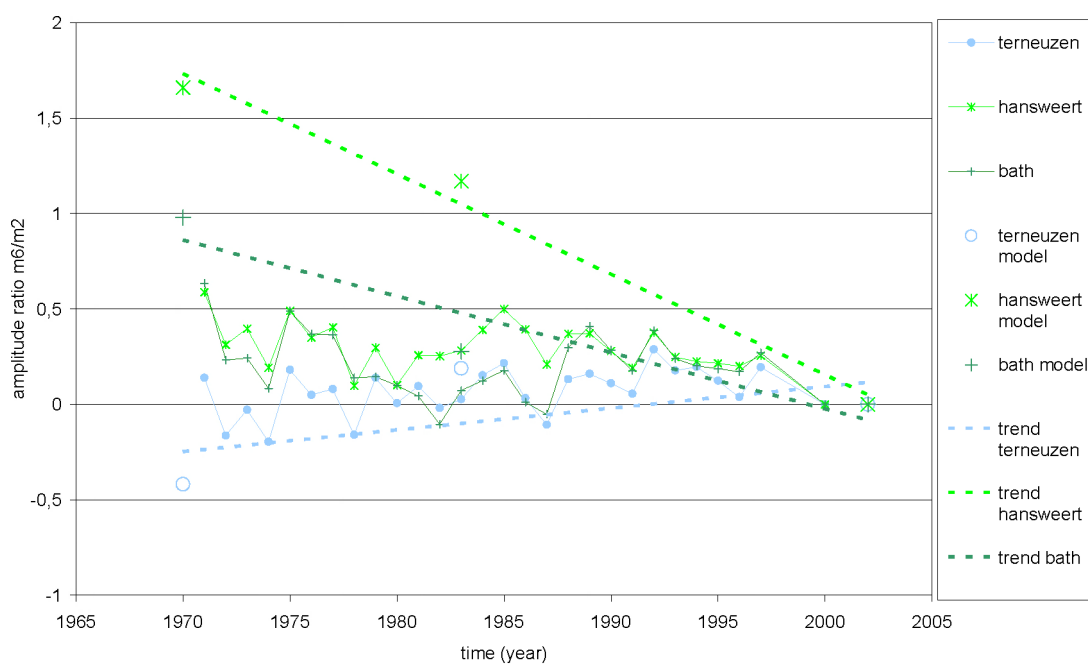


Figure 5-8: Comparison of the phase of the amplitude ratio M_6/M_2 derived from the model (relative to 2002) with the measurements (relative to 2000) at the stations Terneuzen, Hansweert and Bath.

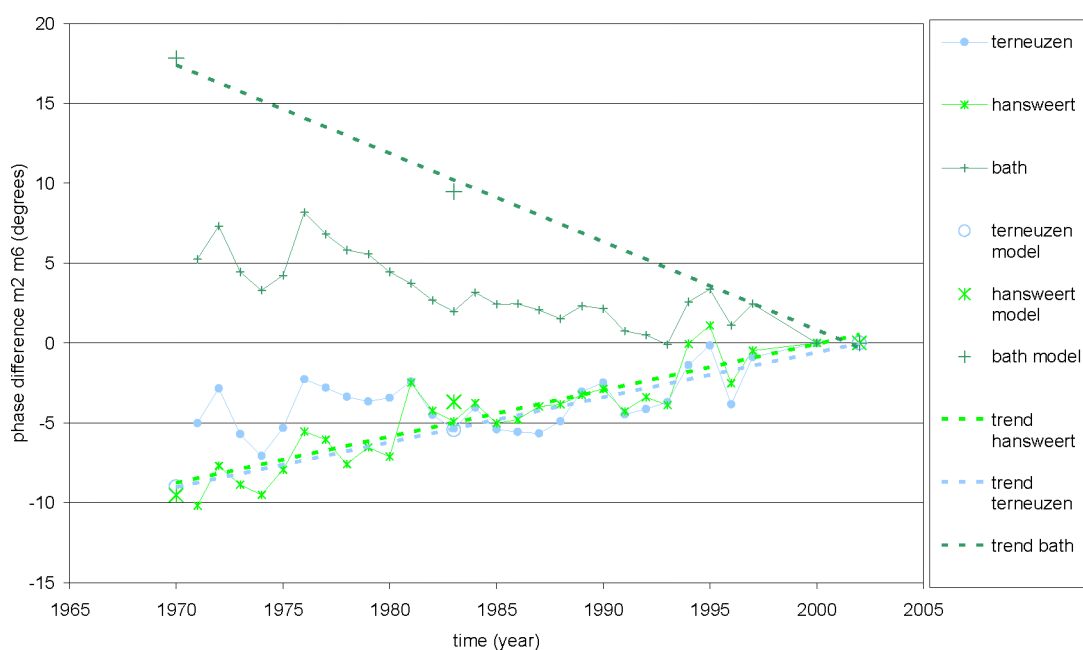


Figure 5-9: Comparison of the phase of phase difference $3\phi_2 - \phi_6$ derived from the model (relative to 2002) with the measurements (relative to 2000) at the stations Terneuzen, Hansweert and Bath.

5.1.3 Conclusions

The model in the present configuration has been set-up in such a way that simulations for the study of the interaction between tide and bathymetry can be run within a reasonable time. Using the morphological tide selected by Kuijper et al. (2004) a representative situation (of 5 days) can be simulated within one night.

The choice of identical boundary conditions for the three years is made to assess the influence of bathymetric change on tidal propagation characteristics and tidal sediment transport patterns. However the schematisation of the boundaries results in an underestimated evolution of the modelled phases and amplitudes of the tidal constituents compared to the observed phases and amplitudes.

On the other hand, the evolution of the amplitude ratios and phase differences within the estuary which describe the strength of the asymmetry and the ebb- or flood-dominance, are well represented. The discrepancy for the station Hansweert could be caused by limitations of the model, but also by the particular location of the measurement station.

Eventhough there are some limitations, the DELFT3D model of the Western Scheldt provides a unique tool to study the influence of the bathymetry on the tidal characteristics and the sediment transport. The trends in the different parameters describing the tidal asymmetry are reproduced well enough to give confidence in the model results and to be able to compare them with other related data.

5.2 Vertical Tidal Asymmetry

Although analysis of the horizontal tidal asymmetry might provide a direct relation to sediment transport, valuable information of the deformation of the tide within the estuary can be obtained by the analysis of the vertical tidal asymmetry. In this section, the evolution of the vertical asymmetry along the estuary is studied and linked to bottom changes. In a following chapter the evolution of the horizontal tidal asymmetry is investigated.

5.2.1 Method

The tidal asymmetry derived from the model results with the bathymetry of the years 1970, 1983 and 2002 are compared. Observation points along the ebb and flood channels were selected in the model (respectively 62 and 53 points) (Figure 5-10). The water level time series at each observation point are harmonically analysed in terms of the amplitudes and phases of the tidal constituents M_2 , M_4 and M_6 . With these results, the amplitude ratios M_4/M_2 and M_6/M_2 , and the phase differences $2\phi_2 - \phi_4$ and $3\phi_2 - \phi_6$ are calculated. In this way the evolution of these tidal characteristics within the estuary and the influence of different bathymetries can be examined.

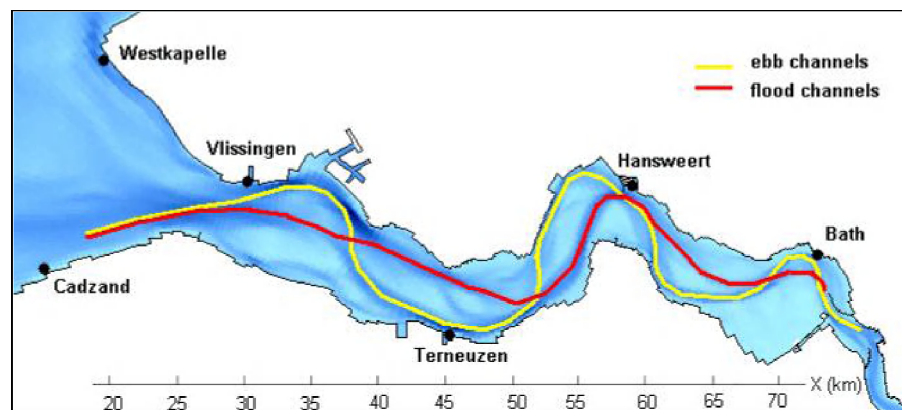


Figure 5-10: Location of the lines of observation points in the model along the ebb and flood channels.

5.2.2 Results

The evolution of the vertical tide within the estuary is presented for the M_2 , M_4 and M_6 constituent on a number of graphs. Each graph compares the years 1970, 1983 and 2002, and shows the evolution within the estuary. The horizontal axis of the graphs agrees with the coordinates of the observation points, expressed on a length scale which is west-east

directed. Table 5-3 gives the position of a number of stations and the locations where ebb and flood channels meet. The same length scale is shown on Figure 5-10.

Table 5-3: Location of the measurement stations and the crossings of the ebb and flood channels.

	Location	Distance (km)
Measurement Station	Vlissingen	30
	Terneuzen	46
	Hansweert	59
	Walsoorden	61
	Bath	73
Crossing ebb and flood channel	Drempel van Borsele	38
	Ebschaar Everingen / Straatje van Willem	52
	Bocht van Hansweert	59
	Drempel van Valkenisse	69

Amplitude and Phase

The evolution of the amplitude of the M_2 , M_4 and M_6 constituent along the ebb and flood channels is shown in respectively Figure 5-11 and 5-12. The amplitude of M_2 is continuously increasing except for the year 1970, where it starts decreasing upstream from Walsoorden (km 61). This is a shortcoming of the model and doesn't represent the historical situation.

By comparing the different years, it becomes clear that the M_2 amplitude increased along the entire estuary over the years. This increase becomes larger upstream. The highest difference (0.15 m) between 1970 and 1983 is found upstream from Hansweert. In this part the change between 1983 and 2002 is in the same order of magnitude, whereas between Terneuzen and Hansweert the amplification of the amplitude is much larger than before 1983 (0.04 vs. 0.02 m). The abrupt jumps in the curves are located at the crossings of the ebb and flood channels.

The M_4 amplitude shows a different development. It slightly increases from 0.15 to 0.16 m towards Vlissingen (km 30) in the ebb channel, and towards the 'Drempel van Borsele' (km 38) in the flood channel. Then the M_4 amplitude decreases towards a local minimum in Hansweert (from 0.16 to 0.12 m), increasing again further upstream. This last increase

differs heavily from the considered bottom: the M_4 amplitude becomes 0.18, 0.15 and 0.14 m near Bath in respectively the year 1970, 1983 and 2002. Only in the most upstream part there is a continuing decrease in time. In the central part the highest values for the M_4 amplitude are found for 1983 and the lowest for 2002. In the most western part near Vlissingen there is little difference between the three years.

The amplitude of M_6 increases till Walsoorden (km 61) in the ebb channel and till the ‘Drempel van Valkenisse’ in the flood channel (km 69) (from 0.18 to 0.24 m). A remarkable evolution is the decrease between 1970 and 2002 east of km 53 (respectively 55) in the ebb (flood) channel and the increase west from Terneuzen. In the middle, the amplitude is temporarily higher in 1983.

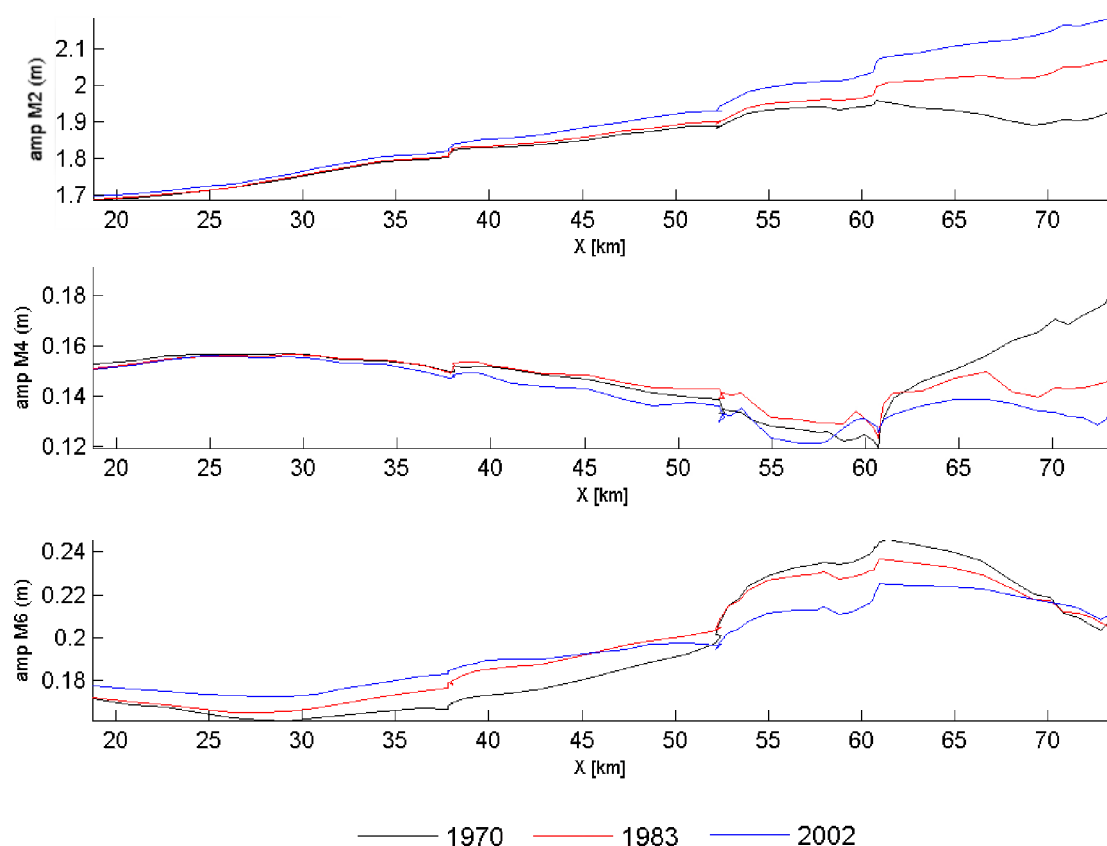


Figure 5-11: Evolution of the amplitude of M_2 , M_4 and M_6 along the ebb channels in the Western Scheldt.

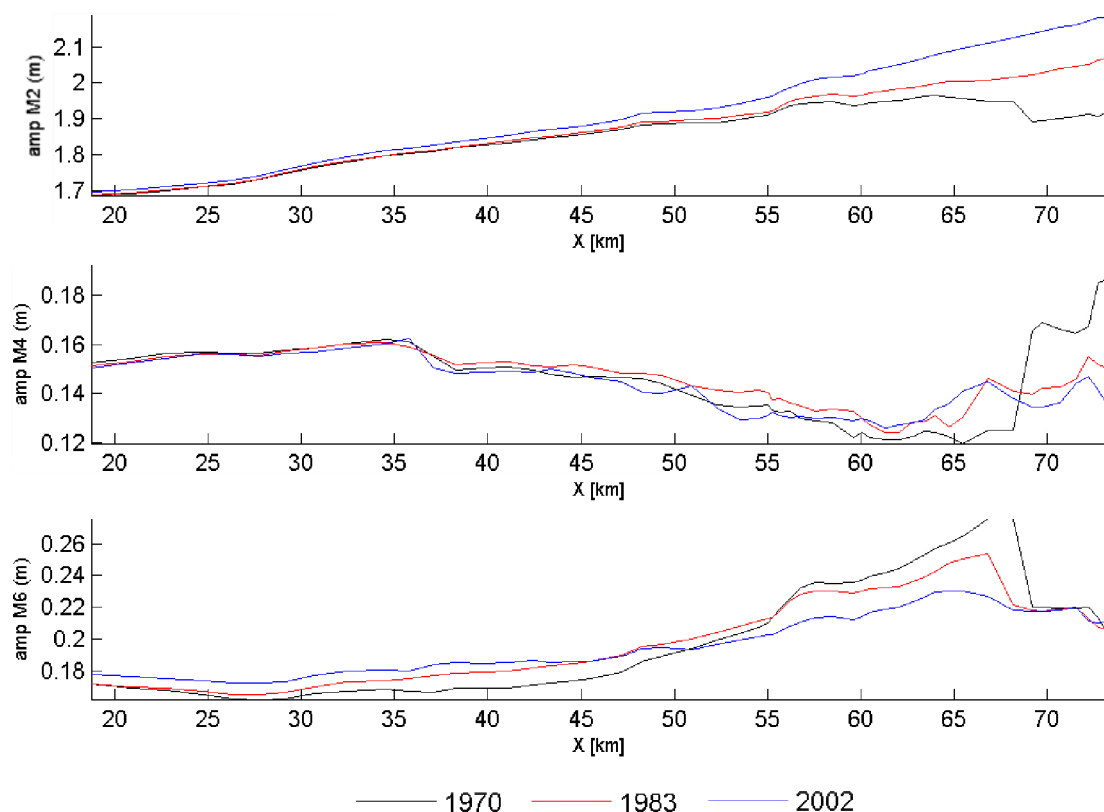


Figure 5-12: Evolution of the amplitude of M_2 , M_4 and M_6 along the flood channels in the Western Scheldt.

The change of the phase of the M_2 , M_4 and M_6 tidal components within the estuary is presented in Figures 5-13 and 5-14. The magnitude is expressed relative to the most seaward observation point. All constituents increase along the estuary. From the most seaward point to Bath an increase with 45° of φ_2 is noticed, 70 to 80° for φ_4 and slightly more than 180° for φ_6 . West of the ‘Ebschaar van Everingen’ the difference between the three years is smaller than east of this point. φ_2 decreases with 8° from 1970 to 2002 near Bath. Conversely φ_4 increases with 16° in this area. The increase of φ_4 near Hansweert is smaller, around 4° . The phase of φ_6 decreases slightly with 5° . In all these cases the change between 1983 and 2002 is larger than between 1970 and 1983.

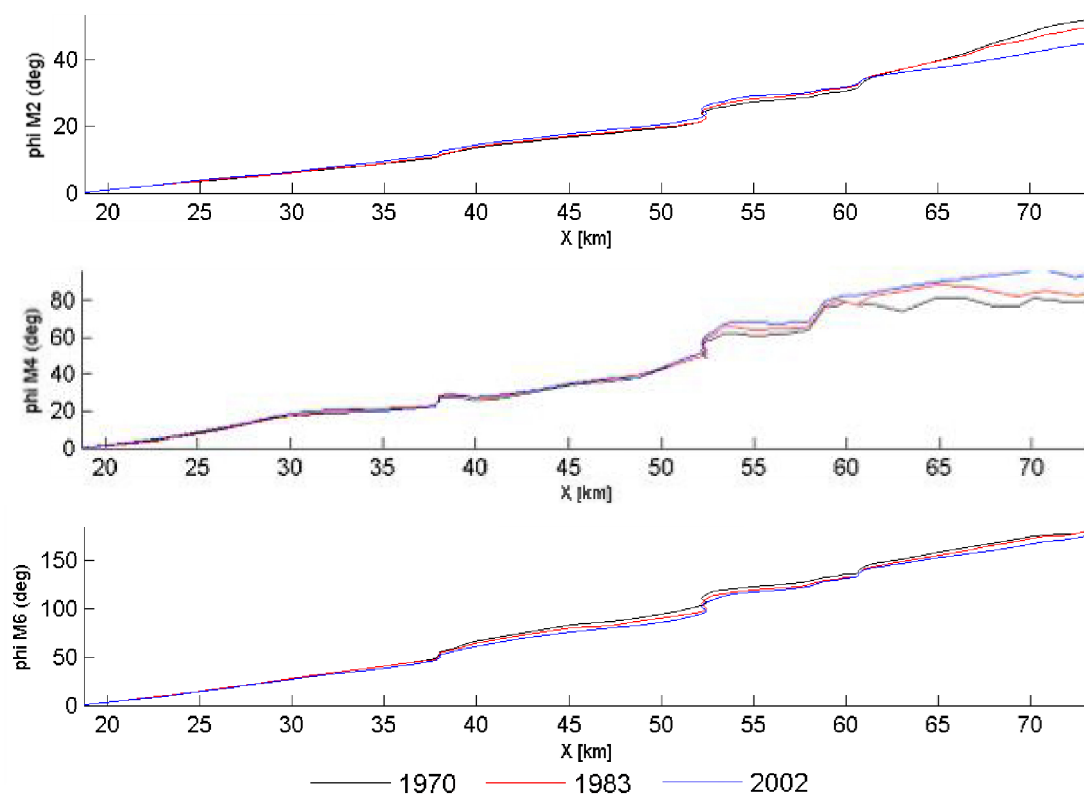


Figure 5-13: Evolution of the phase of M_2 , M_4 and M_6 along the ebb channels in the Western Scheldt.

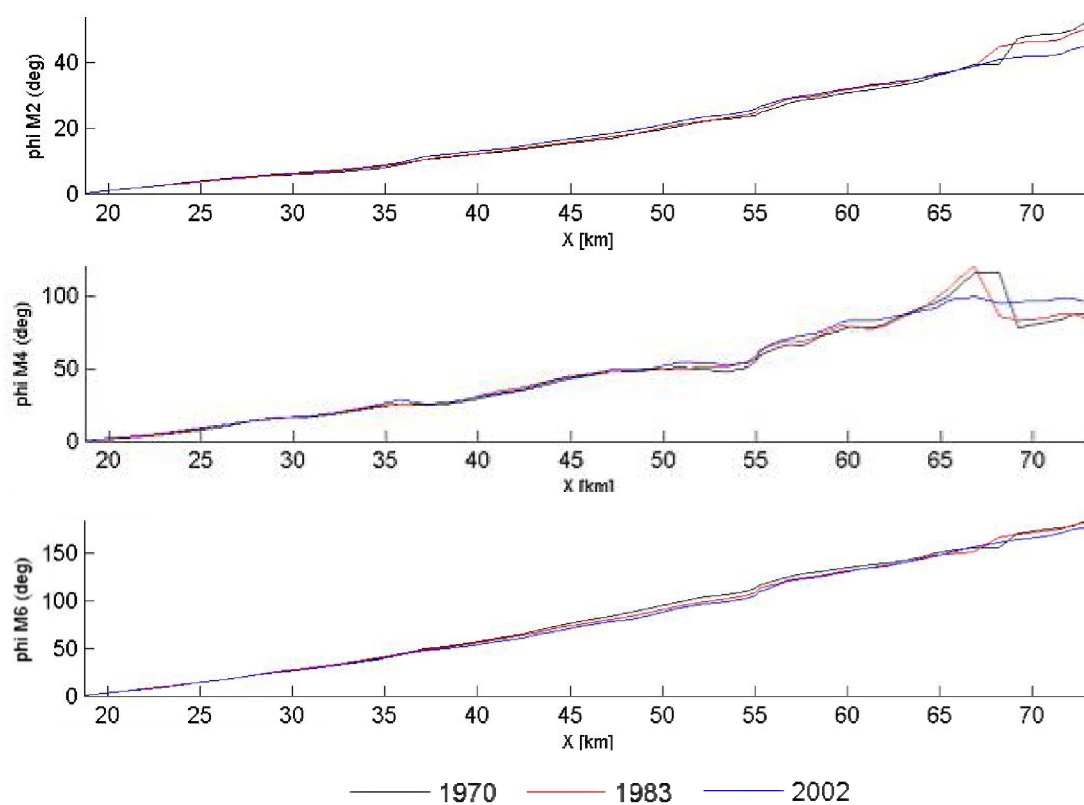


Figure 5-14: Evolution of the phase of M_2 , M_4 and M_6 along the flood channels in the Western Scheldt.

The abrupt jumps in the graphs near km 68 are caused by the ‘Drempel of Valkenisse’. The bathymetry in this region has undergone drastic changes over the years (Figure 5-15). The typical shallow bar at the landward end of the flood channel influences the flow in this region significantly.

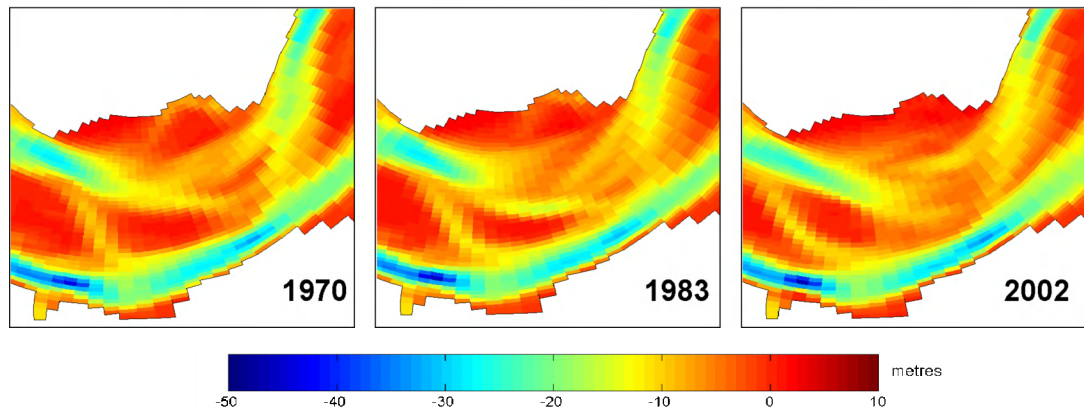


Figure 5-15: Bathymetry near the ‘Drempel of Valkenisse’ for the years 1970, 1983 and 2002.

Amplitude Ratio and Phase Difference

The tidal asymmetry in the Western Scheldt can be described according to Wang et al. (2002) by:

- the amplitude ratio M_4/M_2 which determines the strength of the asymmetry
- the phase difference $2\phi_2 - \phi_4$ which indicates the flood or ebb-dominance (for a positive respective negative difference, i.e. flood dominant if the relative phase is between 0° and 180°)

Similarly, the relation between the M_2 and M_6 tidal constituents is expressed with the amplitude ratio M_6/M_2 and the phase difference $3\phi_2 - \phi_6$.

These four parameters are calculated at every observation point, and as such their evolution within the estuary is examined. Figures 5-16 and 5-17 show the amplitude ratios M_4/M_2 and M_6/M_2 in respectively the ebb and flood channels.

The ratio M_4/M_2 decreases in the estuary from 0.09 at the seaward end to 0.065 near Hansweert, wherefrom it starts increasing again. West of ‘the Drempel van Borsele’ the ratio decreased between 1970 and 2002. In the part east from this point up to Hansweert, the highest values are found for 1983 and the lowest for 2002. In the part east from the ‘Drempel of Valkenisse’ the largest changes have occurred: 0.1 towards 0.075 from 1970 to 1983 and a further decrease to 0.065 in 2002.

Also the ratio M_6/M_2 decreases from the seaward end towards Vlissingen. Then it slowly starts increasing towards the ‘Drempel van Valkenisse’, after which it decreases again. In the part west of Terneuzen the ratio increases between 1970 and 2002, whereas it decreases east of this point. However, there is a big difference between the three years: whereas the ratio evolves highly within the estuary in 1970, it becomes more and more levelled along the estuary through the years.

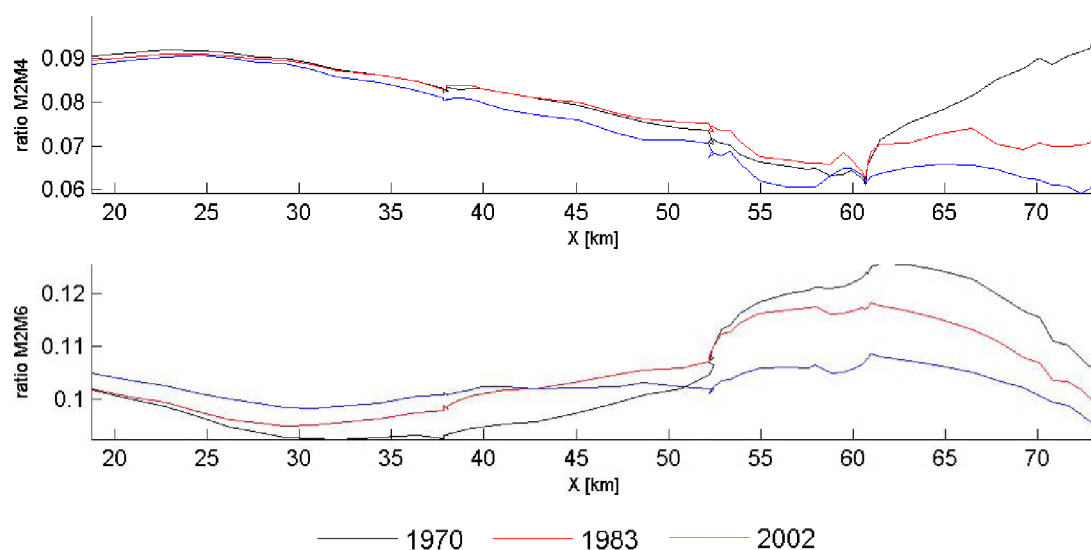


Figure 5-16: Evolution of the amplitude ratios M_4/M_2 and M_6/M_2 along the ebb channels in the Western Scheldt.

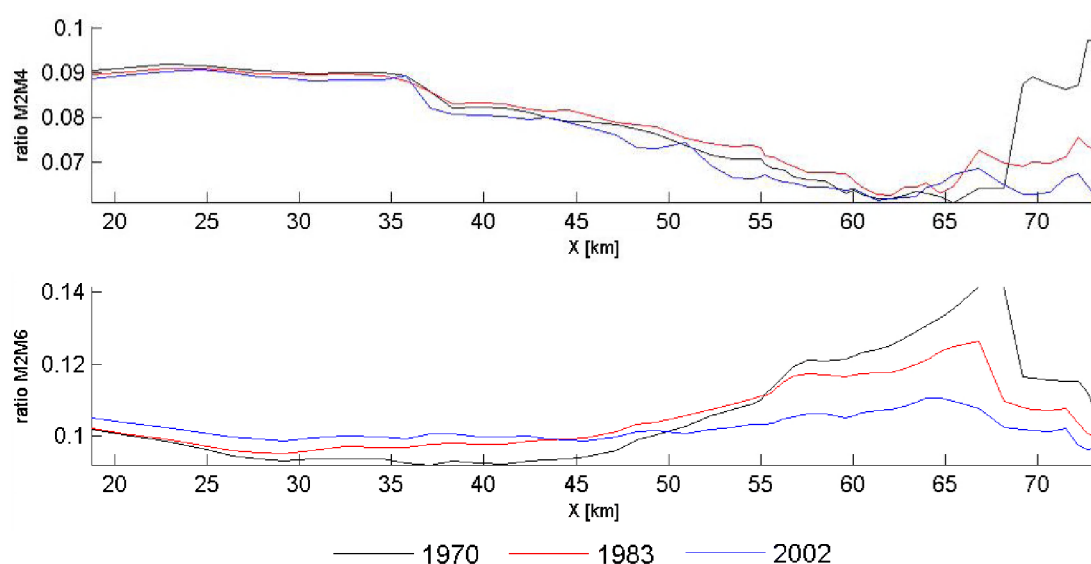


Figure 5-17: Evolution of the amplitude ratios M_4/M_2 and M_6/M_2 along the flood channels in the Western Scheldt.

The changes in the phase differences in the flood channels are concentrated in the most eastern part of the estuary where both $2\phi_2 - \phi_4$ and $3\phi_2 - \phi_6$ decrease during time (Figure 5-18 and 5-19). In the western part $2\phi_2 - \phi_4$ hardly changes. Concerning $3\phi_2 - \phi_6$ there are changes throughout the entire estuary. In the part west of Hansweert the difference increases in time, whereas in the most eastern part there is a decrease. Whereas for 1970 $3\phi_2 - \phi_6$ decreases to Hansweert where after it start increasing again, there is a continuing increase going upstream in 2002.

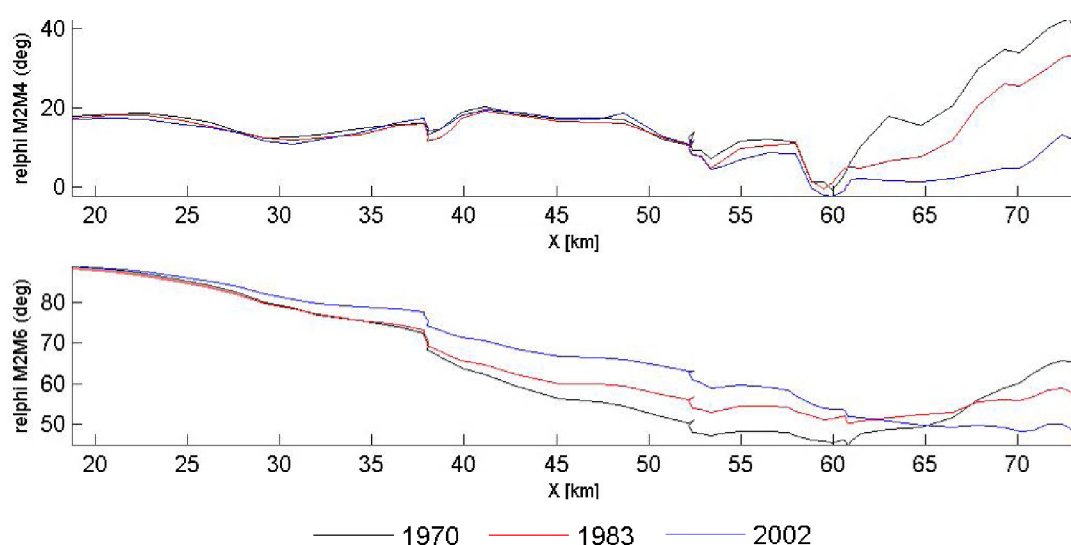


Figure 5-18: Evolution of the phase differences $2\phi_2 - \phi_4$ and $3\phi_2 - \phi_6$ along the ebb channels in the Western Scheldt.

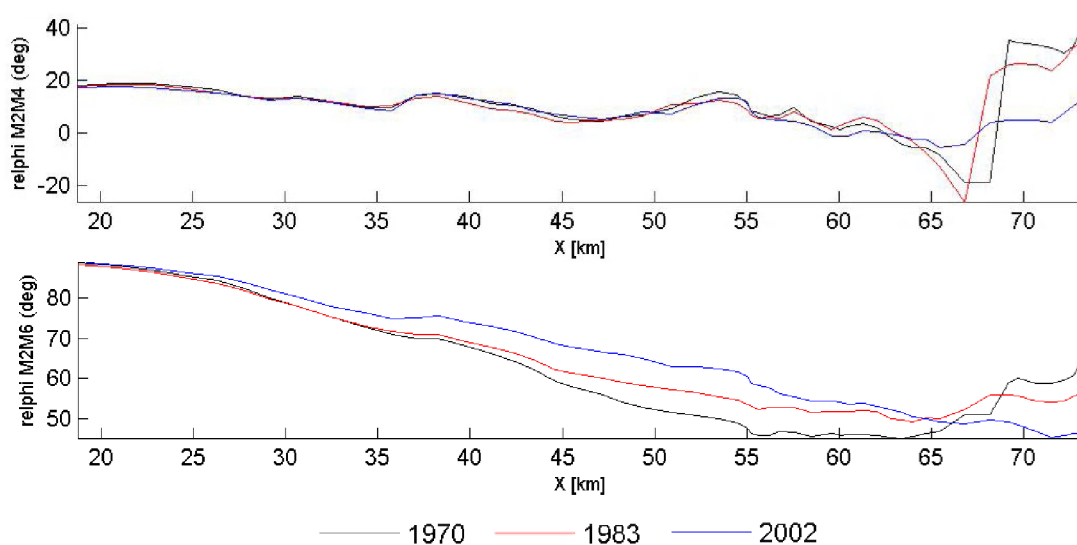


Figure 5-19: Evolution of the phase differences $2\phi_2 - \phi_4$ and $3\phi_2 - \phi_6$ along the flood channels in the Western Scheldt.

5.2.3 Discussion

A closer investigations shows that the location of the macro cells can clearly be distinguished on the graphs. The borders coincide with the crossings between ebb and flood channels. As such it is possible to describe the evolution of the characteristics of the vertical tide within each macro cell. Hereafter the changes in the bathymetry within each macro cell are described as well as the human interventions which took place.

Only macro cell 6 is completely described below. For the other cells only the most important findings are discussed. A complete description for these cells, even as maps with the depth differences between the different bathymetries and cross-sections of the river bed can be found in Appendix A.7.

Macro Cell 6

The amplitude of M_2 increases significantly in both channels between 1970 and 2002 whereas the amplitude of M_4 decreases significantly. The biggest change occurs in the period 1970 to 1983. The amplitude of M_6 increases slightly in the ebb channel, but hardly changes in the flood channel. ϕ_2 decreases and ϕ_4 increases heavily in both channels from 1970 to 2002. ϕ_6 decreases as well, but changes less than ϕ_4 .

These changes result in a significant decrease of M_4/M_2 , M_6/M_2 , $2\phi_2-\phi_4$ and $3\phi_2-\phi_6$ in this macro cell. The decrease of the amplitude differences is more pronounced in the period 1970-1983, whereas for the phase differences the largest change occurs in the period 1983-2002.

Both ebb and flood channel became deeper from 1970 to 2002 (Figure 5-20). It's also clearly visible that the ebb channel became wider during the years. This evolution is caused by high amounts of dredging which took place in areas A and B in the ebb channel (Table 5-4). Further, steepening and a northwards movement of the southern border of the flood channel are noticed. This is due to the dumping of material in area B. High amounts have been dumped in area B until 1991, from then the amount has halved. As a result the flood channel becomes smaller but also somewhat deeper. In the period 1970-1983 sedimentation took place at the landward end of the flood channel.

Deepening of both channels gave rise to an increase of the M_2 amplitude and a decrease of the amplitude of M_4 . Deepening of the ebb channel through the entire macro cell occurred from 1970 to 1983 which explains why the biggest change is noticed in this period.

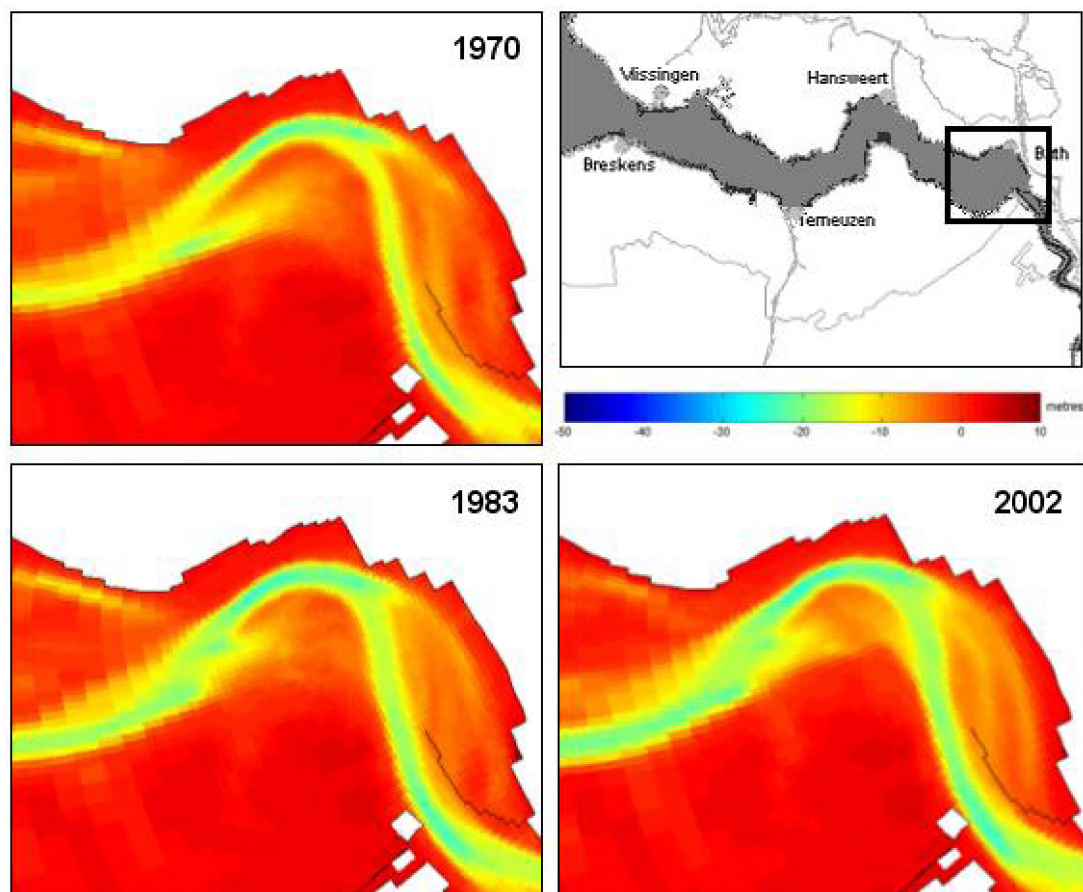
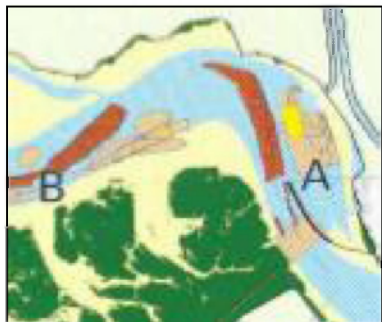


Figure 5-20: Bathymetry in macro cell 6 and 7 for the years 1970, 1983 and 2002.

Table 5-4: Overview of the dredging, dumping and sand mining in macro cell 6.

Activity	Amount (m ³ /year)	Period (years)	
Dredging in area B	1000000	1955 – 1969	
	2500000	1969 – 2000	
Dredging in area A	2300000	1955 – 1985	
	3200000	1985 – 1989	
	1500000	1989 – 2000	
Dumping in area B	2200000	1955 – 1973	
	4500000	1973 – 1991	
	2000000	1991 – 1997	
Dumping in area A	800000	1955 – 1971	
	200000	1971 – 1983	
Sand mining in area A	800000	1964 – 1970	
	100000	1972 – 1976	
	300000	1980 – 1986	

Other Macro Cells

In macro cell 1 M_4/M_2 decreases lightly and M_6/M_2 increases. The phase hardly changes between 1970 and 2002, although $3\phi_2-\phi_6$ increases between 1983 and 2002. These evolutions occur in both the ebb and flood channel.

Between 1970 and 1983 a slight increase of M_4/M_2 and a decrease from 1983 to 2002 is noticed in macro cell 3. The ratio M_6/M_2 also decreases from 1970 to 1983 but in the period afterwards the M_6/M_2 ratio decreases only in the upstream part of the cell. The phase difference $2\phi_2-\phi_4$ remains stable from 1970 to 2002, whereas $3\phi_2-\phi_6$ increases during this period, with the highest change after 1983.

The most important bathymetric changes are the deepening of the ebb channel from 1970 to 2002 (dredging in area Q) and sedimentation in the downstream part of the flood channel from 1983 to 2002 (dumping in area M).

In macro cell 4 M_4/M_2 slightly increases between 1970 and 1983 and decreases afterwards. M_6/M_2 decreases from 1970 to 2002. The phase difference $2\phi_2-\phi_4$ decreases from 1970 to 2002, whereas $3\phi_2-\phi_6$ increases significantly during this period.

These changes are accompanied by the deepening and widening of the flood channel (dredging in area O, sand mining in area J) Also significant sedimentation of the ebb channel is noticed. The different evolution in both channels can explain why ϕ_4 increases more in the ebb channel than in the flood channel.

A significant decrease of M_4/M_2 and M_6/M_2 is noticed in the ebb channel of macro cell 5. M_4/M_2 slightly decreases in the flood channel. The ratio M_6/M_2 decreases significantly in this part. The phase difference $2\phi_2-\phi_4$ decreases heavily from 1970 to 2002 in the ebb channel. $3\phi_2-\phi_6$ increases in the most western part of macro cell 5 but decreases in the eastern part.

The significant deepening (dredging in area B and E) of the ebb channel of macro cell 5 from 1970-2000 and the sedimentation of the flood channel can explain why the amplitude of M_4 increases slightly in the flood channel but decreases significantly in the ebb channel. The bigger changes in the ebb channel give rise to the significant increase of ϕ_4 in the ebb channel. The different evolution in the west and east of macro cell 5 can be brought in relation with the evolution of $3\phi_2-\phi_6$ which increases in the west of this cell but decreases in the east.

5.2.4 Conclusions

The M_2 amplitude continuously increases from Vlissingen to Bath. The M_4 and M_6 amplitudes show opposite evolutions: where M_4 increases, M_6 decreases (and vice versa). The phase of the different components continuously increases through the estuary, although the amount of increase depends on the local bathymetry. Therefore the vertical tidal asymmetry is influenced by changes in the bathymetry. Higher differences for the amplitudes, phases, amplitude ratios and phase differences are found when the bathymetry is more modified.

From 1970 to 2002 the asymmetry of the vertical tide changes the most in the eastern part of the Western Scheldt between Hansweert and Bath. A significant decrease of M_4/M_2 , M_6/M_2 , $2\phi_2-\phi_4$ and $3\phi_2-\phi_6$ is noticed in macro cell 6 between 1970 and 2002. This is accompanied by a deepening of the flood and ebb channels due to the high amounts of dredging which took place in this area.

In the part west of macro cell 4 the M_4/M_2 amplitude ratio decreases whereas the M_6/M_2 ratio increases. The phase difference $3\phi_2-\phi_6$ clearly increases, but the difference $2\phi_2-\phi_4$ hardly changes.

Deepening of the ebb channel is in general accompanied by a decrease of the amplitude ratios M_4/M_2 and M_6/M_2 , although the effect is more pronounced for the last one. This evolution is found in macro cells 3, 4, 5 and 6.

The phase difference $3\phi_2-\phi_6$ increases in most macro cells (1, 3, 4 and 5), whether or not deepening of the channels occurs. The increase is higher when significant sedimentation has occurred as for example in the flood channel of macro cell 4. However in the most eastern part the difference $3\phi_2-\phi_6$ decreases.

5.3 Horizontal Tidal Asymmetry

5.3.1 Method

For the analysis of the horizontal tide in the Western Scheldt, observation points and cross-sections in the ebb and flood channel in each macro cell are selected in the model. In contrast to the stations where the vertical tide has been analysed, these are located in the centre of the channels. The locations of the observation points and the cross-sections are shown in Figure 5-21, the according names in the model can be found in Appendix A.8.

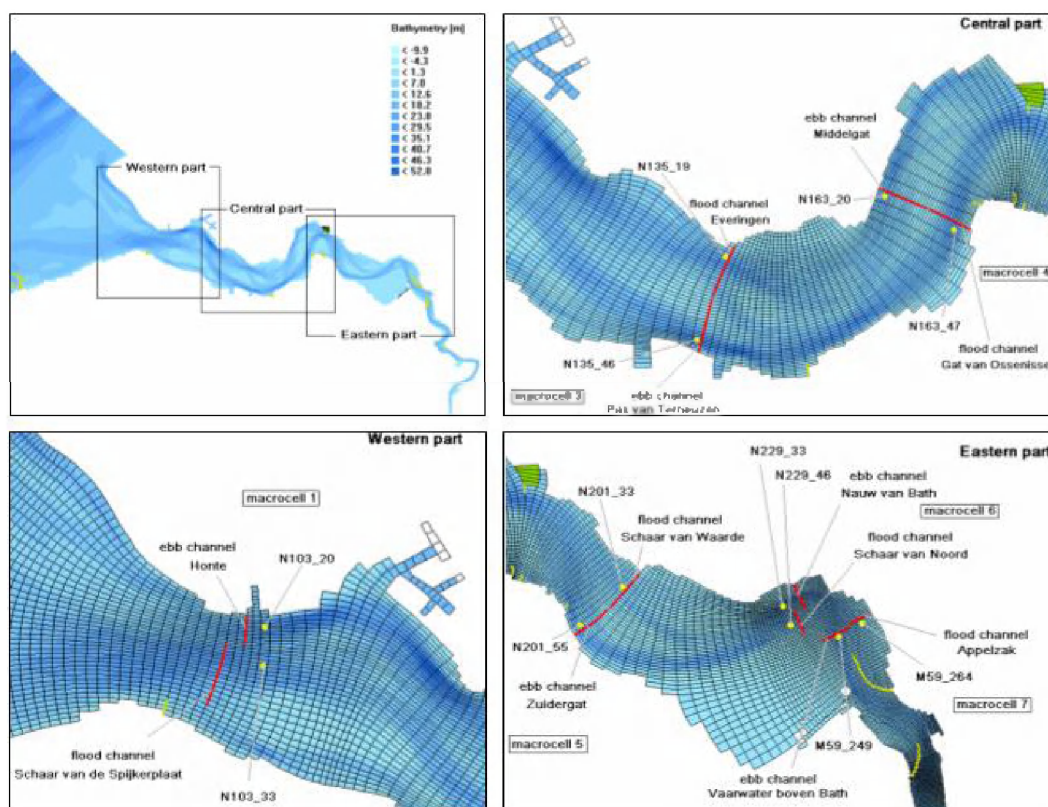


Figure 5-21: Location of the observation points and cross-sections in the model.

Since channels are known to move over the years, the observation points are located in the middle of the ebb and flood channel to avoid abrupt changes in depth. The cross-sections are located across the entire ebb or flood channel so that at each time step the discharge through the whole channel is measured. The profile of the cross-section in macro cell 6 with an

indication of the observation points can be seen on Figure 5-22. The cross-sections in the other cells can be found in Appendix A.8.

In every observation point time series (every 10 minutes) of the velocities are available. The depth averaged velocity components in accordance with the grid are chosen, since they are directed along and perpendicular to the channel direction. The assumption is that in the centre of the channel the velocities are more or less uni-directional (in the direction of the channel). Therefore a major and minor axis of the velocities can be discerned. The time series are harmonically analysed to get the contribution of the most important tidal constituents. The same is done for the discharge data from every cross-section.

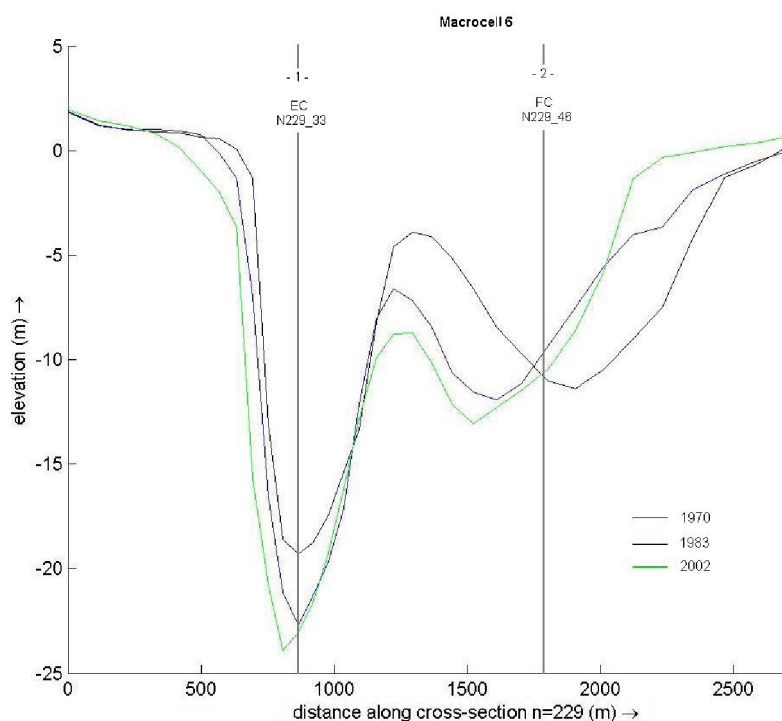


Figure 5-22: The profile of the cross-section in macro cell 6. The vertical lines indicate the position of the observation points in the flood and ebb channel (respectively FC and EC).

A harmonic analysis was also performed for all the observation points along the entire length of the ebb and flood channels in the estuary. The same points as in chapter 4 are used. This allows to study the variation of the horizontal tidal asymmetry within the estuary. Since more results are used, local irregularities can be spotted and a more general result comes out.

5.3.2 Results

Flow Velocity

The depth-averaged flow velocity records are harmonically analysed to investigate the characteristics of the asymmetry of the horizontal tide. Since the flow velocity is a vector, each tidal constituent is represented by an ellipse which is characterised by the direction of the principal axis, the amplitude along the two axes and the corresponding phase. These parameters are determined from the model results for the years 1970, 1983 and 2002 at each observation point. The ellipses for the observation points in the flood and ebb channel in macro cell 6 are shown in respectively Figures 5-23 and 5-24. The ellipses for the other observation points and a Table with the derived parameters are given in Appendix A.8.

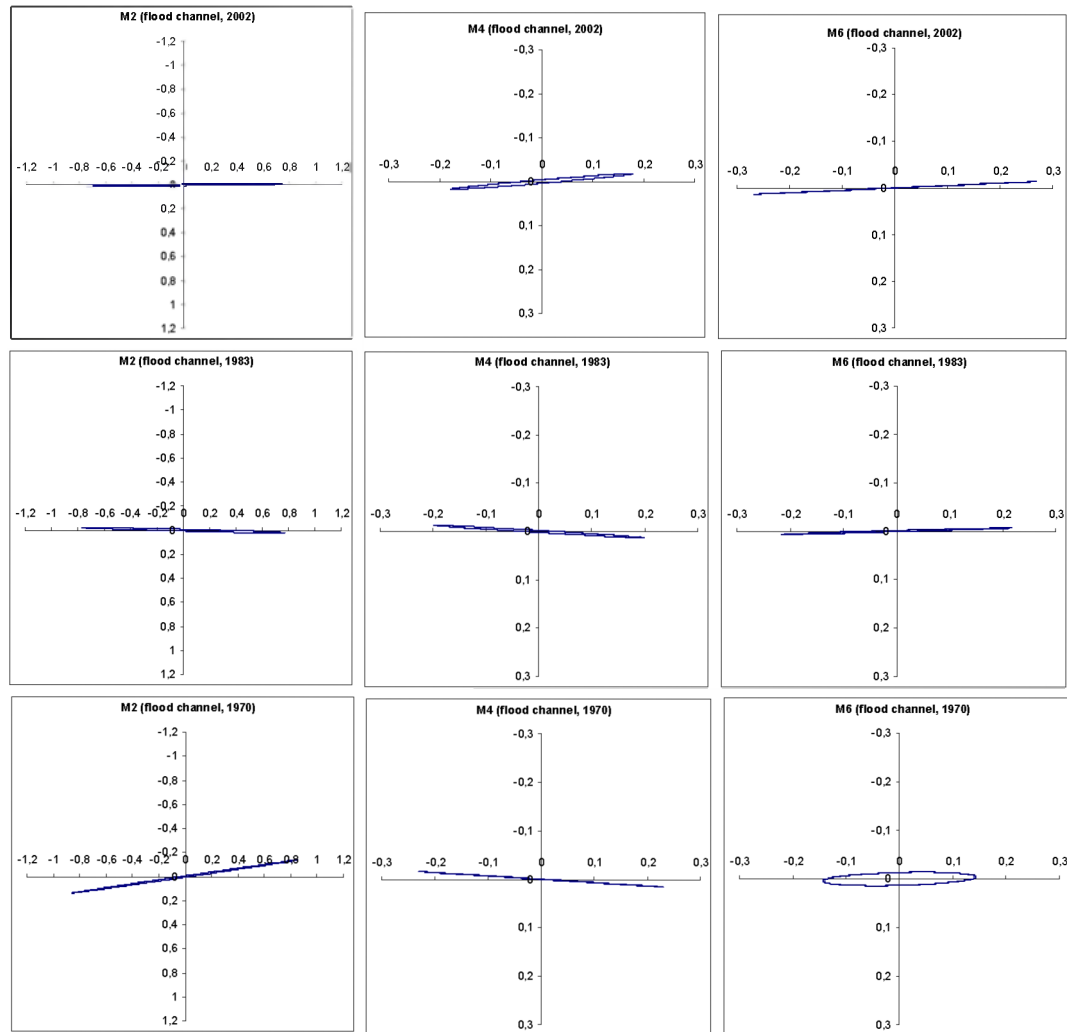


Figure 5-23: Tidal ellipses for the M_2 , M_4 and M_6 tidal constituents derived from the model results for the years 1970, 1983 and 2002 for the observation point in the flood channel of macro cell 6 (velocities in m/s).

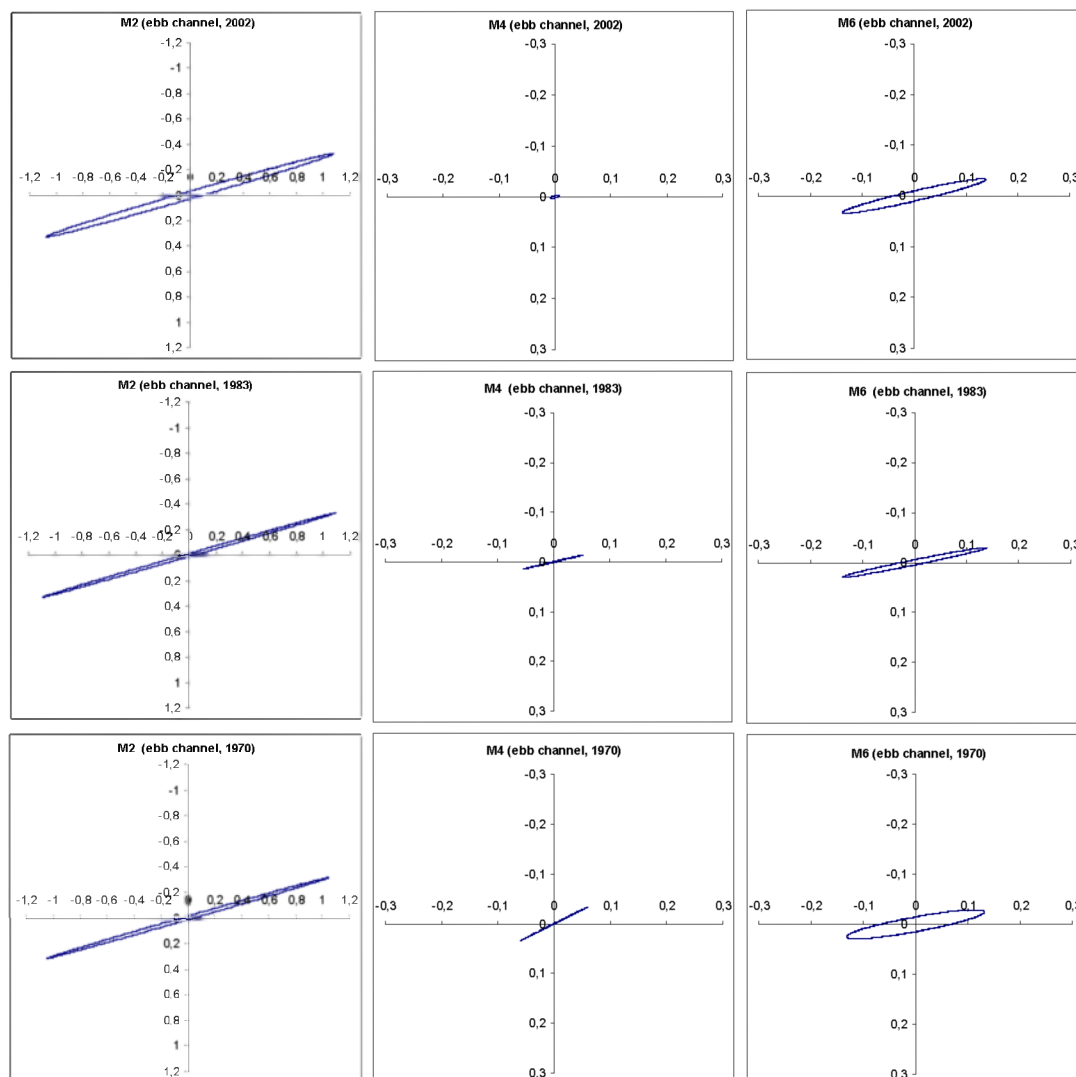


Figure 5-24: Tidal ellipses for the M_2 , M_4 and M_6 tidal constituents derived from the model results for the years 1970, 1983 and 2002 for the observation point in the ebb channel of macro cell 6 (velocities in m/s).

For macro cell 6, there can be seen from Figures 5-23 and 5-24 that the orientation of the M_2 component of the depth-averaged velocity in the ebb channel remained the same, whereas a change occurred in the flood channel after 1970. The amplitude only slightly changed. The amplitude of the M_4 and M_6 components are clearly smaller, between 0.5 and 0.2 m/s. In the flood channel the amplitude of the M_4 decreased, whereas the amplitude of the M_6 increased. The decrease of the M_4 component is even more pronounced in the ebb channel. The M_4 component in the ebb channel is very small and varies in direction. The direction of the M_4 component in the flood channel changed after 1983.

In general the ellipses are very flat and orientated along the mainstream of the currents. On the graphs this corresponds with the horizontal axis, which is aligned with the along-channel

orientated grid axis. The M_2 constituent has the largest amplitude, varying between 0.3 and 1.4 m/s depending on the location. The M_4 and M_6 constituents have the same order of magnitude and are smaller than 0.27 m/s.

In macro cells 1, 3 and 4 in the western part of the Western Scheldt, the ellipses show only little difference between the 3 years, compared to the other three cells located more upstream in the river. For example in the flood channel of macro cell 5 the principal axis of the M_2 and M_6 constituents fluctuates around the mainstream of the channel. In the ebb channel the M_4 component is very small and the direction of the principal axis is different for the three years. The ellipses in macro cell 7 become flatter during the years and more orientated along the mainstream in both channels.

The next step is the calculation of the amplitude ratios M_0/M_2 , M_4/M_2 and M_6/M_2 , and the phase differences $2\phi_2-\phi_4$ and $3\phi_2-\phi_6$ of the velocity component in the mainstream direction at each observation point. The results for the years 1970, 1983 and 2002 for macro cell 6 are presented on the graphs in Figure 5-25. The results for the other macro cells and a Table with all the amplitudes and phases can be found in Appendix A.8.

As can be seen on Figure 5-25 there is a decrease of the M_4/M_2 ratio of the current velocities in both the flood and the ebb channel of macro cell 6 from 1970 to 2002, together with increasing M_0/M_2 and M_6/M_2 ratios in the flood channel. The phase difference $2\phi_2-\phi_4$ in the ebb channel strongly increases in 2002, whereas there is only little change in the $3\phi_2-\phi_6$ difference. Both phase differences increase in the flood channel over the period 1970-2002.

Some remarkable findings in the other macro cells are:

- the negative M_0/M_2 ratio in the flood channel of macro cell 3 for the years 1970 and 1983,
- the irregular phase difference $2\phi_2-\phi_4$ in the ebb channel of macro cell 5 for the year 1970,
- the evolution of the phase difference in the flood channel of macro cell 7.

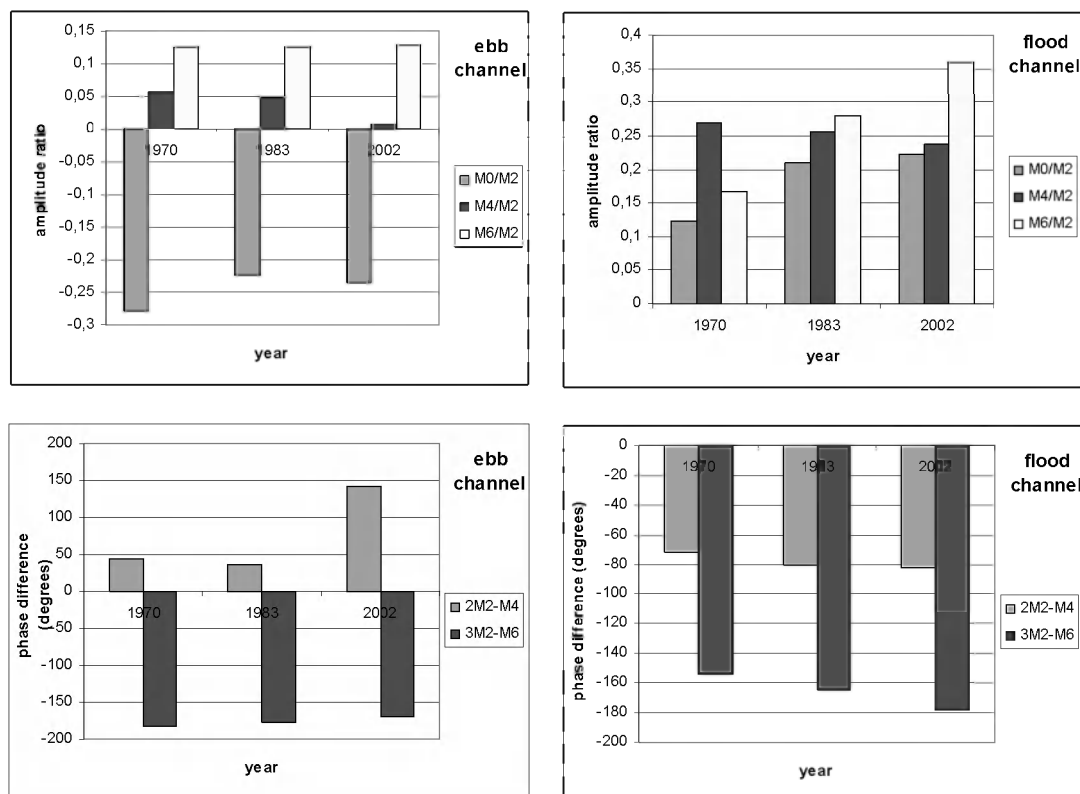


Figure 5-25: The amplitude ratios M_0/M_2 , M_4/M_2 and M_6/M_2 and the phase differences $2\phi_2 - \phi_4$ and $3\phi_2 - \phi_6$ of the velocity component in the mainstream direction at the observation points in the ebb and flood channel of macro cell 6 derived from the model results for the years 1970, 1983 and 2002.

Other points of interest are:

- a decrease of the ratio M_6/M_2 in the ebb channel of macro cell 3,
- an increasing phase difference $3\phi_2 - \phi_6$ in the ebb and flood channel of macro cell 3, 4 and 5,
- an increasing phase difference $2\phi_2 - \phi_4$ in the ebb channel of macro cell 4 and the flood channel of macro cell 3,
- an increasing M_4/M_2 ratio in the ebb channel and decreasing M_4/M_2 and M_6/M_2 ratios in the flood channel of macro cell 4,
- an increase of the M_0/M_2 ratio in the flood channel of macro cell 5 and 7, whereas the M_4/M_2 ratio in the ebb channel decreases.

Discharges

At the specified cross-sections in the channels, time-series of the instantaneous discharges are determined. As for the water levels and the velocities, a harmonic analysis was carried out for the period of one morphological tide. The amplitude ratios M_0/M_2 , M_4/M_2 and M_6/M_2

are determined and the results for the years 1970, 1983 and 2002 are compared. The results for macro cell 6 are presented in Figure 5-26. The graphs for the other macro cells can be found in Appendix A.8. There must be remarked that the sum of the ebb and flood channel cross-section is not always equal to the entire river cross-section due to the selection of the individual cross-sections in each channel. There has been opted for cross-sections which entirely stay in the same channel in the three different years.

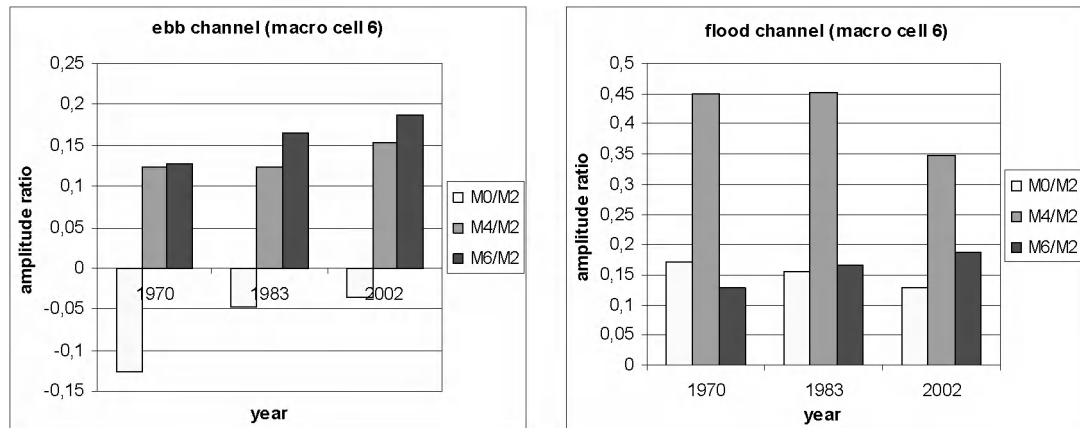


Figure 5-26: The amplitude ratios M_0/M_2 , M_4/M_2 and M_6/M_2 for the discharge through the cross-sections in the ebb and flood channel of macro cell 6 derived from the model results for the years 1970, 1983 and 2002.

In macro cell 6 the contribution of M_6 increases in both channels over the years (Figure 5-26). However where the contribution of the M_4 component augments in the ebb channel of macro cell 6, it decreases in the flood channel in 2002. The contribution of M_0 decreases in both the ebb and flood channel.

Remarkable findings in the other cells are:

- In macro cell 1 the contribution of M_6 to the discharge decreases over the years in both channels, and in the ebb channel this is also the case for the contribution of M_4 .
- The amplitude ratios in macro cell 3 and 5 don't show an unambiguous trend.
- The contribution of the M_4 component in the ebb channel of macro cell 4 increases, whereas its role reduces in the flood channel.
- In macro cell 7 the input of M_6 increases in the ebb and flood channel over the years. This is the same evolution as in cell 6. However where the contribution of the M_4 component augments in the ebb channel of macro cell 6, it decreases in macro cell 7.

In most cases the contribution of the M_4 exceeds that of M_6 in the flood channels (except from macro cell 3: 2002, and macro cell 7: 2002), whereas in the ebb channels the contribution of M_6 is more important than that of M_4 (except from macro cell 4: the opposite, macro cell 3: 1983 and macro cell 7: 1970).

Along-channel Variation of the Horizontal Tidal Asymmetry

Amplitude and Phase

The M_2 amplitude of the velocity in the western part increased in general over the years (Figure 5-27 and 5-28). Near the upstream part of the flood channel in macro cell 1, a temporary higher value in the year 1983 is found. This has to do with the evolution of the shoals in this part. However after Hansweert (km 59) the amplitude decreased in the ebb channels, whereas it increased in most flood channels.

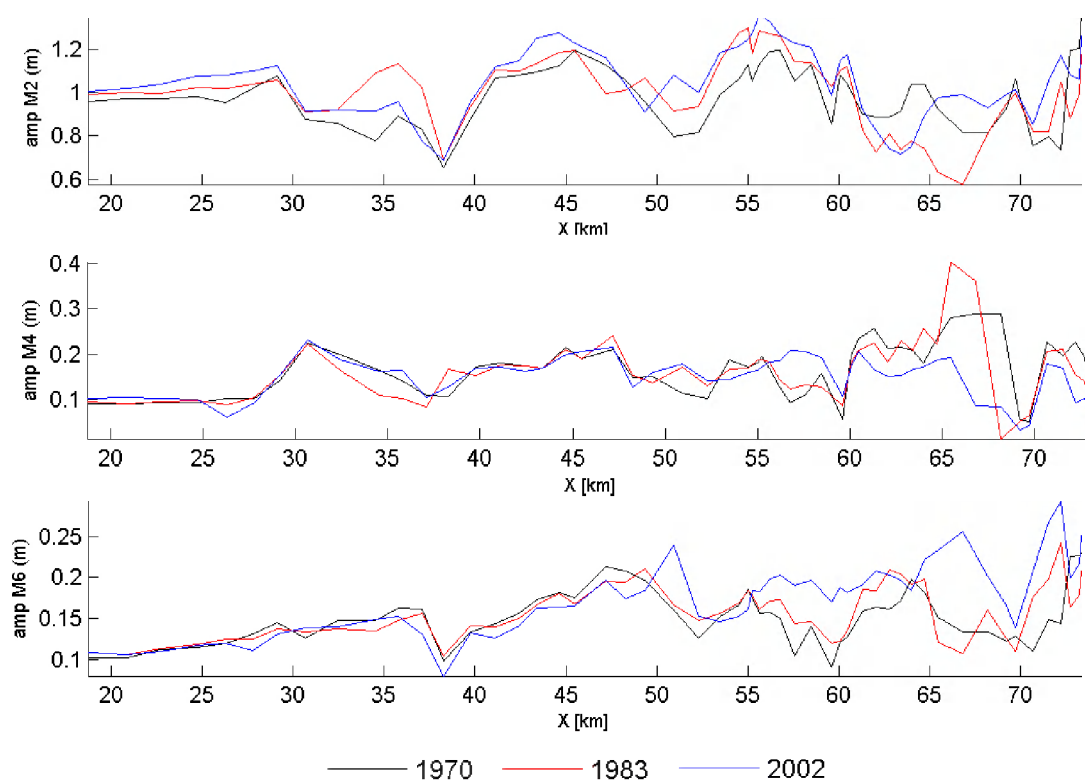


Figure 5-27: Evolution of the amplitude of the M_2 , M_4 and M_6 components of the horizontal tide along the flood channels in the Western Scheldt.

The amplitude of M_4 seems to fluctuate around a local value. The most important change is the decrease from 1970 to 2002 in the part upstream from Hansweert.

The amplitude of M_6 slightly decreases in the downstream part, however upstream from Hansweert it increases from 1970 to 2002 with temporary higher values in the ebb channels for 1983.

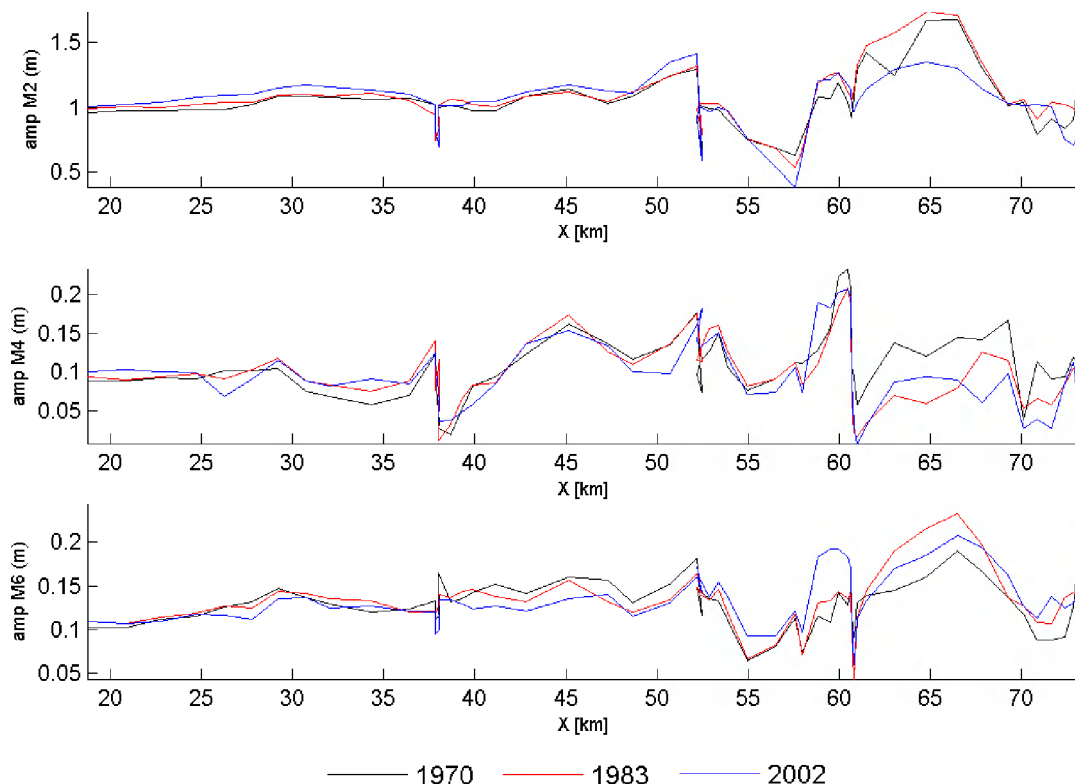


Figure 5-28: Evolution of the amplitude of the M_2 , M_4 and M_6 components of the horizontal tide along the ebb channels in the Western Scheldt.

The amplitude of the phase is strongly dependent from the location in the estuary (Figures 5-29 and 5-30). Jumps occur near macro cell 4 (km 50-58) and 6 (km 68-73) in both channels and also near Vlissingen in the ebb channel. It's hard to draw conclusions about the evolution of the phase over the years, although the changes are clearly higher in the eastern part of the estuary, where the phase decreases. A better evaluation can be made when the phase differences are considered (See further).

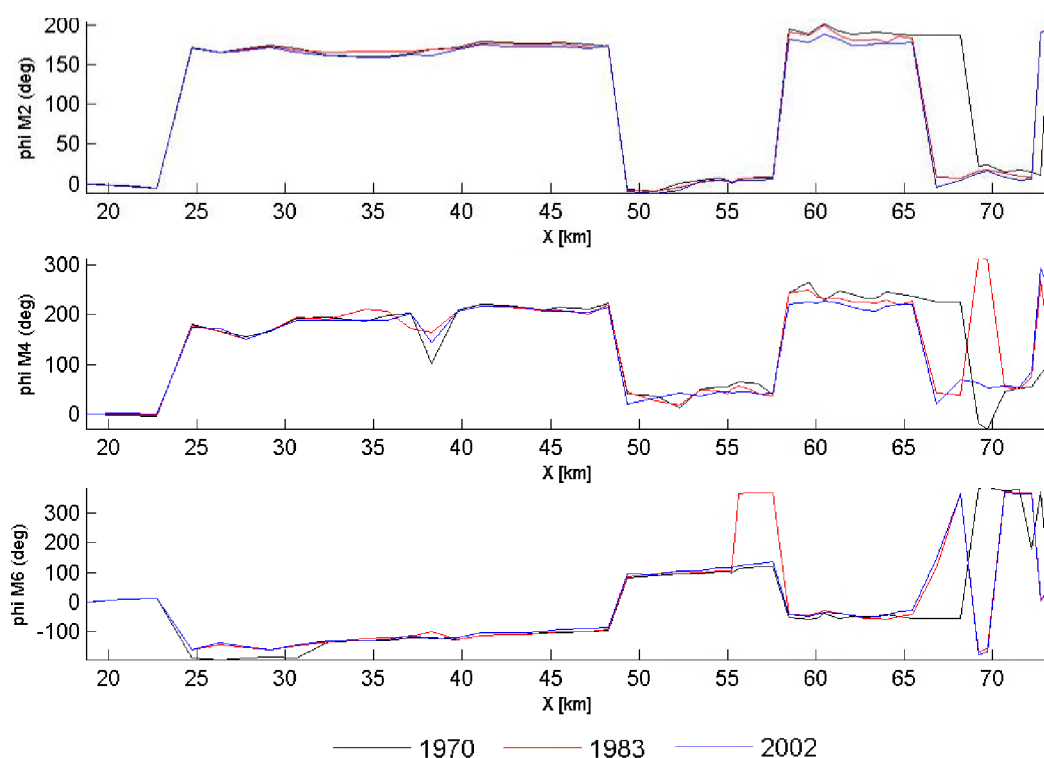


Figure 5-29: Evolution of the phase of the M_2 , M_4 and M_6 components of the horizontal tide along the flood channels in the Western Scheldt.

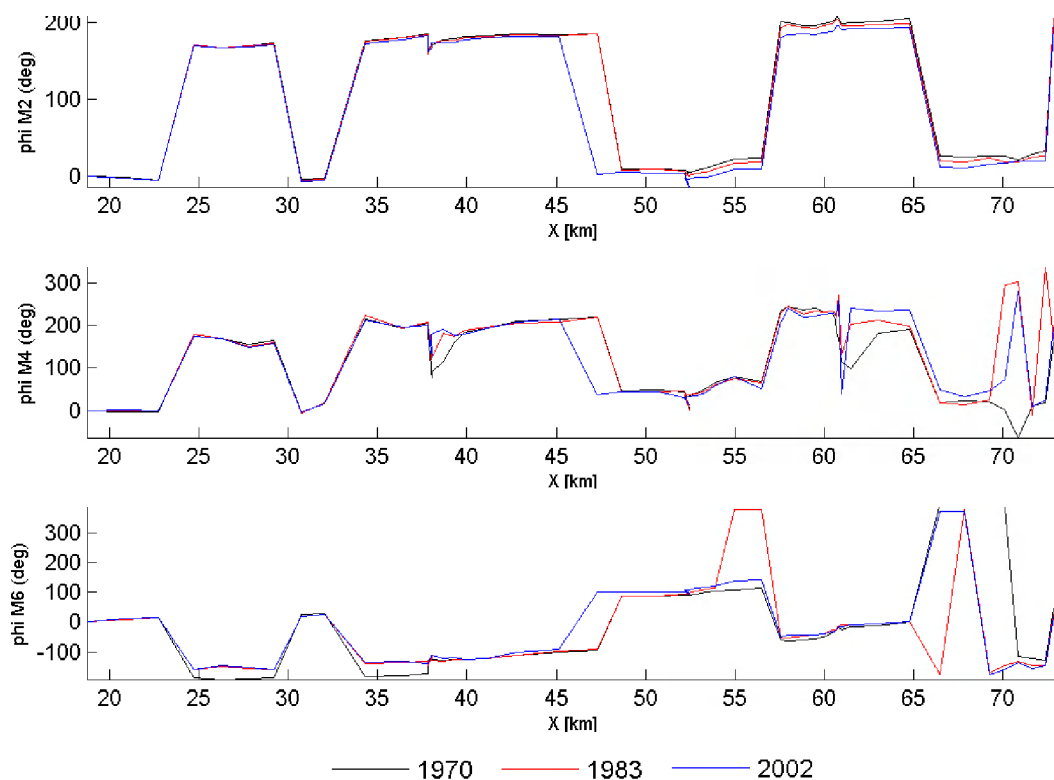


Figure 5-30: Evolution of the phase of the M_2 , M_4 and M_6 components of the horizontal tide along the ebb channels in the Western Scheldt.

Amplitude Ratio and Phase Difference

The amplitude ratio M_4/M_2 does not change significantly in the most downstream part (Figures 5-31 and 5-32). Only near the ‘Drempel of Borsele’ (km 38) sudden changes occur. In the part upstream from Hansweert (km 59) more changes are noticed. In general the ratio decreases, only for 1983 higher values are found in the flood channel. Other sudden changes are found near the ‘Drempel of Valkenisse’ (km 69).

A decrease of the ratio M_6/M_2 is noticed up to km 52 in the ebb channels and up to Hansweert in the flood channels. More upstream the ratio increases from 1970 to 2002. Here again, sudden changes are noticed near the bars at the end of the channels.

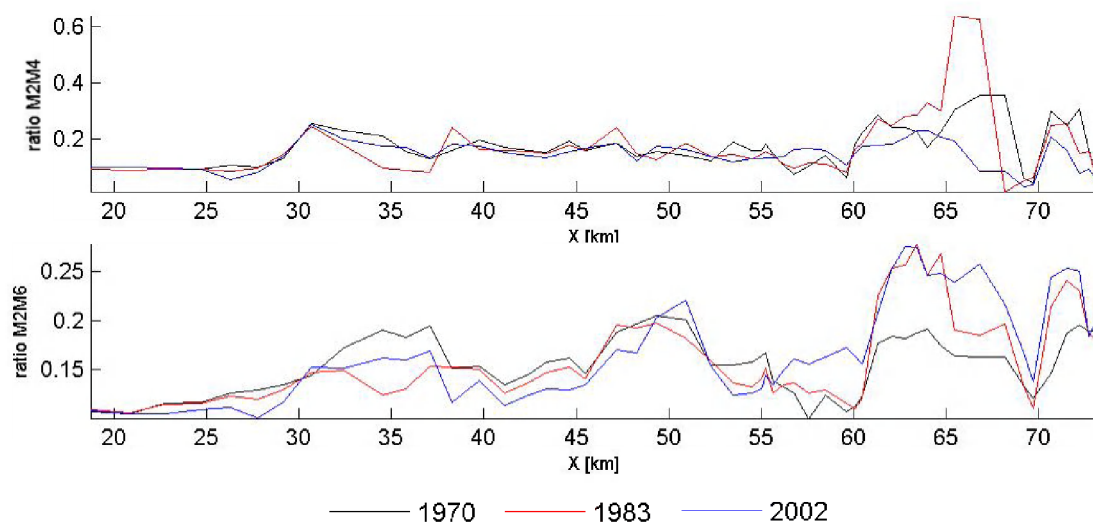


Figure 5-31: Evolution of the amplitude ratio of the M_2 , M_4 and M_6 components of the horizontal tide along the flood channels in the Western Scheldt.

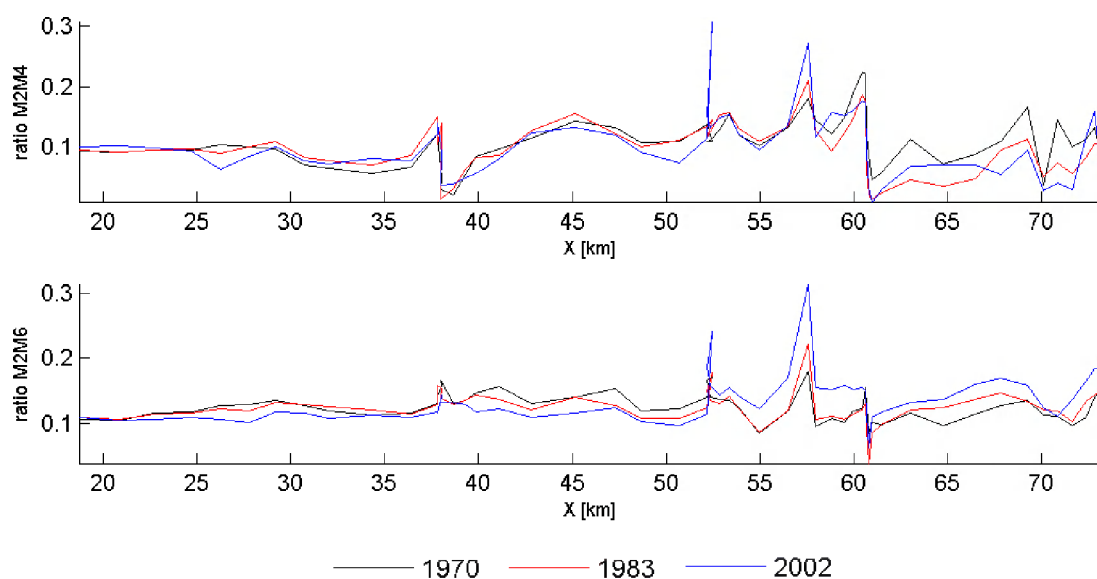


Figure 5-32: Evolution of the amplitude ratio of the M_2 , M_4 and M_6 components of the horizontal tide along the ebb channels in the Western Scheldt.

The phase differences $2\phi_2 - \phi_4$ and $3\phi_2 - \phi_6$ show a significant different behaviour (Figure 5-33 and 5-34). Whereas $3\phi_2 - \phi_6$ becomes more and more negative going upstream (always ebb-dominance), $2\phi_2 - \phi_4$ changes sign in some parts. Whereas the difference $2\phi_2 - \phi_4$ is in general positive, it becomes negative at the most seaward end, between Terneuzen and Hansweert and near Bath in both channels, and also near Vlissingen in the ebb channel only.

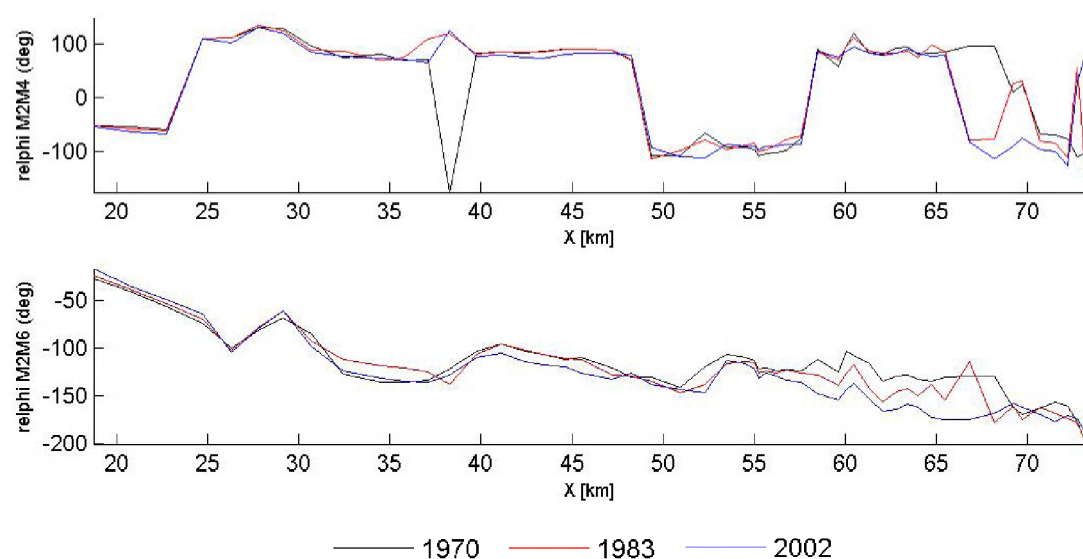


Figure 5-33: Evolution of the phase differences of the M_2 , M_4 and M_6 components of the horizontal tide along the flood channels in the Western Scheldt.

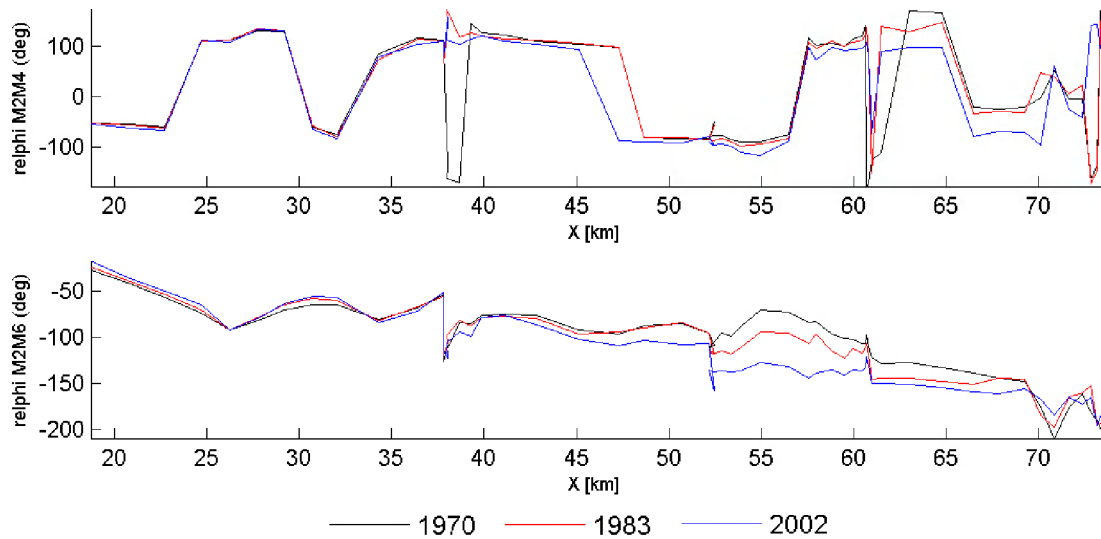


Figure 5-34: Evolution of the phase differences of the M_2 , M_4 and M_6 components of the horizontal tide along the ebb channels in the Western Scheldt.

Near the ‘Drempel van Borsele’ jumps occur in $2\phi_2 - \phi_4$. In general, this difference decreases over the years in the part between Hansweert and Bath. Also the length of the negative difference between Terneuzen and Hansweert in the ebb channel changes for the year 2002. The phase difference $3\phi_2 - \phi_6$ decreases from 1970 to 2002 in some parts. Significant changes are noticed upstream of macro cell 3 (km 52) in both channels. The decrease is also noticed in macro cell 3, although the change is smaller than upstream, and occurs mostly between 1983 and 2002. Here again, jumps are noticed at the locations of the bars.

5.3.3 Discussion

To enable the correct interpretation of the change of the horizontal tidal asymmetry, the bottom changes during each period need to be considered as done previously for the vertical tide. Representative cross-sections of the Westerns Scheldt bathymetry for each of the macro cells can be found in Appendix A.7.5, maps with the bathymetry of each cell and an overview of the human interventions in Appendix A.7.3, and maps with the depth differences between the years in Appendix A.7.4.

The drastic changes of the different parameters in for example the flood channel of macro cells 5 and 7 are correlated with important bottom changes and movement of the deepest part of the flood channel. Higher values for the amplitude along the secondary axis of the ellipse for the M_4 constituent are typically found when the channel has moved and the local depth has decreased with several meters. When the observation point is situated in a shallow

part of the channel, the relative contribution of the M_4 constituent is higher. This can be observed from the relative change in amplitude ratio M_4/M_2 and the phase difference $2\phi_2 - \phi_4$ of the velocities and the amplitude ratio M_4/M_2 of the discharges.

The ebb channel of macro cell 7, which is the most upstream located cell, became deeper and wider during the years. This is a consequence of the human interventions which took place in this area. Concerning discharges the morphological evolution gives rise to a higher contribution of the M_6 constituent, whereas the influence of M_4 decreases. The same trend is noticed for the phase difference of the velocities. The amplitude ratios of the velocities show a decrease of the contribution of the M_4 component. The same evolution of these parameters is found when the years 1970 and 1983 are compared in macro cell 5.

Also the ebb channel in macro cell 6 became deeper during the years; however in this case only the decrease of M_4/M_2 of the velocities and the increase of M_6/M_2 of the discharge are clearly visible.

The opposite evolution takes place in the ebb channel of macro cell 4: during the years the channel became shallower and smaller. This is accompanied by an increase of the amplitude ratio M_4/M_2 of the velocities and the discharges.

In macro cell 3 and 4 the amplitude ratio M_4/M_2 of the discharge decreases, while the ratio M_6/M_2 increases. This is accompanied by a widening of the flood channel and in the case of macro cell 3 also a decreasing maximal depth.

The along-channel analysis of the vertical tide includes a high number of locations through the ebb and flood channels. As such it is less sensible to local irregularities. High local variations are typically found at the crossing of ebb and flood channels or near bars.

However, in general the values found in the analysis of the individual points agree with those found in the along-channel analysis.

The evolution of the phase differences through the estuary, shows an alternation of positive and negative values for $2\phi_2 - \phi_4$. This difference becomes negative at the most seaward end, between Terneuzen and Hansweert (macro cell 4) and near Bath in both channels, and also near Vlissingen in the ebb channel only. Especially in macro cell 4, the impact of human interventions is important. The flood channel was significantly deepened whereas the ebb channel became narrow and shallow.

The phase difference $3\phi_2 - \phi_6$ becomes more negative upstream. In both channels this difference is always negative.

The comparison with previous studies is included in Appendix A.7.7.

5.3.4 Conclusions

Due to the specific location of the individual, single observation points it is hard to draw unambiguous conclusions from these results. As shown before, the location of the point within the channel section influence the results significantly since velocities are highly affected by the local bathymetry. However the obtained values agree in general with those derived from the along-channel analysis. This analysis is based on a high number of observation points distributed in the ebb and flood channels. Therefore general trends within an area are better represented, and local abrupt changes can be distinguished.

Also in this along-channel analysis the most significant changes are observed in the upstream part of the Western Scheldt (east of Hansweert): the amplitude ratio M_6/M_2 increases, and the ratio M_4/M_2 and the phase differences $2\phi_2 - \phi_4$ and $3\phi_2 - \phi_6$ decrease. Downstream from Hansweert the ratio M_6/M_2 and the phase difference $3\phi_2 - \phi_6$ decrease. The ratio M_4/M_2 and the difference $2\phi_2 - \phi_4$ do not show a clear trend in this part.

Deepening of a channel decreases of the M_6/M_2 amplitude ratio (as observed in macro cell 3 and 4) and the M_4/M_2 ratio (see cell 4, 5 and 6). The phase difference $3\phi_2 - \phi_6$ is continuously increasing in macro cells 3, 4 and 5. Interaction with changes in the bathymetry influences the magnitude of the increase. Sedimentation in a channel results in an increase of the $2\phi_2 - \phi_4$ phase difference (see cell 3 and 4) and an increase of the M_4/M_2 amplitude ratio (see cell 4). Apart from the last finding, similar interactions between modified bathymetry and vertical tide were observed (see section 5.2).

6 Sediment Transport

This chapter discusses the influence of the bathymetry on the tide-driven sediment transport. First we focus on the influence of different bottoms on the residual sediment transport patterns. The second part describes the residual main sediment transport directions in the estuary together with the erosion/sedimentation in the different macro cells as determined in the sand balance derived from the model. This leads to conclusions about the contribution of the tide-driven sediment transport to the import/export of sediments at the river mouth.

6.1 Residual Sediment Transport Patterns

6.1.1 Method

Chapter 4 describes the results of the numerical simulations performed with the Western Scheldt model forced with bathymetries for the years 1970, 1983 and 2002. Each of these simulations was combined with two fundamentally different transport formulations: Van Rijn (2003) and Engelund Hansen (1967). The Engelund Hansen formulation is based on a total load approach. The Van Rijn formulation distinguishes between bed-load and suspended load (See section 4.2).

The sediment transport analysis focuses on the residual transport patterns calculated as the integral of the instantaneous transport over one tidal cycle, and is thus equal to the difference between the ebb- and flood-transport. This is calculated directly with DELFT3D for one morphological tide. Only the tide-driven sediment transport is computed, since no wind, waves or density differences are modelled. Comparison is made between the results for the different years and the different transport formulations.

Only a selection of maps for the western part of the Western Scheldt is presented in this section. Appendix A.9 presents all other relevant maps (also for the central and eastern part).

6.1.2 Results

The residual sediment transport patterns as found with the total load formula from Engelund Hansen (Figure 6-1) confirms the existence of circulation cells in the various macro scale ebb and flood channel systems in the Western Scheldt as described by Jeuken (2000) and Winterwerp (2000). Such an estuarine section consists of two large, parallel-aligned channels, divided by tidal flats. The largest residual sediment transport is clearly situated within the ebb- and flood channels (in respective the ebb- and flood-direction), whereas on the shoals there is hardly any residual transport.

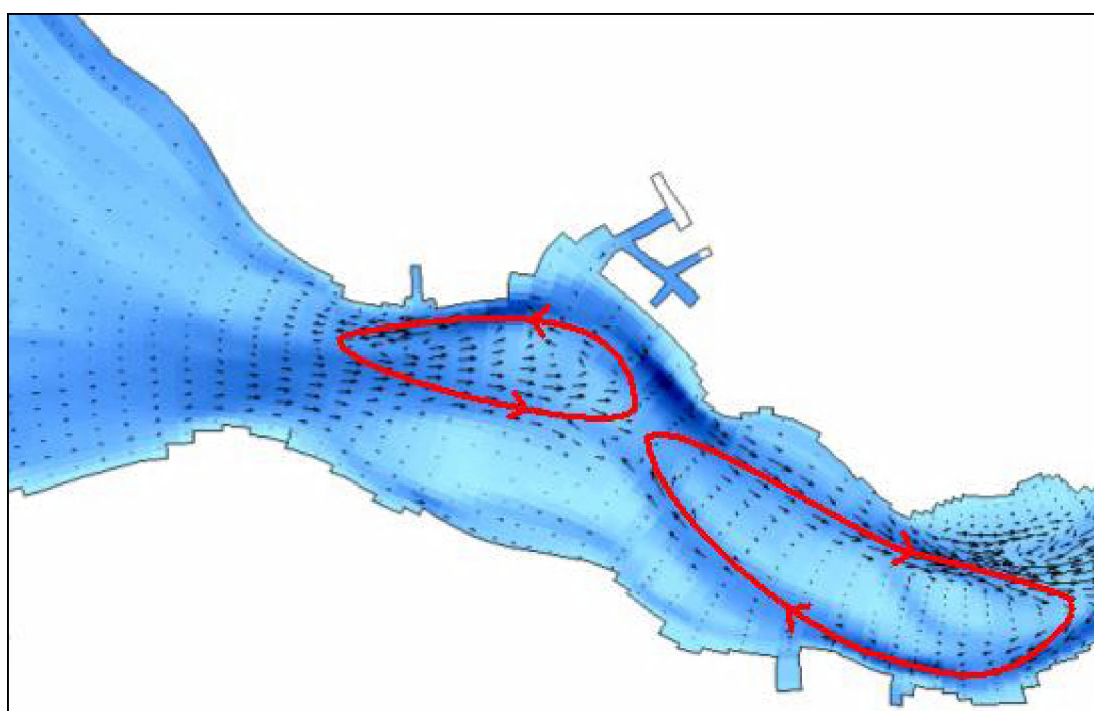


Figure 6-1: Residual transport patterns in the western part of the Western Scheldt for 2002 according to the Engelund Hansen formulation for the total load.

In Figure 6-2 the residual sediment transport patterns for both 1970 and 2002 for the total load calculated with the Engelund Hansen formula are shown. No drastic changes in the overall patterns occur, however some local differences are noticed. In area I, which is located just south of Vlissingen, there can be seen that the residual transport in the ebb and flood channel is slightly higher in 2002. The flood channel is also extended more to the east compared to 1970.

In the second area (the green circle) there can be seen that the direction of the residual transport in the ebb channel has somewhat changed between 1970 and 2002. The flow

became a bit more westward oriented in 2002. In area III, there can be seen that the transport patterns were modified due to changes in the bathymetry and the location of the channels. The westward directed transport increased in the southern part of the flood channel, and the component going to the north at the edge of the Figure became less important. Maps with direction and magnitude differences of the residual transport between the two years are included in Appendix A.9.2.

In the central and eastern part similar small changes occur. These Figures can be found in Appendix A.9. A modified transport direction is usually correlated with a movement of the channels and shoals. The location of the circulation cells hardly changes.

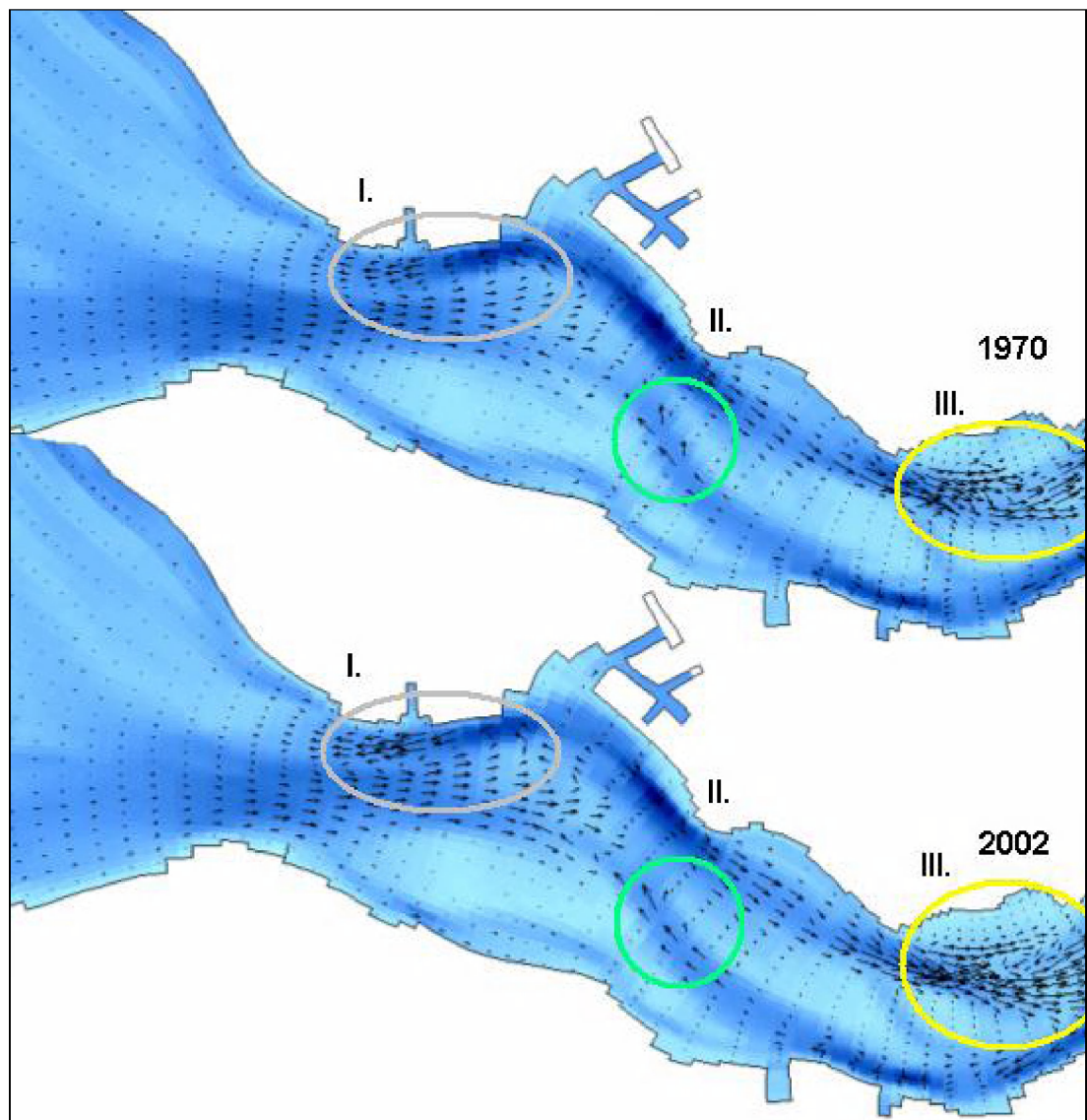


Figure 6-2: Residual transport patterns in the western part of the Western Scheldt for 1970 (top) and 2002 (bottom) according to the Engelund Hansen formulation for the total load. The vectors for both years have the same scale.

The Van Rijn formulation allows comparing the sediment transport patterns from the suspended load (Figure 6-3) and the bed-load (Figure 6-4). Since the calculated bed-load is only 3% of the total transport, these vectors are reproduced on a larger scale to make the sediment transport patterns visible. Although bed-load and suspended load are forced by two different mechanisms, the residual transport patterns are very similar. Only small differences, such as in the marked area in Figures 6-3 and 6-4 can be noticed. A map with the differences in direction between the two transport modes is given in Appendix A.9.2. The same conclusions apply for the results for the central and eastern part of the Western Scheldt (Appendix A.9).

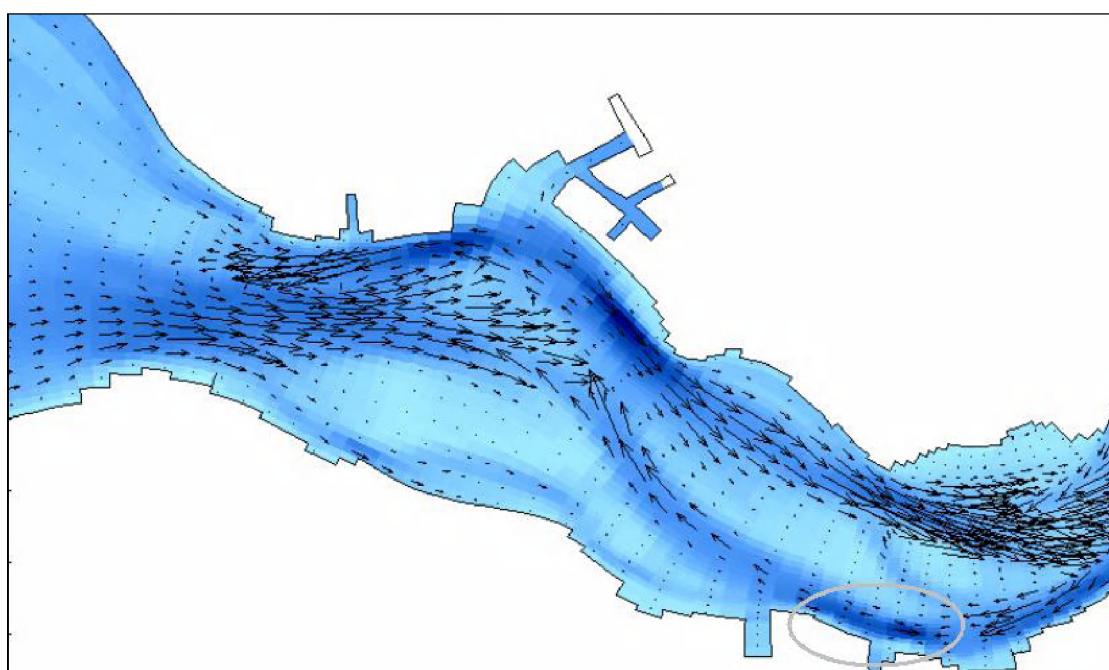


Figure 6-3: Residual transport patterns in the western part of the Western Scheldt for 2002 according to the Van Rijn formulation for suspended load.

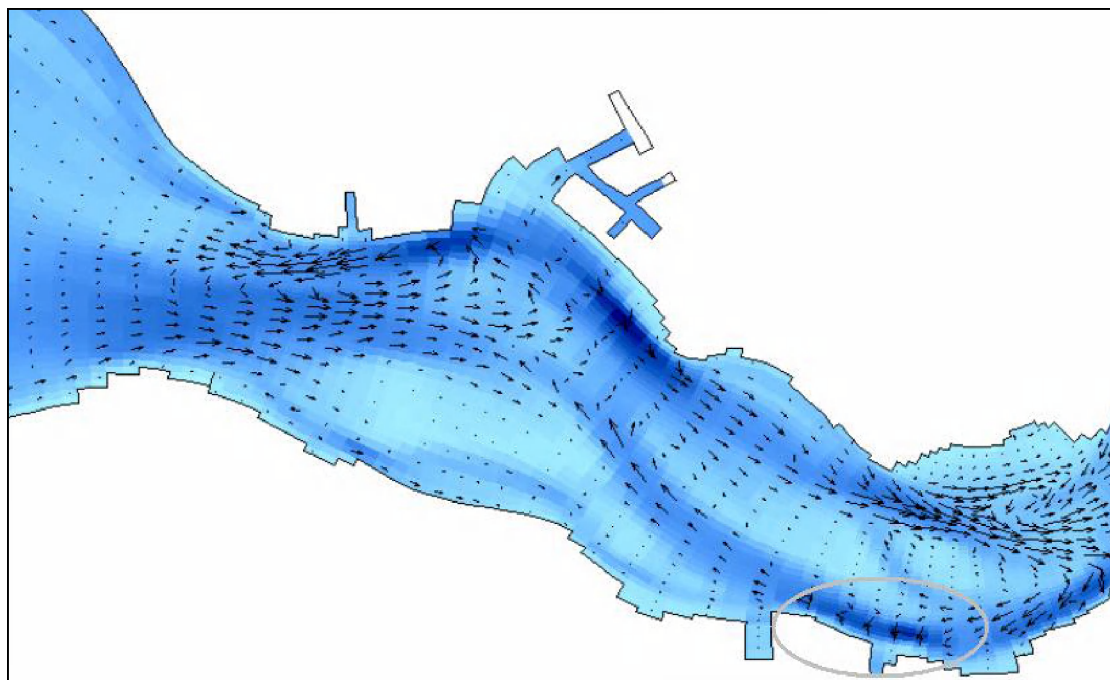


Figure 6-4: Residual transport patterns in the western part of the Western Scheldt for 2002 according to the Van Rijn formulation for bed-load. The vectors have a different scale as on Figure 6-3.

In Figure 6-5 the residual transport patterns as calculated in DELFT3D with the Van Rijn formulation for suspended load in the western part of the Western Scheldt are compared for 1970 and 2002. In areas I, II and III the same evolution as discussed above for the total load calculated with the Engelund Hansen formula is visible. The transport vectors near Vlissingen (area I) are a bit larger in 2002 compared to 1970. Also the somewhat larger extent of the flood channel of this circulation cell to the east is noticed again. The differences in area II are less clear, although in 2002 the ebb channel is a little wider than in 1970.

Around areas III, IV and V the influence is visible of the modified bathymetry. The channel in the grey circle (area IV) moved to the east and lost importance. As a result, the transport in both the ebb (area V) and flood channel (area III) increased. In the flood channel also a change in the transport directions occurred.

Maps with direction and magnitude differences between the two transport formulations are given in Appendix A.9.2. Also here, similar observations are made in the central and eastern part of the Western Scheldt (Appendix A.9).

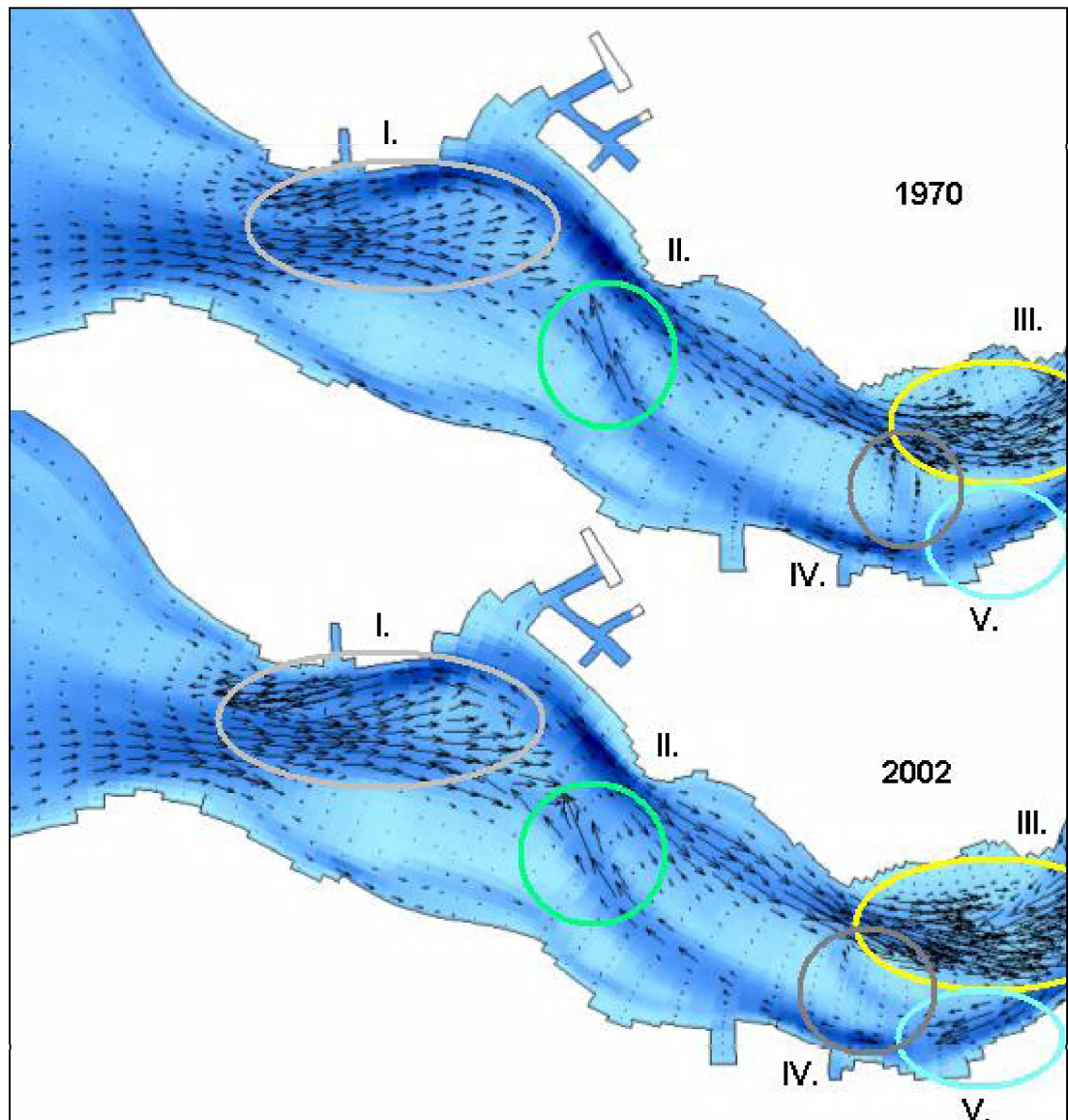


Figure 6-5: Residual transport patterns in the western part of the Western Scheldt for 1970 (top) and 2002 (bottom) according to the Van Rijn formulation for suspended load.

6.1.3 Discussion

The natural morphological development is the result of interactions between the water motion, sediment transport and bed topography (Wang and Jeuken, 2000). In an estuary like the Western Scheldt where tidal action is an important forcing factor, it is the residual sediment transport which determines the morphological development.

However, this also has the consequence that the ebb- and flood transport are almost equal to each other, which means that the magnitude of the residual transport is an order smaller than that of the ebb- or flood-transport (ibid.).

The residual sediment transport pattern is closely related to the bathymetry of the estuary. Movements of the channels can be seen in area III on Figures 6-2 and 6-5, and are accompanied by modified residual sediment transport patterns. Also Wang and Jeuken (2000) mentioned the importance of the geometric and bathymetric characteristics of the estuary in relation to the residual circulation.

The main ebb channels exhibit an ebb-dominant transport, whereas the main flood channels are clearly flood-dominant. This agrees with the 2DH model results from Winterwerp (2000) and observations from Jeuken (2000).

Whereas different transport formulations are known to give different quantitative results (Wang and Jeuken, 2000; Pinto et al., 2006), the patterns for the residual sediment transport are very similar.

6.1.4 Conclusions

The Van Rijn transport formulation and the Engelund Hansen formula give similar residual transport patterns. Although the driving mechanisms for suspended load and bed-load are different, the residual transport patterns in the model according to the Van Rijn formulation are very alike. The calculated bed-load is only around 3% of the total transport.

The circulation cells on the scale of the ebb and flood channels in the estuary are well represented in the model and hardly move between the three different years. The most important changes in the transport pattern are caused by the movement of channels and shoals in the estuary.

6.2 Tidally Averaged Bed-load Transport

6.2.1 Method

The local residual sediment transport is directly related to the asymmetry of the horizontal tide. Van de Kreeke and Robaczewska (2003) found that the long-term mean bed-load transport is determined by the flow velocities associated with M_0 , M_2 and its overtides M_4 and M_6 . The tidally averaged bed-load transport can be expressed with the following dimensionless expression:

$$\frac{\langle q \rangle}{\hat{u}^3 f} = \frac{3}{2} \varepsilon_0 + \frac{3}{4} \varepsilon_4 \cos \beta + \frac{3}{4} \varepsilon_4 \varepsilon_6 \cos(\beta - \gamma) \quad \text{Equation 6-1}$$

$$(M_0, M_2) \quad (M_2, M_4) \quad (M_2, M_4, M_6)$$

where:

- q = volumetric rate of sand transport per unit width
- \hat{u} = amplitude of the M_2 tidal current
- $\varepsilon_0, \varepsilon_4, \varepsilon_6$ = amplitude ratio of the residual M_0 , M_4 , M_6 and the M_2 tidal current respectively
- f = function of sediment and fluid characteristics
- γ = phase of tidal current M_6 relative to the M_2 tidal current
= $3\phi_2 - \phi_6$
- β = phase of tidal current M_4 relative to the M_2 tidal current
= $2\phi_2 - \phi_4$

The first term gives the contribution of the residual M_0 to the transport, the second term that from the interaction between M_2 and M_4 , and the last one also includes the influence of the M_6 constituent.

6.2.2 Results and discussion

A harmonic analysis of the flow velocity during one morphological tide was performed for the observation points in the ebb and flood channel of every macro cell as described in section 5.3. The different contributing terms and the total dimensionless tide-averaged bed-load transport according to Van de Kreeke and Robaczewska (2003) are calculated in every observation point. This gives an idea of the relative contributions of the tidal constituents to

the bed-load transport. The results for macro cell 6 are visualised in Figure 6-6. The graphs for the other macro cells can be found in Appendix A.8.

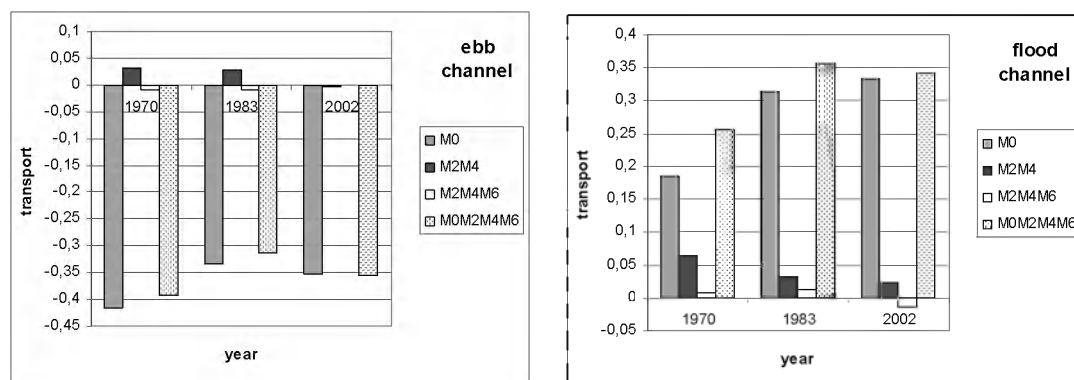


Figure 6-6: The different contributing terms and the total dimensionless tide-averaged bed-load transport according to Van de Kreeke and Robaczewska (2003) based on the velocity component in the mainstream direction at the observation points in the ebb and flood channel of macro cell 6 derived from the model results for the years 1970, 1983 and 2002.

On the graphs above there can be seen that the contribution of M_4 in both the ebb and flood channel decreases, whereas the M_0 residual increases in the flood channel. In both channels, the M_0 component has the highest contribution to the residual transport, and even determines the transport direction.

6.2.3 Conclusion

There is a major difference between the ebb and flood channels. In the ebb channels M_0 is determinative for the transport, whereas in the flood channels also the contribution of M_4 and M_6 is important.

The main ebb channel is characterised by strongly ebb-dominant residual currents (Jeuken, 2000; Wang and Jeuken, 2000). The direction of residual sand transport is determined by the effect of the relatively small residual current. The contribution of the overtides to the residual transport is several times smaller (Wang and Jeuken, 2000).

Changes in the contribution of the different terms to the total residual transport are directly related to the observed changes in the amplitude ratios of the M_0 , M_4 , M_6 and the M_2 tidal current respectively (Section 5.3).

6.3 Sand Balance Derived from the Model

6.3.1 Method

The sand balance derived from the model in this study quantifies the erosion and sedimentation of sand under influence of the tide-driven sediment transport occurring for a certain bathymetry. For this balance the Western Scheldt division into macro cells (Winterwerp et al., 2000) is used with a few adaptations (Figure 6-7): macro cell 1 and meso cell 2 form one entity, as well as macro cells 6 and 7. The latter entity is formed because it isn't possible to define cross-sections between these two cells to determine the sediment exchange between them due to the orientation of the grid in this part of the Western Scheldt.

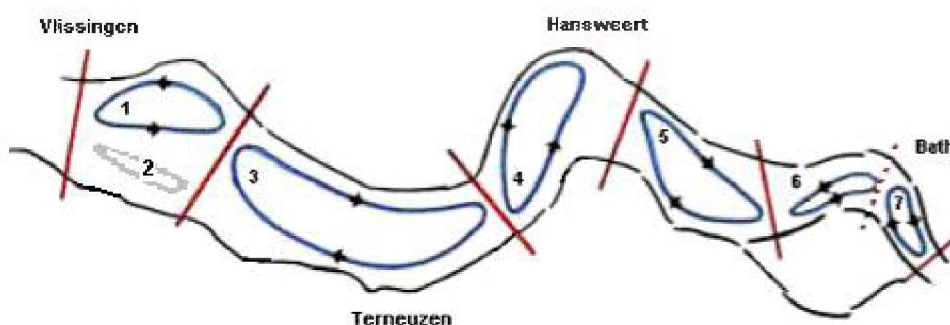


Figure 6-7: Division of the Western Scheldt in cells for the sand balance. The blue loops are macro cells, the grey one is a meso cell. The red full lines represent the borders between the compartments used in the sand balance (Schematical representation after Nederbragt and Liek (2004)).

The volume change within a compartment during one tidal cycle is calculated as follows:

$$\Delta V = V_{sb} - V_{lb} \quad \text{Equation 6-2}$$

where V_{sb} = the volume sediments passing through the seaward cell boundary during one tidal cycle (in m^3)

V_{lb} = the volume sediments passing through the landward cell boundary during one tidal cycle (in m^3)

ΔV = the volume change within the cell during one tidal cycle (in m^3)

Landward transport is counted positive, seaward transport negative. Therefore erosion will be represented by a negative volume change and sedimentation by a positive value.

Calculating the sand balances using the transport between macro cells through one cross-section representing the cell boundary, gives different values and even different trends at some locations compared to when the averaged transport through more cross-sections in the border area between two cells is used. This difference is the most noticeable in macro cells 3, 4 and 5. A comparison for the seaward border of cell 1 is given in Appendix A.10. Differences can amount to 50% for two successive cross-sections.

In the following discussion the sand balance derived from the averaged transport will be used. In this way local irregularities have less influence on the general trend. An overview of the cross-sections selected for this calculation and their location in the model is given in Appendix A.10.

6.3.2 Results

Table 6-1 gives the transport calculated with the Van Rijn formulation across the borders of the macro cells in $\text{m}^3/\text{tidal cycle}$. In most cases sediments are transported upstream in the estuary. Only between macro cells 1&3 the transport is directed downstream. Regarding the transport direction, bed-load and suspended load behave the same.

Table 6-1: Transport across the macro cell borders in $\text{m}^3/\text{tidal cycle}$ (+ = import; - = export) according to the Van Rijn formulation.

		Transport across the macro cell borders in $\text{m}^3/\text{tidal cycle}$ (+ = import; - = export)					
downstream		delta	cell 1	cell 3	cell 4	cell 5	cell 7
upstream		cell 1	cell 3	cell 4	cell 5	cell 6	upstream
1970	total load	1998	-705	1658	2403	1470	2512
	bed-load	21	-21	31	50	49	45
	suspended load	1978	-684	1627	2354	1421	2467
1983	total load	2246	-1204	2042	2490	1196	923
	bed-load	24	-24	29	43	37	20
	suspended load	2222	-1180	2012	2447	1158	903
2002	total load	1969	-395	2639	3381	436	1346
	bed-load	11	-41	28	58	2	27
	suspended load	2027	-353	2611	3322	434	1319

The transport between the cells is visualised in Figure 6-8. These graphs show that the total transport between cells 3&4 and 4&5 increases from 1970 to 2002, whereas the opposite is

true on the border of cells 5&6. In the other cell borders no clear trend is visible: the transport remains in the same direction all the years, only the value fluctuates. The same trends are visible for the suspended transport.

The bed-load transport shows another evolution. The transport from cell 3 towards cell 1 increases from 1970 to 2002, so more sediment is moving downstream. On the borders of cell 3&4 and 5&6, the (upstream) transport decreases. The import from the mouth towards cell 1 is clearly smaller in 2002 than in 1970 and 1983.

Comparing bed-load and suspended load shows that they don't follow exactly the same evolution. Since bed-load is only 3% of the suspended load, the trends of the suspended load are dominant. Upstream of macro cell 5, bed-load and suspended load evolve in the same way.

The erosion and sedimentation in the macro cells is given in Table 6-2 in $\text{m}^3/\text{tidal cycle}$. Erosion is noticed in macro cells 3 and 4. In cell 6+7 this happens only in 1970 and 2002. In all the other cases sedimentation occurs. Also here bed-load and suspended load have in general the same influence, only in cell 6+7 bed-load and suspended load have an opposite influence in 1970. Again the trend from the suspended load is dominant.

Table 6-2: Erosion and sedimentation in the macro cells in $\text{m}^3/\text{tidal cycle}$ according to the Van Rijn formulation (+ = sedimentation; - = erosion).

		Erosion (-) and Sedimentation (+) in the Macro Cells				
		(in $\text{m}^3/\text{tidal cycle}$)				
Macro Cell		cell 1+2	cell 3	cell 4	cell 5	cell 6+7
1970	total load	2703	-2363	-745	933	-1042
	bed-load	42	-52	-19	1	4
	suspended load	2662	-2311	-727	933	-1046
1983	total load	3450	-3246	-448	1294	273
	bed-load	48	-53	-14	6	17
	suspended load	3402	-3192	-435	1289	255
2002	total load	2364	-3034	-742	2945	-910
	bed-load	52	-69	-30	56	-25
	suspended load	2380	-2964	-711	2888	-885

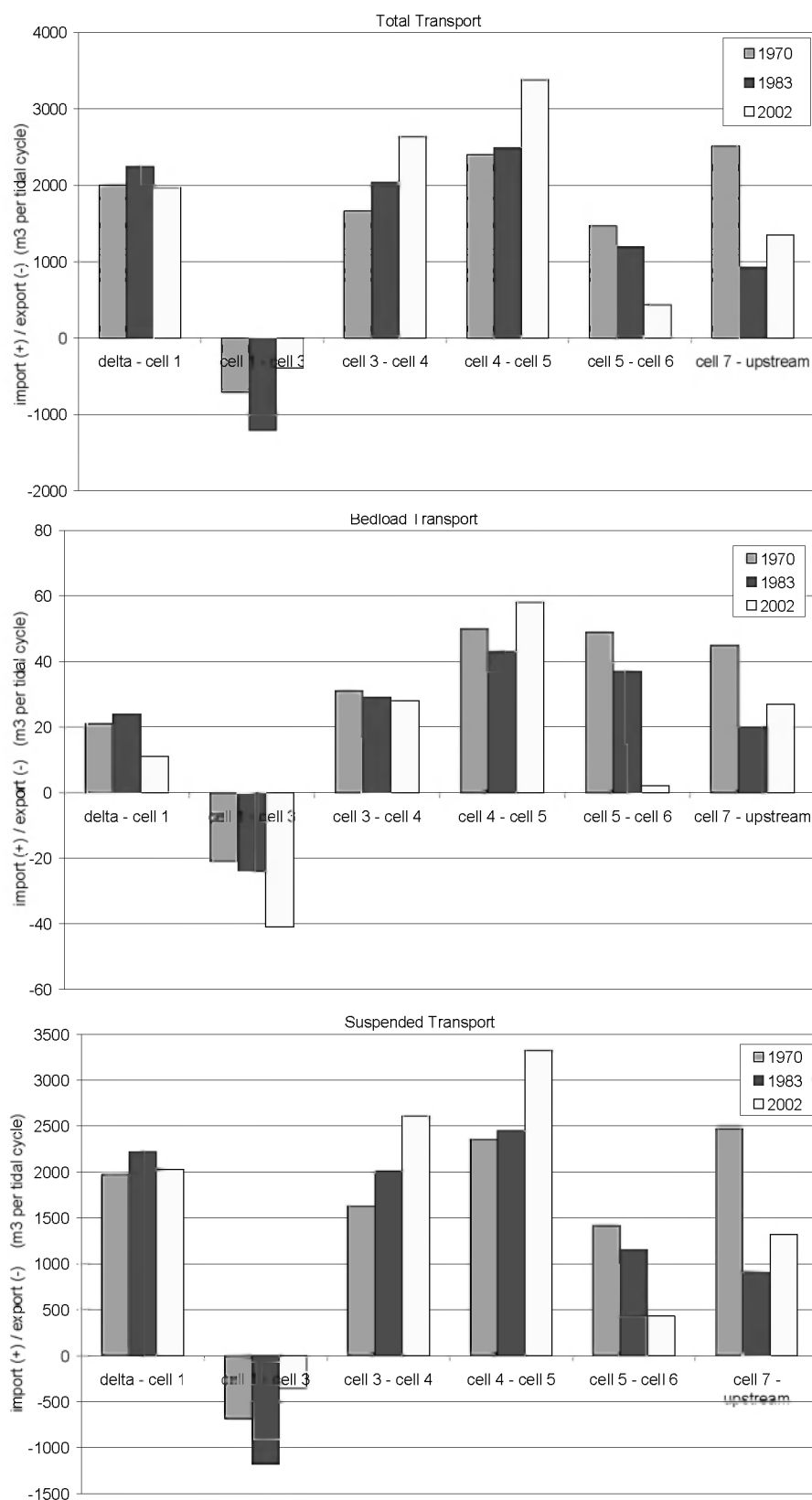


Figure 6-8: Transport between the macro cells in the Western Scheldt in $\text{m}^3/\text{tidal cycle}$ for the total, bed-load and suspended transport according to the Van Rijn formulation (+ = import or transport to the east, - = export or transport to the west).

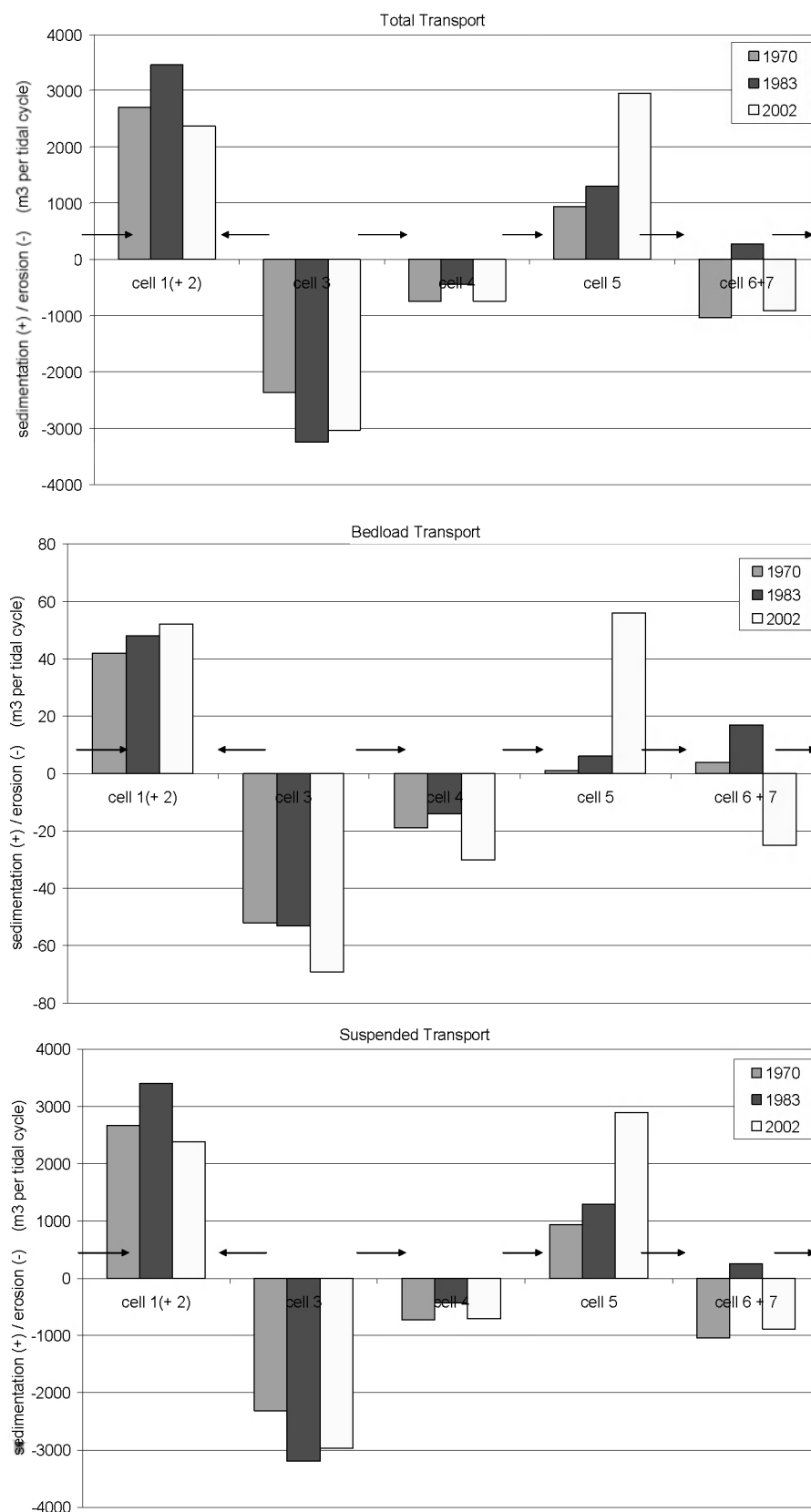


Figure 6-9: Sedimentation (+) and erosion (-) in the macro cells in the Western Scheldt in m³/tidal cycle for the total, bed-load and suspended transport according to the Van Rijn formulation. The arrows show the direction of the sediment transport between the cells.

Figure 6-9 visualises the erosion/sedimentation in the macro cells for the three different years. Only macro cell 5 shows a clear trend of increased sedimentation. This is visible for both bed-load and suspended load. Also here some different trends can be noticed for the influence of bed-load only. In cell 1 the sedimentation increases between 1970 and 2002, whereas in cell 3 the erosion augments

The same analysis was made for the transport calculated with the Engelund Hansen formula. This formulation directly gives the total load. The transport between the cells is 30 to 50% lower compared to Van Rijn. However the same trends appear as for the total load calculated with van Rijn. Considering the erosion/sedimentation within the cells, the pattern is slightly different in cell 4 and cell 6+7. The latter compartment shows the same evolution as the bed-load calculated with the Van Rijn formulation. These results can be found in Appendix A.10.

6.3.3 Discussion

The sand balance derived from this model is different from the approach when field data is used. Typically erosion/sedimentation in every department is calculated from the depth differences between two selected years. This is normally done for periods of several years. The volume changes together with an upstream boundary condition result in the transport between the compartments.

In this study, the opposite procedure has been followed. Erosion and sedimentation volumes are calculated from the transport between the compartments. Another point of difference is the time scale: sediment transport has been calculated for one ebb-flood cycle and no intervention data were included for this short period.

The sand balance from the model doesn't show a change from import to export at the mouth. Only for bed-load (which is only 3% of the total transport) the sediment import at the mouth decreased significantly from 1970 to 2002, whereas the export from cell 3 towards cell 1 increased. The suspended load, which dominates the total transport, doesn't show this evolution.

The comparison with previous studies and the identification of possible errors are described in Appendix A.10.

6.3.4 Conclusion

The increasing transport from west to east as found by Stikvoort et al. (2003) in the central part of the Western Scheldt is well represented in the model.

The change from import to export at the mouth is not reproduced in the model. When only the bed-load from the Van Rijn approach is considered, an increasing seaward transport is found from cell 3 towards cell 1 during the period 1970-2002. On the borders of cell 3&4 and 5&6, the upstream transport decreases. The import from the mouth towards cell 1 is also clearly smaller in 2002 compared to the other two years. However, even for bed-load only, no export at the mouth occurs.

Bed-load and suspended load do not show exactly the same evolution. A clear increase in eastward directed transport in the central part of the Western Scheldt is found for the suspended load, whereas this evolution is absent for bed-load only.

The transport formulation largely affects the results. The Engelund Hansen formulation typically gives lower values (30 to 50%) compared to Van Rijn. However the trends in the total transport calculated with both formulas correspond.

6.4 Relation Sediment Transport & Tidal Asymmetry

The Table below gives an overview of the most important evolutions of the amplitude ratios and the phase differences of the M_2 , M_4 and M_6 components of the horizontal tide. These evolutions are compared with the changes in sediment transport between the different macro cells and the sedimentation or erosion within each area according to the sand balance derived from the model as described in section 6.1 (See figures 6-7 and 6-8).

Table 6-3: Most important evolutions of the amplitude ratios and the phase differences of the M_2 , M_4 and M_6 components of the vertical tide.

Macro Cell	M_4/M_2	M_6/M_2	$2\phi_2 - \phi_4$	$3\phi_2 - \phi_6$
1	-	-	-	-
3	-	decrease	increase	increase
4	decrease (FC) increase (EC)	decrease	increase	increase
5	decrease	-	-	increase
6	decrease	-	-	-
7	decrease	-	-	increase
FC = flood channel, EC = ebb channel, - = no significant or clear evolution				

The decrease of the amplitude ratio M_4/M_2 in macro cells 5, 6 and 7 indicates a decrease of the strength of the tidal asymmetry. Combined with the positive phase difference $2\phi_2 - \phi_4$ a decrease of the eastward sediment transport through these cells is to be expected. This agrees with the decreasing transport from cell 5 towards cell 6 as found in the sand balance derived from the model. Also more sedimentation occurs in cell 5.

The bottom changes only influence the amount of increase of the phase difference $3\phi_2 - \phi_6$ in macro cells 3, 4, 5 and 7. This phase difference remains negative and does not change the transport significantly.

The amplitude ratio M_6/M_2 decreases in cell 3 and 4. Because the phase difference $3\phi_2 - \phi_6$ is negative, this means a decrease of the seaward transport. The decrease of M_4/M_2 in the flood channel of macro cell 4 in combination with the negative phase difference $2\phi_2 - \phi_4$ in this part, influences the transport in the same way. The sand balance shows an increase of the landward transport from cell 3 towards cell 5. Also more erosion occurs in macro cells 3 and

4. However, both changes in tidal asymmetry only decrease the transport and do not provide the driving force for an increased landward transport.

The trends in the sand balance can not be fully explained by the changes in tidal asymmetry due to a modified bathymetry. However, as mentioned before, many human interventions took place in the Western Scheldt. When dredging, dumping and sand mining are considered, the change in strategy after the second deepening seems to be important. Before 1997 the dredged material in the eastern part was dumped nearby in the secondary channels. After 1997 more material is dumped in the western and middle part of the Western Scheldt. The increased eastward transport from macro cell 3 towards cell 5 is probably related to this strategy.

Also more local, changes in dredging and dumping amounts can be responsible for the evolution of the transport between the cells. For example the dredging in area M and the dumping of sediments in area R can cause transport from cell 3 towards cell 1.

When macro cell 5 is considered, the numbers for the interventions clearly show an increase in the sediment demand. More dredging occurs since 1970, more sand mining since 1980 and less dumping since 1980. As such sediment supplied from downstream will be trapped in cell 5 and not transported further upstream. The sand balance from the model shows a decrease of the transport from cell 5 to 6, whereas the sedimentation within macro cell 5 clearly increases.

At the upstream border of the Western Scheldt, an important influence of the interventions in the Sea Scheldt can be expected. The sand balance study from Haecon (2006) shows a lot of dredging and almost no dumping in the Sea Scheldt around 1970. In 1983 and 2002 there is less dredging and more dumping. As such, the sediment demand decreases and less sediment is transported from the Western Scheldt towards the Sea Scheldt. This evolution is also present in the sand balance derived from the model.

The dredging strategy seems to have an important influence on the sediment transport occurring in the estuary. Parts of the channel where a lot of dredging occurred and almost no dumping show a clear sediment demand. Transport towards these locations and sedimentation in these areas will be high.

7 Conclusions

Is there a change in tidal asymmetry over the years?

Does the asymmetry of the vertical tide determined from the model agree with the asymmetry derived from field measurements?

For the model in this study the morphological tide selected by Kuijper et al. (2004) is applied. Identical boundary conditions were chosen for the three years since in this way only the changes of the bathymetry will influence the outcomes of the simulations. This has however the consequence that in the most downstream stations the slight evolution of the phase and amplitude of the tidal constituents noticed in the observations is not present in the model results.

On the other hand, the evolution of the amplitude ratios and phase differences within the estuary which describe the strength of the asymmetry and the ebb- or flood-dominance, are well represented. Only for the station Hansweert significant different trends come out from the model. This could be caused by limitations of the model, but also by the particular location of the measurement station.

Taking the limitations of the model into account, the DELFT3D model of the Western Scheldt provides a unique tool to study the influence of the bottom geometry on the tidal characteristics and the sediment transport. The trends in the different parameters describing the tidal asymmetry are reproduced well enough to give confidence in the model results and to be able to compare them with other related data.

How does the asymmetry of the vertical tide in the estuary change over the years?

The asymmetry of the vertical tide changes between 1970 and 2002. The highest differences occur in the eastern part of the Western Scheldt between Hansweert and Bath. There the amplitude ratios M_4/M_2 and M_6/M_2 , and the phase differences $2\varphi_2 - \varphi_4$ and $3\varphi_2 - \varphi_6$ decrease significantly in macro cell 6 between 1970 and 2002. This decrease is accompanied by a deepening of the flood and ebb channels due to the high amounts of dredging which took place in that area.

In the part west of macro cell 4 the M_4/M_2 amplitude ratio decreases whereas the M_6/M_2 ratio increases. The phase difference $3\varphi_2-\varphi_6$ clearly increases between 1970 and 2002. The amount of the increase is influenced by the changes in the bathymetry. The difference $2\varphi_2-\varphi_4$ hardly changes.

How does the asymmetry of the horizontal tide in the estuary change over the years?

The asymmetry of the horizontal tide changes between 1970 and 2002. The highest differences are found upstream from Hansweert: the amplitude ratio M_6/M_2 increases, and the ratio M_4/M_2 and the phase differences $2\varphi_2-\varphi_4$ and $3\varphi_2-\varphi_6$ decrease. Downstream from Hansweert the ratio M_6/M_2 and the phase difference $3\varphi_2-\varphi_6$ decrease. The ratio M_4/M_2 and the phase differences $2\varphi_2-\varphi_4$ do not show a clear trend in this part.

Deepening of a channel leads to a decrease of the amplitude ratio M_6/M_2 (cell 3 and 4) and M_4/M_2 (cell 4, 5 and 6). The phase difference $3\varphi_2-\varphi_6$ is continuously increasing in macro cells 3, 4 and 5, only the amount of increase is influenced by the changes in bathymetry. Sedimentation in a channel gives rise to an increase of the phase difference $2\varphi_2-\varphi_4$ (cell 3 and 4) and an increase of the amplitude ratio M_4/M_2 (cell 4). Apart from the last finding, similar reactions of the vertical tide to a modified bathymetry were found.

How do changes in the bathymetry modify the tidal asymmetry?

Is there a relation between the changes in the tidal asymmetry and the import/export of sediments at the mouth?

Which changes in the bathymetry have influenced the tidal asymmetry the most?

Both the analysis of the vertical and the horizontal tide related the deepening of channels to a decrease of the amplitude ratios M_6/M_2 and M_4/M_2 . Sedimentation in a channel gives rise to an increase of the phase difference $2\varphi_2-\varphi_4$ and the amplitude ratio M_4/M_2 of the horizontal tide. Both evolutions of the bathymetry are in most cases due to human interventions. Dredging, dumping and sand mining occur throughout the estuary and induce important bathymetric changes. These clearly have an impact on the tidal asymmetry in the estuary.

Does the residual transport derived from the model agree with previous sand balances?

In this study, no quantitative comparison was made with previous sand balances, since different periods are looked at. Whereas in the traditional sand balances typically the evolution over different years is looked at, in this study the evolution during one tidal cycle in combination with different bathymetries has been looked at.

The change from import to export at the mouth is not reproduced in the recent model. When only bed-load is considered in the Van Rijn approach, an increasing seaward transport is found from cell 3 towards cell 1. On the borders of cell 3&4 and 5&6, a decrease of the upstream transport is noticed. The import from the mouth towards cell 1 is also clearly smaller in 2002 compared to the other two years. However, even for bed-load only, no export at the mouth occurs.

On the other hand the increasing transport from west to east as found by Stikvoort et al. (2003) in the central part of the Western Scheldt is well represented in the model.

The last finding shows that the changes in the residual transport are (at least) locally influenced by the tide-bathymetry interaction. However, the absence of export in the 2002 situation indicates that some factors are still missing. Possibly wind and waves are important for the residual transport as well. Their influence hasn't been investigated in this study.

The dredging strategy seems to have an important influence on the sediment transport occurring in the estuary. Parts of the channel where a lot of dredging has occurred and almost no dumping show a clear sediment demand. Transport towards these locations and sedimentation in these areas is high.

Does bed-load & suspended load follow different trends?

In this study the Van Rijn transport formulation has been applied to calculate the bed-load and suspended load separately. The calculated bed-load is only around 3% of the total transport.

Although the driving mechanisms for suspended load and bed-load are different, the residual transport patterns in the model are very similar. However, as seen from the sand balance derived from the model, bed-load and suspended load don't follow exactly the same evolution. A clear increase in eastward directed transport in the central part of the Western Scheldt is found for the suspended load, whereas for bed-load only this evolution is absent.

Can different transport formulations influence the results significantly?

The transport formulation can largely affect the results. The Engelund Hansen formulation typically gives lower values (30 to 50%) compared to Van Rijn. Regarding qualitative results, more similarities are present. The Van Rijn transport formulation and the Engelund Hansen formula give for example similar residual transport patterns. Also the trends in the total transport calculated with both formulas correspond.

Which characteristics of the bottom geometry are responsible for the import/export of sediments at the Western Scheldt mouth?

The change from import to export at the mouth is not reproduced in the model. This can be explained by three different reasons:

- Insufficient accuracy in forcing of the model. In this study irregularities in the water level upstream from Hansweert were found for the 1970 situation. A solution would be to calibrate the model again and to improve the schematisation of the most upstream part.
- Sediment transport due to interaction of the tide with the bathymetry isn't representative for the residual sediment transport. Also non-tidal mechanisms such as estuarine circulation, wind and waves can contribute significantly to the transports in a tidal inlet. These mechanisms haven't been included in the model for this study.
- The effect of human interventions might be underestimated and dominate over the natural changes.

Further research is needed to determine the influence of all these different processes (See recommendations).

Which are the mechanisms governing the sediment exchange between the Dutch coast and the tidal basin Western Scheldt?

The change from import to export at the mouth is not reproduced in the model. This can have different reasons as described above. On the other hand the increasing transport from west to east in the central part of the Western Scheldt is well represented in the model. This finding shows that the changes in the residual transport are (at least) locally influenced by the interaction of bathymetry and tide. Also the dredging strategy seems to have an important influence on the sediment transport occurring in the estuary.

However, the absence of export in the 2002 situation indicates that some factors are still missing. Possibly wind and waves are important for the residual transport as well. Their influence hasn't been investigated in this study. Further research is needed to identify the relative importance of the different mechanisms. Recommendations for further research are formulated in the next chapter.

8 Recommendations

The subject of the sediment exchange at the Western Scheldt mouth is very extensive and a lot of different processes can contribute to the observed evolution. This study should be seen as a small step forward in getting insight in this mechanism. Some recommendations for further research are formulated below.

Sea Scheldt

Data concerning the bathymetry of the Sea Scheldt are limited. Measurements have been performed only once every 10 years (Haecon, 2006). For all intermediate years interpolation of the available data is used, however these bottoms can differ significantly from the real situation.

Also the discharges near Rupelmonde, which is the upstream boundary of the numerical model, are not well-known. The use of more accurate boundary conditions can significantly improve the model performance and reliability.

Spring-Neap Cycle

Wang et al. (1999) described the temporal variation of the asymmetry of the vertical tide and highlighted a number of possible errors due to the selection of a morphological tide. These limitations have been taken into account during this study. However the intensity of the bathymetry-induced residual circulations in the ebb and flood channels goes through a spring-neap tidal cycle (ibid.). Results for simulations forced by a spring-neap cycle should be compared to those with a morphological tide.

Shoals

Figure 8-1 shows a comparison of the shoal area “de Hooge Platen” located in the western part of the Western Scheldt near Breskens between 1996 and 2001. The picture clearly shows that “De Bol” has become higher and even vegetation is present in 2001 since there occurs less flooding. It is not known how accurate the bathymetric data are concerning the shoals in the Western Scheldt. However the accurate representation of the shoals in a numeric model can have an important influence on the tidal volumes and the propagation of

the tide in the estuary. There should be investigated how sensitive the tidal characteristics in the Western Scheldt are to changes in the height of the shoals.



Figure 8-1: Aerial photo of the shoals “de Hooe platen” in 1996 (left) and 2001 (right). The red spots are vegetated areas. (Picture from the “ Meetkundige Dienst” in Peters et al., 2003)

Wind & Waves

In this study only the tide-driven residual sediment transport was considered. However in addition to the tidal forcing also non-tidal mechanisms such as estuarine circulation, wind and waves can contribute significantly to the transports in a tidal inlet as found for the Marsdiep by Elias et al. (2006). Although the Western Scheldt is a significantly different inlet, these processes should probably be included as well to explain the change from import to export at the mouth.

Other Influences on the Estuary

A number of other impacts on the estuary are still not included. Upstream, in the port of Antwerpen, the numerous docks have a clear influence on the sand evolution in the Sea Scheldt (Haecon, 2006). Not only the construction caused transport variations, but also now sediment exchanges between the docks and the Sea Scheldt (ibid.).

The influence of the canals along the Western Scheldt (canal Gent-Terneuzen, canal through Zuid-Beveland, canal through Walcheren) should be investigated more in detail (Haecon, 2006). Also a number of brooks flow into the port of Antwerp.

The impact of the human interventions on the morphological evolution of the mouth is still unknown. However it's expected that the expansion of the port of Zeebrugge and the delta-

plan with the storm-surge barrier on the Eastern Scheldt have influenced the Voordelta (Peters, 2006; Port of Zeebrugge, 2006). Research is needed to determine the morphological evolution of this region, also in relation to the Western Scheldt since an important interaction exist between these two areas (Peters, 2006).

References

- Ackers P. and White W.R., 1973, *Sediment transport: new approach and analysis*, Journal of the hydraulics division, ASCE 99 (11), 2041-2060.
- Aubrey D. G. and Speer P. E., 1985, *A study on non-linear tidal propagation in shallow inlet/estuarine systems: 1. Observations*, Estuarine, Coastal and Shelf Science, 21, 185-205.
- Bailard J., 1981, *An energetic total load sediment transport model for a plane sloping beach*, Journal of Geophysical Research, 86, C11, 10938-10954.
- Bijker E., 1968, *Littoral drift as function of waves and current*, 11th Coastal Engineering Conf. Proc. ASCE, London, UK, 415-435.
- Bonekamp H., Ridderinkhof H., Roelvink D. and Luijendijk A., 2002, *Sediment transport in the Texel tidal inlet due to tidal asymmetries*, ICCE 2002.
- Boon J.D., 1988, *Temporal variation of shallow-water tides in basin-inlet systems*, in Aubrey D.G. and Weishar L. (Eds.), *Hydrodynamics and sediment dynamics of tidal inlets*, Springer-Verslag, New York.
- Boon J.D. and Byrne R.J., 1981, *On basin hypsometry and the morphodynamic response of coastal inlet systems*, Marine Geology, 40, 27-48.
- Camenen B. and Larroudé P., 2003, *Comparison of sediment transport formulae for the coastal environment*, Coastal Engineering, 48, 111-132.
- Dauwe B., 2001, *Monitoring van de effecten van de verruiming 48'-43'*, *Samenvatting van de ontwikkelingen in de Westerschelde (tussenstand 2000)*, RAPPORT 6, Rapport RIKZ/2001.025.
- de Bok C., 2002, *Zandbalans van het deelsysteem "Delta"*, Werkdocument RIKZ/OS/2002/114x, Rijksinstituut voor Kust en Zee/RIKZ.
- De Jong J.E.A., 2000, *Zandbalans Westerschelde en monding. Periode 1955-1999*, Notitie NWL-00.16, Rijkswaterstaat, directie Zeeland.
- Dibajnia M. and Watanabe A., 1992, *Sheet flow under non-linear waves and currents*, Coastal Engineering, 2015-2029.
- Dronkers J., 1985, *Tide-induced residual sediment transport of fine sediment*, Rijkswaterstaat, Delta Department, The Netherlands.
- Dronkers J., 1986, *Tidal asymmetry and estuarine morphology*, Netherlands Journal of Sea Research, 20, 117-13.
- Dronkers J., 1998, *Morphodynamics of the Dutch Delta*, in: Dronkers J. and Scheffers M. (1998), *Physics of Estuaries and Coastal Seas*, A.A. Balkema, Rotterdam.
- Dronkers J., 2005, *Dynamics of Coastal Systems*, Advanced Series on Ocean Engineering – Volume 25, World Scientific.

- Du Four I., Schelfout K., Vanheteren S., Van Dijk T. and Van Lancker V., 2006, *Geologie en sedimentologie van het Westerscheldemondingsgebied*, in: Coosen J., Mees J., Seys J. en Fockedeij N. (Eds.). *Studiedag: De Vlakte van de Raan van onder het stof gehaald. Oostende, 13 oktober 2006*, Vlaams Instituut voor de Zee (VLIZ), VLIZ Special Publication, 35, Oostende, België. iii + 135 p.
- Duin R.N.M., 2005, *Trends in de zandhuishouding van het Nederlandse kuststelsel*, werkdokument RIKZ/KW/2005.132w, Rijksinstituut voor Kust en Zee/RIKZ.
- Dumon G., Balcaen N., Huygens M., Hyde P. and Haerens P., 2006, *Hydrodynamica ter hoogte van de vlakte van de Raan*, in: Coosen J., Mees J., Seys J. en Fockedeij N. (Eds.). *Studiedag: De Vlakte van de Raan van onder het stof gehaald. Oostende, 13 oktober 2006*, Vlaams Instituut voor de Zee (VLIZ), VLIZ Special Publication, 35, Oostende, België. iii + 135 p.
- Dyer K.R., 1997, *Estuaries: a physical introduction*, John Wiley and Sons Ltd., 2nd edition.
- Elias E.P.L., Cleveringa J., Buijsman M.C., Roelvink J.A. and Stive M.J.F., 2006, *Field and model data analysis of sand transport patterns in Texel Tidal inlet (the Netherlands)*, Coastal Engineering, 53, 505-529.
- Elias E.P.L., 2006, *Morphodynamics of Texel Inlet*, PhD-thesis, Delft University.
- Engelund F. and Hansen E., 1967, *A monograph on sediment transport in alluvial streams*, Teknisk Forlag, Technical University of Denmark.
- Fortunato A.B. and Oliveira A., 2005, *Influence of intertidal flats on tidal asymmetry*, Journal of Coastal Research, 21 (5), 1062-1067.
- Friedrichs C.T., and Aubrey D.G., 1988, *Non-linear tidal distortion in shallow well-mixed estuaries: a synthesis*, Estuarine, Coastal and Shelf Science, 27, 521-545.
- Friedrichs C.T., and Aubrey D.G., 1996, *Uniform bottom shear stress and equilibrium hypsometry of intertidal flats*, in: Pattiaratchi C. (Ed.), *Mixing processes in Estuaries and Coastal Seas*, Estuarine and Coastal Studies Series, American Geophysical Union, Washington, DC, 405-429.
- Friedrichs C.T., Aubrey D.G. and Speer P.E., 1990, *Impacts of relative sea-level rise on evolution of shallow estuaries*, In Cheng R.T., (Ed.), *Residual current and long-term transport*, Springer Verslag, New York.
- Friedrichs C.T., Lynch D.R. and Aubrey D.G., 1992, *Velocity asymmetries in frictionally-dominated tidal embayments: longitudinal and lateral variability*, in: Prandle D. (Ed.), *Dynamics and exchanges in estuaries in the coastal zone*, American Geophysical Union, Washington D.C., 277-312.
- Fry V.A., Aubrey D.G., 1990, *Tidal velocity asymmetries and bed-load transport I*, Estuarine coastal and shelf science, 30 (5) p453-473, 1990.
- Gautier C. and Van De Boomgaard M., 2003, *Rapportage veldmetingen Westerschelde september 1997 t/m december 2002*, RIKZ/2003.052, Rijksinstituut voor Kust en Zee/RIKZ.

- Groen P., 1967, *On the residual transport of suspended load matter by an alternating tidal current*, Netherlands Journal of Sea Research, 3, 564-674.
- Groenendaal E., 2005, *Westerschelde: import of export? Invloed van de bodemligging op sedimenttransport in de Westerschelde*, MSc dissertation TU Delft.
- Haecon, 2000, *Zandbalans WS-Mond Belgisch gedeelte*, Rapport NST2155-25, Haecon Harbour & Engineering Consultants.
- Haecon, 2006, *Actualisatie van de zandbalans van de Zee- en Westerschelde*, Haecon (Soresma), report 1249760008/lvp.
- Hayes M.O., 1975, *Morphology of sand accumulation in estuaries: an introduction to the symposium*, In: Cronin L.E. (Ed.), *Estuarine Research II*, Academic Press, New York, 3-22.
- Heathershaw A.D., 1988, *Sediment transport in the sea, on beaches and in rivers: Part II – Sediment movement*, Journal of Naval Science, 14(4), 221-234.
- Hibma A., Stive M.J.F. and Wang Z.B., 2004, *Estuarine Morphodynamics*, Coastal Engineering, 51, 765-778.
- Huijs S. M., Groenenberg, van Westenbrugge K., de Kock G., Santbergen L., van Hoek H., Polfliet A., van Herk S., Roelse P., 2000, *Zand in de hand: Beleidsplan Zandwinning Westerschelde 2001-2011*, Nota NWL-00.05, Rijkswaterstaat, Directie Zeeland, Middelburg.
- Hulström F., 1935, *Studies in the morphological activity of rivers as illustrated by the river Fyris*, Geological Institute of the University of Upsala Bulletin, 25, 221-528.
- Jeuken M.C.J.L., 2000, *On the morphologic behaviour of tidal channels in the Westerschelde estuary*, PhD-thesis, Utrecht University, 378pp.
- Jeuken C., Ruessink G. and Wang Z.B., 2002, *Adviezen voor het maken van een gezamenlijke zandbalans voor Westerschelde en monding*, Z3213, WL | Delft Hydraulics.
- Jeuken M.C.J.L., Wang Z.B., Van der Kaaij T., Van Helevert M., Van Ormondt M., Bruisma R. and Tanczos I., 2004, *Morfologische ontwikkelingen in het Schelde estuarium bij voortzetting van het huidige beleid en effecten van een verdere verdieping van de vaargeul en uitpolderingen langs de Westerschelde, Deelovereenkomst 2 en 3 Morfologie*, Arcadis/Technum/ WL | Delft Hydraulics.
- Kang J.W. and Jun K.S., 2003, *Flood and ebb-dominance in estuaries in Korea*, Estuarine, Coastal and Shelf Science, 56(1), 187-196.
- Karim M.F. and Kennedy J.F., 1990, *Menu of couple velocity and sediment discharge relations for rivers*, Journal of Hydraulic Engineering, 116, 8, 978-996.
- Kornman B., Arends A. and Dunsbergen D., 2000, *Westerscheldemonnd 1970 – 2020: Een morfologische blik op de toekomst*, Ministerie van Verkeer en Waterstaat, Directoraat-Generaal Rijkswaterstaat, Rijksinstituut voor Kust en Zee/RIKZ.

- Kuijper C., Steijn R., Roelvink D., van der Kaaij T. and Olijslagers P., 2004, *Morphological modelling of the Western Scheldt, Validation of DELFT3D*, Report Z3648 / A1198, WL Delft Hydraulics and Alkyon.
- Li C., and O'Donnell J., 1997, *Tidally driven residual circulation in shallow estuaries with lateral depth variation*, Journal of Geophysical Research, 102(C13), 27915-27929.
- LTV, 2001, *Langetermijnvisie Schelde-estuarium met toelichting (LTV 2030)*, Ministerie van verkeer en Waterstaat, Rijkswaterstaat Directie Zeeland en ministerie van de Vlaamse Gemeenschap.
- Marijs K. and Parée E., 2004, *Nauwkeurigheid vaklodingen Westerschelde en monding; "de praktijk"*. Rapport ZLMD-04.N.004, Rijkswaterstaat, Meetinformatiedienst Zeeland.
- Mol G., van Berchum A.M. and Krijger G.M., 1997, *De toestand van de Westerschelde aan het begin van de verdieping 48'/43'*, Rapport RIKZ-97-049.
- Nederbragt G. and Liek G.-J., 2004, *Beschrijving zandbalans Westerschelde en monding*, Rapport RIKZ/2004.020, Rijkswaterstaat, Rijksinstituut voor Kust en Zee/RIKZ.
- Nederbragt G., 2006, *Zandvoorraden van het kuststelsel, Onderbouwing van een conceptueel model met behulp van trends van de winst- en verliesposten over de periode 1973-1997*, Rapport RIKZ/2005.033, Rijkswaterstaat, Rijksinstituut voor Kust en Zee/RIKZ.
- OS2010, *Ontwikkelingsschets 2010 Schelde-estuarium*, <http://www.ontwikkelingsschets2010.nl>, on 11 august 2006.
- Paphitis D., 2001, *Sediment movement under unidirectional flows: an assessment of empirical threshold curves*, Coastal Engineering, 43, 227-245.
- Peters B.G.T.M., Liek, G.A., Wijsman J.W.M., Kuijper M.W.M., van Eck G.Th., 2003, *Monitoring van de effecten van de verruiming 48'/43'*, Een verruimde blik op waargenomen ontwikkelingen, MOVE Evaluatierapport 2003, MOVE-rapport 8, Deel B: Hoofdrapport, Rapport RIKZ/2003.027, Rijkswaterstaat, Directie Zeeland.
- Peters J.J., 2006, *Belang van de vlakte van de Raan voor de morfologische evolutie van het Schelde-estuarium*, in: Coosen J., Mees J., Seys J. and Fockedeij N. (Eds.). *Studiedag: De Vlakte van de Raan van onder het stof gehaald. Oostende, 13 oktober 2006*, Vlaams Instituut voor de Zee (VLIZ), VLIZ Special Publication, 35, Oostende, België. iii + 135 p.
- Pinto L., Fortunato A.B. and Freire P., 2006, *Sensitivity analysis of non-cohesive sediment transport formulae*, Continental Shelf Research, in press.
- Port of Zeebrugge, 2006, www.portofzeebrugge.be, on 30/10/2006.
- Postma H., 1967, *Sediment transport and sedimentation in the estuarine environment*, Estuaries, G. H. LAUFF, ed., AAAS Publ., 158-179.
- Postma H., 1981, *Exchange of materials between the North Sea and the Wadden Sea*, Marine Geology, 40, 199-213.

- Prandle D., 2004, *How tides and river flows determine estuarine bathymetries*, Progress in Oceanography, 61, 1-26.
- Ribberink J., 1998, *Bed-load transport for steady flows and unsteady oscillatory flows*, Coastal Engineering, 34, 52-82.
- Ridderinkhof H., 1988a, *Tidal and residual flows in the Western Dutch Wadden sea, I: Numerical model results*, Netherlands Journal of Sea Research, 22(1), 1-21.
- Ridderinkhof H., 1988b, *Tidal and residual flows in the Western Dutch Wadden sea, II: An analytical model to study the constant flow between connected tidal basins*, Netherlands Journal of Sea Research, 22(3), 185-198.
- Ridderinkhof H., 1989, *Tidal and residual flows in the Western Dutch Wadden sea, III: Vorticity balances*, Netherlands Journal of Sea Research, 23(1), 9-26.
- RIKZ, *Rijksinstituut voor Kust en Zee*, 2006, www.rikz.nl, on 10 September 2006.
- Schoeman P.K., 2000, *Getij-asymmetrie in de Westerschelde*, Master thesis, Delft University of Technology, Faculty of Civil Engineering.
- Shields A., 1936, *Application of Similarity Principles and Turbulence research to Bed-load Movement* (English translation of the original German manuscript), Hydrodynamics Laboratory, California Institute of Technology, Publication No. 167.
- Speer P.E. and Aubrey D.G., 1985, *A study of non-linear tidal propagation in shallow inlet/estuarine systems, Part II: theory*, Estuarine, Coastal and Shelf Science, 21, 207-224.
- Speer P.E., Aubrey D.G. and Friedrichs C.T., 1991, *Non-linear hydrodynamics of shallow tidal inlet/bay systems*, in Parker B.B. (Ed.), Tidal Hydrodynamics, Wiley, New York.
- Stikvoort E. (ed.), Berrevoets C., Kuijper M., Lefèvre F., Liek G-J., Lievaart M., van Maldegem D., Meininger P., Peters B., Pouwer A., Schippers H. and Wijsman J., 2003, *Monitoring van de effecten van de verruiming 48'-43', MOVE-rapport 7: MOVE hypothesendocument 2003, Onderliggende rapportage bij MOVE-rapport 8 (deel A en B) Evaluatierapport 2003, Rapport RIKZ/2003.009, Middelburg.*
- Technische Scheldec commissie, 1984, *Verdieping Westerschelde programma 48'/43', Studierapport, deel 1 en 2*, Subcommissie Westerschelde, Middelburg en Antwerpen.
- TeeT.K., 1976, *Tide-induced residual current, 2D non-linear numerical tidal model*, Journal of Marine Research, 34, 603-628.
- Uit den Bogaard L.A., 1995, *Resultaten zandbalans Westerschelde 1955-1993*, IMAU rapport R95-08, Universiteit Utrecht.
- Van De Kreeke J., Robaczewska K., 1993, *Tide-induced residual transport of coarse sediment; application to the Ems estuary*, Netherlands Journal of Sea Research 31, 3, 209-220.

- Van den Berg J.H., Jeuken M.C.J.L., and Van der Spek A.J.F., 1996, *Hydraulic processes affecting the morphology and evolution of the Westerschelde estuary*, in: Nordstrom K.F. and Roman C.J. (Eds.), *Estuarine shores: Evolution, Environments and Human Alterations*. John Wiley, Chichester, p157-184.
- van der Kaaij T., Roelvink D. and Kuijper K., 2004, *Morphological modelling of the Western Scheldt, Intermediate report Phase I: Part I: Hydrodynamic model set-up, calibration and verification; Part II: Wave model set-up*, Z3648/A1198, WL Delft Hydraulics and Alkyon.
- van der Male C., 1993, *Euleriaanse reststromen op de Westerschelde berekend met DETWES*, Werkdocument GWWS 93.839x, Rijkswaterstaat, Rijksinstituut voor Kust en Zee/RIKZ, Middelburg.
- van der Spek A.J.F., 1997, *Tidal asymmetry and long-term evolution of Holocene tidal basins in the Netherlands: simulation of paleo-tides in the Scheldt estuary*, *Marine Geology*, 141, 71-90.
- Van der Slikke M.J., 1997, *Grootschalige zandbalans van de Westerscheldemonding. Een inventarisatie van dieptegegevens (1800-1996)*, IMAU Rapport R97-18, Universiteit Utrecht.
- Van der Slikke M.J., 1998, *Grootschalige en interne zandbalans van de Westerscheldemonding. (1969-1993)*, IMAU Rapport R98-05, Universiteit Utrecht.
- van Rijn L.C., 1984a, *Sediment transport, part I: bed-load transport*, *Journal of Hydraulic Engineering* 110, 10, 1431-1456.
- van Rijn L.C., 1984b, *Sediment transport, part II: suspended load transport*, *Journal of Hydraulic Engineering* 110, 11, 1631-1641.
- Van Straaten L. M. J. U. and Kuenen P. H., 1957, *Accumulation of fine-grained sediments in the Dutch Wadden Sea*, *Geologie en Mijnbouw*, 19, 329-354.
- van Veen J., 1950, *Ebb- and flood channel systems in the Netherlands tidal waters (in Dutch, English summary)*, KNAG, 2e series, part 67, Republished, translated and annotated by Delft University of Technology, 2001, ISBN 9040723389.
- Verfaillie E., Van Lancker V. and Van Meirvenne M., in press, *Multivariate geostatistics for the predictive modelling of the surficial sand distribution in shelf sea*, *Continental Shelf Research*.
- Verlaan P.A.J., 1998, *Mixing of marine and fluvial particles in the Scheldt estuary*, Ph.D., Delft University of Technology.
- Voogt L., Van Rijn L.C. and Van Den Berg J.H., 1991, *Sediment transport of fine sands at high velocities*, *Journal of Hydraulic Engineering*, 117, 869-890.
- Vroon J., Storm C., Coosen J., 1997, *Westerschelde: stram of struis? Eindrapport van het project Oostwest, een studie naar de beïnvloeding van fysische en verwante biologische patronen in een estuarium*, RIKZ-97.023, Rijkswaterstaat, Rijksinstituut voor Kust en Zee/RIKZ.

- Walburg L., 2006 (in preparation), *Zandbalans van het Nederlandse kustsysteem*, Werkdocument RIKZ/KW/2005.133w, Rijksinstituut voor Kust en Zee/RIKZ.
- Wang Z.B., Jeuken M.C.J.L., de Vriend H.J., 1999, *Tidal asymmetry and residual sediment transport in estuaries. A literature study and application to the Western Scheldt*, Z2749, WL | Delft Hydraulics.
- Wang Z.B., Jeuken M.C.J.L., Gerritsen H., de Vriend H.J., Kornman B.A., 2002, *Morphology and asymmetry of the vertical tide in the Westerschelde estuary*, Journal of Continental Shelf Research 22 (2002) 2599-2609.
- Winterwerp J.C., Jeuken M.C.J.L., Stive M.J.F. and de Vriend H.J., 2000, *Lange termijnvisie Westerscheldecluster morfologie*, Z2798, WL | Delft Hydraulics.
- WL|Delft Hydraulics, 2005, *User Manual DELFT3D-FLOW: Simulation of multi-dimensional hydrodynamic flows and transport phenomena, including sediments*, Delft, the Netherlands.
- WL|Delft Hydraulics, 2006, *DELFT3D*, Delft, the Netherlands.
- Zimmerman J.T.F., 1978, *Topographic generation of residual circulation by oscillatory (tidal) currents*, Geophysics. Astrophys. Fluid Dynamics, 11, 35-47.
- Zimmerman J.T.F., 1980, *Vorticity transfer by tidal currents over an irregular topography*, Journal of Marine Research, 38 (4), 601-630.
- Zimmerman J.T.F., 1981, *Dynamics, diffusion and geomorphological significance of tidal residual eddies*, Nature, 290, 549-5.